

Cover

Geochemical modelling is an important pillar of the safety assessment studies. Thermodynamic data of safety relevant elements (insert) and their compounds have been reviewed and documented in the new release of the PSI/Nagra thermodynamic database TDB-12/07.

PAUL SCHERRER INSTITUT



Progress Report 2014

**Laboratory for Waste Management
Nuclear Energy and Safety Department**



See also our web-page
<http://www.psi.ch/les/>

Preface

The main task of the Laboratory for Waste Management is to carry out an R&D programme to strengthen the scientific basis for radioactive waste management.

The Laboratory serves an important national role by supporting the Swiss Federal Government and Nagra in their tasks to safely dispose of radioactive wastes from medical, industrial and research applications as well as from nuclear power plants. The activities are in fundamental repository geochemistry, chemistry and physics of radionuclides at geological interfaces and radionuclide transport and retardation in geological media and man-made repository barriers. The work performed is a balanced combination of experimental activities in dedicated laboratories for handling radioactive elements, field experiments and modelling. The work is directed towards repository projects and the results find their application in comprehensive performance assessments carried out by Nagra. In particular, a major priority for LES over the next decade or so will be to contribute to the Sachplan geologische Tiefenlagerung ("Sectoral Plan").

This report summarises the activities and results achieved in the reporting period. It is organised as an overview followed by individual reports on the six waste management group/sub-programme activities.

We gratefully acknowledge the help of the institute's management and of Nagra in our work.

TABLE OF CONTENTS

1	OVERVIEW	5
1.1	Introduction.....	5
1.2	General.....	5
1.3	Sectoral Plan for Deep Geological Disposal.....	7
1.4	Repository near field.....	8
1.4.1	Repository chemistry	8
1.4.2	Clay systems	8
1.4.3	Cement.....	9
1.4.4	Interfacial processes.....	10
1.5	Repository far field	11
2	GEOCHEMICAL MODELLING	13
2.1	Overview.....	13
2.2	Activities in support of the Sectoral Plan.....	13
2.2.1	PSI/Nagra Chemical Thermodynamic Database 12/07.....	13
2.2.2	Critical assessment of silicate species.....	13
2.2.3	Solubility of chemotoxic elements.....	15
2.3	FIRST-Nuclides project.....	15
2.3.1	Introduction.....	15
2.3.2	X-ray spectroscopy	16
2.4	Thermodynamic databases and GEM software	19
2.5	Solid solution – aqueous solution systems.....	19
2.6	Water-rock interactions in Icelandic hydrothermal systems.....	23
2.7	References.....	24
3	TRANSPORT MECHANISMS	27
3.1	Overview.....	27
3.2	Activities in support of the Sectoral Plan.....	28
3.2.1	Geochemical evolution of the L/ILW near field.....	28
3.2.2	Interface Evolution in the engineered Gas Transport System (EGTS).....	29
3.2.3	Influence of a low-pH liner on the near field of a HLW repository	29
3.2.4	DR-A field experiment in the Mont Terri Underground Rock Laboratory.....	30
3.2.5	Multispecies random walk simulations in radial symmetry – model concept, benchmark and application to HTO, ²² Na and ³⁶ Cl diffusion in clay.....	30
3.2.6	Uncertainty propagation of the Linear-Free-Energy-Relationship sorption parameters when applied in reactive transport calculations.....	32
3.2.7	Experimental observation of porosity change at a cement-clay interface.....	33
3.3	Fundamental understanding of transport and sorption mechanisms	34
3.3.1	Water transport in cement revealed by NMR relaxometry and molecular simulations	34
3.3.2	Multi-scale molecular modelling of ion sorption by C-S-H phases.....	34
3.3.3	Up-scaling of diffusion coefficients: Scale dependent mobility of aqueous species	35
3.3.4	Up-scaling of diffusion coefficients: Influence of interparticle pore width distribution	37
3.4	Benchmarking and validation of coupled codes	38
3.4.1	Cooperation with Centre for Environmental Research, Leipzig.....	38
3.4.2	Experimental benchmarks for the verification and validation of reactive transport codes	38
3.5	References.....	39
4	CLAY SORPTION MECHANISMS	41
4.1	Overview.....	41
4.2	Activities in support of the Sectoral Plan.....	41
4.3	Mechanistic sorption modelling.....	42
4.3.1	Sorption modelling of Eu, Th and UO ₂ on Opalinus Clay and Boda Clay	42
4.3.2	Fe(II) uptake on natural montmorillonites: Macroscopic and spectroscopic characterization and surface complexation modelling (PhD project)	44
4.4	XAS related activities	46
4.4.1	SNF project.....	46
4.4.2	AnXAS 2014.....	46

4.5	References.....	46
5	CEMENT SYSTEMS	49
5.1	Overview.....	49
5.2	Activities in support of the Sectoral Plan.....	49
5.3	Speciation and fate of organic compounds in the cementitious near field.....	50
5.3.1	¹⁴ C project.....	50
5.3.1.1	Identification and quantification of organic compounds released during iron corrosion	50
5.3.1.2	Source of oxidized hydrocarbons during the anoxic corrosion of iron.....	50
5.3.1.3	Coupling HPIEC with accelerator mass spectrometry (AMS) for compound-specific ¹⁴ C analysis.....	52
5.3.1.4	Development of a reactor for the corrosion experiment with activated steel.....	54
5.3.2	Chemical stability of organic compounds under hyper-alkaline conditions.....	54
5.4	Immobilization of redox-sensitive radionuclides by cementitious materials.....	55
5.4.1	Actinides.....	55
5.4.2	Selenium.....	56
5.5	References.....	58
6	COLLOID CHEMISTRY	59
6.1	Overview.....	59
6.2	Activities in the CFM Project.....	59
6.3	Other colloid activities.....	59
6.4	Future work.....	61
6.5	References.....	61
7	DIFFUSION PROCESSES	63
7.1	Overview.....	63
7.2	Activities in support of the Sectoral Plan.....	63
7.3	CatClay.....	64
7.4	Transport phenomena in compacted clay systems (TRAPPHICS).....	66
7.5	Porosity changes in porous media.....	67
7.6	Transport of small organic molecules in dense clay systems.....	68
7.7	Anion exclusion phenomena in low porosity clay rocks (ANPOR).....	68
7.8	References.....	69
8	PUBLICATIONS	71
8.1	Peer reviewed journals.....	70
8.2	PSI and Nagra reports.....	72
8.3	Conference proceedings.....	72
8.4	Conferences/workshops/presentations.....	72
8.5	Invited talks.....	75
8.6	Teaching.....	75
8.7	PhD thesis and master projects.....	75
8.8	Other.....	76

1 OVERVIEW

Sergey V. Churakov

1.1 Introduction

The progress made in the Laboratory for Waste Management (LES) over the period from January 1st, 2014 to December 31st, 2014 is summarized in the first part of the report. The detailed description of main activities carried out in the individual groups is then provided in chapters 2 to 7. The topics are either predominantly "experimental" or predominantly "modelling" in their nature. However, most of the projects are multidisciplinary and require strong interactions between groups and individual group members from both experimental and modelling sides.

1.2 General

The next major milestone in Stage 2 of the Sectoral Plan for Deep Geological Disposal (SGT) will be the selection of at least two potential sites each for spent fuel and high-level (SF/HLW) and low- and intermediate-level (L/ILW) radioactive waste repositories. It was foreseen that Nagra proposes the regions and delivers necessary documentation by the end of 2014 - beginning 2015. The accompanying documentation will be reviewed by the regulatory bodies in 2015-2016. The Government decision on Stage 2 is expected in 2017.

During 2014, LES has continued its strong involvement in the preparation of the numerous databases and scientific reports required in Stage 2 of SGT for the Provisional Safety Analyses (PSAs). As stated in the last annual report, the scope and content of this work has continued to evolve and increase over time resulting in requirements for more comprehensive and detailed documentation. The reports underwent a number of internal and external reviews, and were presented at several technical panels. Despite the tight schedule and increasing complexity the requested reports were delivered in time. Thus, the most important milestone for 2014 has been successfully reached.

LES continues participating in the 7th EU Framework Program: "*Carbon-14 Source Term*", (CAST).

Two other projects with LES participation in the 7th EU Framework Program: "*Processes of Cation Diffusion in Clay Rocks*", (*CatClay*) and "*FIRST-Nuclides*" have finished in May 2014 and December 2014, respectively.

The joint research program with the KFKI Atomic Energy Research Institute in connection with the "Schweizer Erweiterungsbeitrag DEZA/SECO" has

been extended by 6 months and has finished in September 2014.

The main multi- and bi-lateral co-operations with external institutions and universities are summarized in Table 1.1.

Table 1.1: National and international co-operations.

Co-operations
<p>Nagra Major financial contribution Various technical working groups</p>
<p>Multinational 7th EU FP (CatClay, CAST, FIRST-Nuclides) Mont Terri Project (Diffusion retardation, Clay Cement Interaction) Grimsel Test Site (Colloid Formation Migration)</p>
<p>Universities Bern, Switzerland (mineralogy, petrography, water chemistry, C-14 AMS) Surrey, United Kingdom; EPFL, Switzerland (cement systems, molecular modelling) Strasbourg, France (glass) Tübingen, Germany (geosphere transport) ETH Zürich, Switzerland (GEMS) FHNW Muttensz, Switzerland (C-14 gas phase analytics)</p>
<p>Research Centres CEA*, France (near- and far-field) CIEMAT, Spain (colloids) EMPA*, Switzerland (cement) IRE, HZDR*, Germany (XAS, TRLFS) INE, KIT*, Germany (near- and far-field, TRLFS) SCK/CEN, Belgium (clays) UFZ*, Germany (reactive transport) *formal co-operation agreements</p>

Current PhD and postdoc projects being carried out in LES are listed below:

M. Bestel has defended her PhD thesis "*Water dynamics in compacted clay systems*" on May 6th at the University of Bern. The project was completed in four and a half years. The first 4 years were supported by SNF. The final half a year period was equally supported by the Laboratory for Neutron Scattering (PSI), LES and the Institute of Geological Sciences in the University of Bern (LES participation).

Y. Chen (PhD student): *"Retardation of low-molecular weight organic compounds in clays"*. Start date: March 2013 (Funding: Nagra/PSI).

E. L'Hopital has defended her PhD thesis: *"Aluminium and alkali uptake in calcium silicate hydrates (C-S-H)"* on 2nd October 2014 at EPFL. The thesis was funded by SNF-Sinergia collaborative project "CASH", between EMPA-EPFL-ICB-Dijon and PSI (main host EMPA, LES participation).

J. Poonosamy (PhD student): *"Experimental benchmarks for verification and validation of reactive transport codes"*. Start date: October 2012 (Funding: Nagra/PSI).

A. Shafizadeh (PhD student): *"Porosity and structural changes at clay-cement interfaces and their relations to transport properties"*. Start date: September 2012 (Funding: Nagra/PSI, CROSS proposal in collaboration with the Neutron Activation and Imaging Group (NUM)).

D. Soltermann has successfully defended her PhD thesis *"Ferrous iron uptake mechanisms at the montmorillonite-water interface under anoxic and electrochemically reduced conditions"* and received the Doctoral Degree in natural sciences at the ETHZ on July 10th, 2014. The project was completed in 4 years and was funded by SNF.

C. Wigger (PhD student): *"Anion accessibility in low porosity argillaceous rocks"* Start date: February 2014 (Funding: NWMO/PSI)

Dr. A. Leal (postdoc): *"Development of robust and efficient computational methods for geochemical modelling and application of finite element methods for reactive transport modelling"*. Start date: September 2014 (Funding: Nagra).

Dr. B. Thien (postdoc): *"Combined hydrological, geochemical and geophysical modelling of geothermal systems"*. Start date: February 2013 (Funding: SNF Sinergia project COTHERM).

Dr. B. Cvetković (postdoc): *"Development of C-14 AMS-based analytical methods for the identification and quantification of C-14 labeled dissolved and volatile organic compounds"*. Start date: November 2013 (Funding: Swissnuclear).

Within an international project on *"Water transport in cements: A bottom-up approach based on NMR relaxation and imaging analysis and numerical modelling"*. 1 PhD and 1 postdoc are jointly supervised by Physics Dep., Uni. Surrey, UK and LES. The project coordinator is Prof. P. McDonald, Uni. Surrey, UK.

Dr. M. del Henar Rojo-Sanz (guest scientist): *"The fate of selenium and technetium in a cementitious repository near field under reducing conditions"*. Start date: November 2012 (Funding: Verbundprojekt Immorad "Grundlegende Untersuchungen zur Immobilisierung langlebiger Radionuklide durch die Wechselwirkung mit endlagerrelevanten Sekundärphasen". Bundesministerium für Bildung und Forschung, Germany).

Dr. L. Pegado (guest scientist): On 31 October 2013 the SNF-Sinergia project has finished. However, as part of a follow up EPFL-PSI project *"A thermodynamic model for C-S-H/C-A-S-H from a bottom up approach"*, Dr. Pegado works at LES approximately one working day per week till December 2015. The project is funded by Nanocem consortium.

A PhD project *"Detailed understanding of metal adsorption on clay minerals obtained by combining atomistic simulations and X-ray absorption spectroscopy"* was approved by SNF. The project is aimed at explaining the retention mechanism of cations on clay minerals at an atomistic scale by combining molecular simulations and spectroscopic measurements.

During 2014 members of LES participated in a number of international technical review groups: (i) SARG (SFR extension, Application Review Group), SKB, Sweden (ii) Expert Panel on "Radionuclide Migration in Plastic Clay", Ondraf/Niras and SCK-CEN, Belgium. (iii) Review panel of the Belgian program on the behaviour of spent fuel in a cementitious environment, Ondraf/Niras, Belgium.

LES co-organized the 7th Actinide XAS workshop (AnXAS 2014) held from 20th to the 22nd of May 2014 at Schloss Böttstein. The workshop was attended by more than 60 participants. Contributions presented at the workshop covered topics of Actinides, Actinides in Environmental and Life Sciences, Solid State Chemistry and Physics of the Actinides, Theoretical and Modelling Tools, Facility Reports and Upcoming Techniques.

Several personnel changes took place in the reporting year. Dr. M. Bradbury, the former Laboratory Head of LES has retired in December 2013. Because of his strong involvement in the key reports for Stage 2 of the SGT, an arrangement was met to continue Bradbury's employment with 20 % occupation.

Dr. A. Jakob, former member of the Transport Mechanisms group, retired in February 2014.

Prof. S. Churakov has taken the Laboratory Head position on January 1st, 2014.

Dr. N. Prasianakis has taken the vacant Group Leader position in the Transport Mechanisms group on October 1st, 2014. He has a strong background in the Lattice Boltzmann based simulation techniques and will strengthen multi-scale modelling activities in the group.

On March 11-12, 2014, the Waste Management Program Committee met for their annual meeting. The work performed within LES and the future plans were appraised and acknowledged. Refocusing of the research activities at LES according to the needs in Stage 3 of the SGT and the General License Application as well as personnel management and know-how transfer were discussed in detail. The valuable help and advice received from the members of the committee, both at the meeting and throughout the year, are appreciated by the whole Laboratory.

1.3 Sectoral Plan for Deep Geological Disposal

Finalization of datasets and documentation for Stage 2 of the SGT and the PSAs has been the major activities in 2014. The finalized Sorption Data Bases (SDBs) for the PSAs covers all potential host rocks (Opalinus Clay, 'Brauner Dogger', Effingen Member, Helvetic Marl), underlying confining units, and MX-80 bentonite. In addition, scenarios taking into account the influence of a high pH plume on the SDBs for host rocks were included in the documentation.

To validate the methodology used for the development of the SDBs, sorption isotherms were measured on Opalinus Clay, 'Brauner Dogger' Effingen Member and Helvetic Marl. The experimental results were compared to blind predictions calculated using the same methodology developed to derive the sorption values given in the SDBs. The results of the comparisons were very satisfactory.

The reports on the maximum radionuclide solubilities in the near field were essentially finalized in 2013. Only minor revision was requested and was implemented accordingly.

It is currently assumed in PSAs that all materials (waste, backfill, container, etc.) inside the caverns of L/ILW cement-based deep geological repositories are homogeneously distributed, and the whole repository can be treated in a "mixing-tank" approach. The consequence of this is that all radionuclides are distributed homogeneously in the cementitious near field after about 50 years. To assess the plausibility of the "mixing-tank" assumption the reactivity of the heterogeneous waste inside waste packages was evaluated. The waste sorts selected for the study are considered to be representative of important waste

packages to be emplaced in the L/ILW caverns. The chemical processes considered are: i) metal corrosion due to the presence of steel, ii) degradation of organic waste materials present in the waste and/or used as embedding matrix (e.g. bitumen), and iii) dissolution of gravel used for waste conditioning. The results show that the amount of water limits the reactivity of the materials in the waste packages.

An update of the Nagra/PSI Chemical Thermodynamic Data Base 01/01 was started in 2008. The revised database and the comprehensive documentation (PSI/Nagra TDB 12/07) have been completed. The electronic versions of the database are released for GEMS-PSI and PHREEQC chemical speciation software.

Formation of aqueous metal-silicate complexes may influence the solubility of several safety relevant radionuclides. The thermodynamic data for the silicon compounds and complexes have been subjected to an intensive in-house review and were included in the final update of the PSI/Nagra TDB 12/07.

A number of chemical elements have no safety relevant radioactive isotopes but may be relevant from a chemotoxic point of view. However, due to their chemical properties these elements may directly influence the dosis calculation in safety analyses studies due to sorption competition with radionuclides. Thus, solubilities of Cr, Mn, Cu, Zn were estimated in cement environments. The solubility of Cd was estimated in both cement and clay environments.

Available and new experimental data were used to formulate and confirm the extended Archie's relation ("e-Archie") for estimating effective diffusion coefficients of water and ions based on the accessible porosities. In the case of Na, surface diffusion had to be considered in order to explain the observed results. The effective diffusion coefficient estimated by earlier derived Archie's expression had to be corrected according to the in-house developed model for surface diffusion.

Reactive transport simulations, conducted with the coupled code OpenGeoSys-GEM, were focused on the studies of mineralogy and porosity evolutions in the Engineered Gas Transport System (EGTS) with different design of the transition layers between the cavern backfill (concrete) and the tunnel backfill (sand-bentonite mixture) taking into account the influence of the degree of saturation. The results of the study were summarized as a report.

1.4 Repository near field

1.4.1 Repository chemistry

The European collaborative project "*FIRST-Nuclides*" aims at understanding and quantifying the early release of radionuclides from Spent Fuel (SF) subject to aqueous corrosion in a geological repository, the so-called Instant Release Fraction (IRF). LES participated in setting up leaching experiments on high-burnup SF and cladding samples from the Gösgen and Leibstadt nuclear power plants in the HOTLAB at PSI.

Further, LES coordinated the study on the chemical state and spatial distribution of fission products in SF using micro X-ray absorption/fluorescence spectroscopy. EXAFS spectra of two SF micro samples from the Swedish Oskarshamn-3 boiling water reactor, prepared as polished chips using Focused Ion Beam (FIB) milling were measured at the microXAS beamline of the Swiss Light Source (SLS). The comparison of the spectra obtained on spent fuel samples with those of Se reference compounds having different oxidation states (-II, -I, 0, IV and VI) suggests that selenium may occur in the fuel as Se(-II) (selenide). The spent fuel XANES spectra could however be also reconstructed through linear combinations fits of the reference compounds for Se(0) and Se(IV). The currently available XANES data are thus not conclusive and suggest that Se may occur in the studied SF either as a mixture of Se(0) and Se(IV) or entirely as Se(-II).

Thermodynamic calculations in C-H-O systems revealed that, in case of complete thermodynamic equilibrium, the predominant carbon bearing species are $\text{CO}_{2(g)}$, HCO_3^- , CO_3^{2-} , and $\text{CH}_{4(g)}$. However, complete thermodynamic equilibrium is rarely achieved in the C-H-O system at moderate temperatures. The kind of organic compounds that might persist in the repository at partial thermodynamic equilibria is not known. To this aim, the stability of acetic acid and formic acid under hyper-alkaline anoxic conditions were studied. The experiments started in 2013, and were repeated in 2014 to test the reproducibility of the experiments. In addition a blank experiment was set up in which an oxygen-free, portlandite-saturated solution without Na-acetate was sampled up to 150 days to determine possible sources of organics from the Teflon liner and the synthetic fittings in the high pressure autoclave.

A significant concentration of ethene was detected in the gas phase of the blank experiment whereas the concentrations of all other gaseous organic compounds were below the GC-MS detection limit.

The experiment with acetate confirmed the presence of increasing concentrations of ethene as in the blank experiments, but in addition an increasing concentration of butane was observed at very low levels. The reaction leading to the formation of butane in the gas phase is still unknown and need to be further investigated.

Within the COTHERM project (SNF-Sinergia program) the mineralogical and porosity evolution of an Icelandic hydrothermal systems are being modelled using a reactive transport model. The results indicate that the initial porosity is the key factor controlling the evolution of the hydrothermal system. Good agreement between the simulations and the field observations increase our confidence in the thermodynamic databases and simulation tools used in the repository related simulations.

Further development of the geochemical modelling tool GEMS has continued. Through a collaborative project with ETH Zürich substantial improvement of the GEMSFITS module took place. This module is heavily used for the evaluation of in-house experimental data and is essential for the development of multicomponent solid solution models for cement and clay minerals. A postdoc project aimed at improving stability and efficiency of the GEMS numerical kernel and its coupling to the transport codes started in September 2014. The development will lead to an increased performance of the coupled reactive transport simulations with OpenGeoSys-GEMS and will allow modelling of in situ conditions for complex (heterogeneous) repository near fields.

1.4.2 Clay systems

A 4 years collaborative project between LES and the Hungarian Academy of Sciences Centre for Energy Research (Budapest) entitled "*Development of a macro- and microscopic approach to investigate the geochemistry of radioactive waste disposal systems*" has finished on 14 September 2014. The project was funded by "Schweizer Erweiterungsbeitrag DEZA/SECO". In this project the "bottom up" approach, used for the development of SBDs for PSAs, was tested using two very different argillaceous rocks namely Boda Clay, an iron rich fresh water sediment, and Opalinus Clay, a carbonate rich sea water sediment. Sorption isotherms were measured at pH of rock's porewater and the blind predictions of sorption isotherms were made based on the 2SPNE SC/CE model. The sorption isotherms could be predicted better than one log unit over the whole range of concentrations studied. This is a very striking agreement, taking into account the large difference in the mineralogy and the porewater

chemistry of the rocks. Contrary to the expectations, other minerals present in Boda Clay, such as zeolites and iron oxides, apparently do not contribute to the uptake of the studied elements.

The PhD project entitled "The influence of Fe(II) on clay properties, the sorption of Fe(II) on clays and competitive sorption investigations: a combined macroscopic and microscopic study" (SNF Grant 200021-129947) focused on the understanding the Fe(II) uptake by natural iron bearing clay minerals employing wet chemistry studies and spectroscopic investigations. Sorption edges and isotherms were measured under anoxic conditions on a synthetic iron free montmorillonite and three natural Fe-bearing smectites having different structural Fe contents. The batch experiments clearly indicate that the uptake of Fe(II) on the Fe(III)-rich montmorillonite is much more pronounced than on the low Fe-bearing and iron-free clays. Mössbauer spectroscopy analysis revealed that on Fe(III)-rich clay Fe(II) oxidizes and sorbs as an Fe(III) surface-bound complex. In addition, the formation of secondary Fe(III) precipitates was observed at higher Fe(II) equilibrium concentrations.

Thus, the sorption of Fe(II) on Fe poor clay can be well described with the conventional 2SPNE SC/CE sorption model. In contrary, for the sorption modelling on Fe rich montmorillonite oxidation of aqueous Fe(II) at the surface has to be considered. The sorption experiments were also conducted under electrochemically reducing conditions ($E_h = -0.640$ V). The results of these measurements were in agreement with the model prediction and thus validated the extended sorption model for Fe(II) over a wide range of redox conditions (-0.64 V $\leq E_h \leq +0.28$ V) and Fe(II) equilibrium concentrations.

At typical near field conditions ($E_h < -0.20$ V at pH 7.8), the porewater contains relatively high Fe(II) concentrations, ca. 10^{-5} M (saturation with siderite). The sorption model predicted that the iron will sorb predominantly as Fe(II) and therefore competitive sorption with divalent radionuclides in the radioactive waste repository is to be expected.

1.4.3 Cement

Sorption data for actinides are often difficult to determine due to the high dose rates of some actinides (e.g. Pu) or the limited stability of relevant redox states (e.g. U(IV)). Therefore, chemical analogy of the radionuclides with the same redox state was checked by comparing the sorption behaviour of several lanthanides and actinides in different redox states on C-S-H phases, which are the main component of hardened cement paste. Uptake

of Eu(III), Cm(III), Th(IV), Np(IV,V,VI), and U(VI) by C-S-H phases with C:S ratios between 1.07 and 1.2 in artificial cement water was determined. In the case of the trivalent and tetravalent actinides and lanthanides, the R_d values were found to be constant, hence independent of the aqueous concentration of the actinides (linear sorption). The R_d values determined for Eu(III) and Cm(III), as well as for Th(IV) and Np(IV) are identical which supports the assumption that radionuclides with the same redox state show the same sorption behaviour.

In the case of the pentavalent and hexavalent actinides, the R_d values significantly decrease with increasing aqueous concentration (non-linear sorption) indicating that the affinity to the C-S-H phases for these actinides decreases with increasing occupation of sorption sites. In addition, the R_d values for Np(VI) were found to be considerably lower than those for U(VI). The difference in the absolute sorption values of Np(VI) and U(VI) uptake by C-S-H phases can be explained by the difference in the stepwise hydrolysis constants of the dominant aqueous species, whereas the sorption mechanism was shown to be the same. Thus, the chemical analogy can also be applied in the case of hexavalent actinides by C-S-H phases giving a proper account to the hydrolysis constants of the aqueous species.

⁷⁹Se is an important redox-sensitive, dose-determining radionuclide in an L/ILW repository. Although Se(-II) is the dominant species under reducing conditions its uptake by cement phases is poorly known. In 2014, kinetics of the Se(-II) uptake by cement phases, i.e. C-S-H phases with different C:S ratios, monocarbonate (AFm-CO₃) and hemicarbonate (AFm-OH-CO₃) has been studied within the "Immorad" project. The ⁷⁵Se uptake by all the investigated cement phases was found to be fast. The higher R_d values determined for AFm-OH-CO₃ compared to AFm-CO could indicate Se(-II) uptake into the interlayer of the former AFm phase.

In a joint project between EPFL, the University of Bourgogne (Dijon) and LES, multi scale molecular simulations were applied to investigate ion sorption by cement phases. This project was initially funded by the "SNF-Sinergia program" and is further funded by the NANOCEM consortium. In the developed multi scale simulation strategy, the quantum mechanical calculations are used to calculate intrinsic protolysis constants of the OH-sites at the surface of C-S-H. These data provide a basis for titration modelling of C-S-H in various electrolyte solutions and are used to predict ion sorption isotherms at different pH. A good agreement between the simulation results, which were obtained without fitting to experimental data, and earlier laboratory

measurements was obtained.

1.4.4 Interfacial processes

The anaerobic corrosion of steel in a cementitious near field can potentially produce ^{14}C containing low molecular weight (LMW) organic compounds which could be major contributors to the dose released from a L/ILW repository. A number of activities are ongoing with an aim to quantify the processes relevant to ^{14}C release. These include various batch-type experiments with non-irradiated steel and the development of the measurements protocols for ^{14}C quantification.

Within the ^{14}C project, financed by Swissnuclear and by the 7th EU framework project "CAST", the series of batch-type experiments with non-irradiated steel powders was brought to an end. These experiments were necessary to calibrate the equipment and set-up prior to the active measurements and to characterize the organic species released during the corrosion process. The organic compounds were identified and quantified applying gas chromatography (GC) coupled with mass spectrometry (MS) for volatile species and high performance ion exclusion chromatography (HPIEC) coupled with MS for aqueous LMW organics, respectively. The gas phase analysis protocol was developed in collaboration with the Institute for Chemistry and Bioanalytics at the University of Applied Sciences Northwestern Switzerland (ICB/FHNW). The organic compounds detected in the experiments agree well with literature data. Nevertheless, some compounds, such as butylene, pentene, propanoate and butanoate could not be observed. The formation of small amounts of carbonate could not be checked due to the presence of carbonate in the neutral and alkaline solutions.

The time-dependent corrosion experiments with iron powders were carried out in 2014 with the aim of identifying the process responsible for two stage corrosion kinetics, namely the fast release of various organic compounds in the initial stage of the experiments (i.e. volatile and dissolved) and slow release of gaseous compounds in long runs. A large difference in the concentrations of organic compounds determined in the experiments with pre-treated and untreated iron powders was observed. Further investigations suggest that the dissolved hydrocarbons are generated due to oxidizing conditions during pre-treatment of the iron powder. Nevertheless, the reducing hyper-alkaline conditions prevail in the repository in the long term, which suggests a very slow release of predominantly reduced (gaseous) hydrocarbons.

The development of the experimental set-up for the

corrosion experiment with irradiated steel was continued. The overpressure reactor for the long-term corrosion experiment with the activated steel is currently being developed. The reactor is designed in such a way that all manipulations necessary for regular sampling can be carried out without removing the lead shielding to minimize exposure of the experimentalist to radiation. The lead shielding has to be opened only during the transfer of the activated steel. The construction of the reactor will be finished by the end of 2014 and the testing phase with non-activated steel will take place in 2015.

First steps towards the development of the compound-specific ^{14}C AMS technique required to detect ^{14}C bearing compounds at very low concentrations have been undertaken. To this aim, the standard separation techniques (GC, HPIEC) were coupled to the ^{14}C AMS detection system. After the chromatographic separation of the different species, they have to be collected in separate fractions and oxidized to CO_2 . The $^{14}\text{CO}_2$ in each fraction is then measured by AMS. The ^{14}C AMS measurements will be carried out using the MICADAS (Mini Carbon Dating System) at the Laboratory for Environmental and Radiochemistry at the University of Bern, Switzerland. Based on the available data for the corrosion rate, the surface area and the activity of the irradiated steel, the amount of ^{14}C to be released in the leaching experiment were estimated. The calculations confirm the feasibility of ^{14}C measurements using the proposed protocol for the planned corrosion experiment with irradiated steel.

In the current repository design cement materials can come into contact with clay rich host rocks and/or bentonite backfill. The effect of the cement-clay interaction is adverse. It may lead to a simultaneous decrease of the porosity in the clay compartment due to mineral precipitation and an increase of the porosity in the cement compartment due to dissolution. These processes are investigated experimentally at laboratory scale within a PhD project on "*Cement-Clay Interaction*".

Several samples of cement-clay interfaces with reaction time up to one year have become available. Transport properties of the reacted interface were estimated based on conventional diffusion-through experiments with tritiated water (HTO), and using *in situ* measurements of heavy water (D_2O) profiles obtained from radiography measurements with cold neutrons at the ICON facility at the SINQ PSI. The measurements suggest slowdown of mass transport through the cement-clay interface in aged samples.

Modelling of humidity transport and consumption of water in waste packages which is tightly coupled not

only to liquid saturation, but also to several geochemical processes (metal corrosion, carbonation, internal degradation, degradation of organic wastes) have been conducted. This work benefited strongly from our collaboration with the Helmholtz Centre for Environmental Research (UFZ, Leipzig, Germany) on the further development of the OpenGeoSys-GEM coupling.

1.5 Repository far field

The EU project "CatClay" was finished by May 31st. In this project a comprehensive set of diffusion measurements in compacted illite was conducted for $^{85}\text{Sr}^{2+}$, $^{60}\text{Co}^{2+}$ and $^{65}\text{Zn}^{2+}$ in a wide range of pH conditions and background electrolyte concentrations. One of the main objectives followed in the CatClay project was to compile sets of experimental diffusion data, by which the validity of the various models for cation diffusion can be tested. Particular focus was set on the study of surface complexing ions. Initially, the effective diffusion coefficients were derived from the measured steady state fluxes using the concentration gradient in aqueous phase. The obtained values of the diffusion coefficients (larger than the D_e of water) suggest that the mobility of the adsorbed species (interlayer and/or diffuse double layer) and their concentration gradients have to be taken into account. Still, none of the tested models, including the ones taking the surface diffusion into account, were able to describe all available datasets consistently.

Series of diffusion experiments in montmorillonite pre-treated with EDTA were conducted with $^{85}\text{Sr}^{2+}$ in order to investigate the effect of speciation on the diffusion. The results can be interpreted qualitatively in the sense that the diffusion of EDTA and $^{85}\text{Sr}^{2+}$ occurs independently and most probably in different pore types. The larger effective diffusion coefficients of Sr compared to those of EDTA indicate that an equilibrium fraction of $^{85}\text{Sr}^{2+}$ may be present in the interlayers of montmorillonite, while the EDTA molecule is excluded from this porosity.

Small organic molecules released by corrosion of the activated steel are potential carriers of ^{14}C . Their diffusion and retardation have been studied in advective flow column experiments. The experiments with ^{14}C labelled Na-acetate, Na-propanoate, Na-2-hydroxypropanoate, Na-3-hydroxypropanoate, Na-D-gluconate in compacted illite have been conducted so far. Mass balance calculations showed that all compounds were almost completely recovered in the effluents except acetate, gluconate and 3-hydroxypropanoate. The strong sorption of lactate and gluconate was observed which might be caused by the interaction of hydroxyl group in the alpha

position with the mineral surface. This will be verified by studying the retention behaviour of butanoate and 2-hydroxybutanoate. Further experiments with compacted kaolinite and Opalinus Clay are planned.

The DR-A field experiment in the Mont Terri Underground Rock Laboratory aims at investigating the effects of high ionic strength perturbations on retention and transport at a field scale. The samples of overcored Opalinus Clay were collected and the radial profiles of HTO, ^{60}Co , Cl, I, Br and main cations (Na, K, Ca, Mg) were measured. The preliminary data compilation indicates that the concentration profiles of the HTO, ^{60}Co , Cl, I, Br and of the main ions per bulk mass of rock generally follow the expected trends. However, some deviations occur which can be explained by disturbances during the overcoring.

Many laboratory and field experiments can be conceptualized in 1D geometry applying a radial symmetry. A new random walk algorithm for transport simulation in radial geometry has been successfully tested and implemented in the in-house code MCOTAC. The code was applied to re-interpret older diffusion experiment using a fully coupled sorption competition set-up. Thanks to these new capabilities, the models available in MCOTAC can now be applied to simulate the DR-A experiment.

Uncertainties in the values of surface complexation constants of cations on mineral surfaces, estimated based on Linear Free Energy Relationships (LFER), are of the order of ± 1.0 log unit. The effect of these uncertainties on the migration of radionuclides was analyzed using reactive transport simulations. The calculated variations of Ni(II) breakthrough times in a bentonite backfill comprise several hundreds of years, which is apparently not of high significance compared to uncertainties of other processes. The effect of sorption competition phenomena (e.g. interaction with background Fe concentration) turned out to be more important.

Cation and anion accessible porosity in potential host rocks and bentonite has been investigated in cooperation with the Nuclear Waste Management Organisation, Canada (NWMO) and the University of Bern using different experimental techniques such as mercury intrusion, N_2 , H_2O and CO_2 adsorption, NMR spectroscopy and cryoporometry. The goal of the project is to understand the interplay between the anion accessible porosity and mineralogy, specific surface area and pore size distribution in the potential host rocks.

Macroscopic diffusion coefficients measured at laboratory and field scales depend on structural

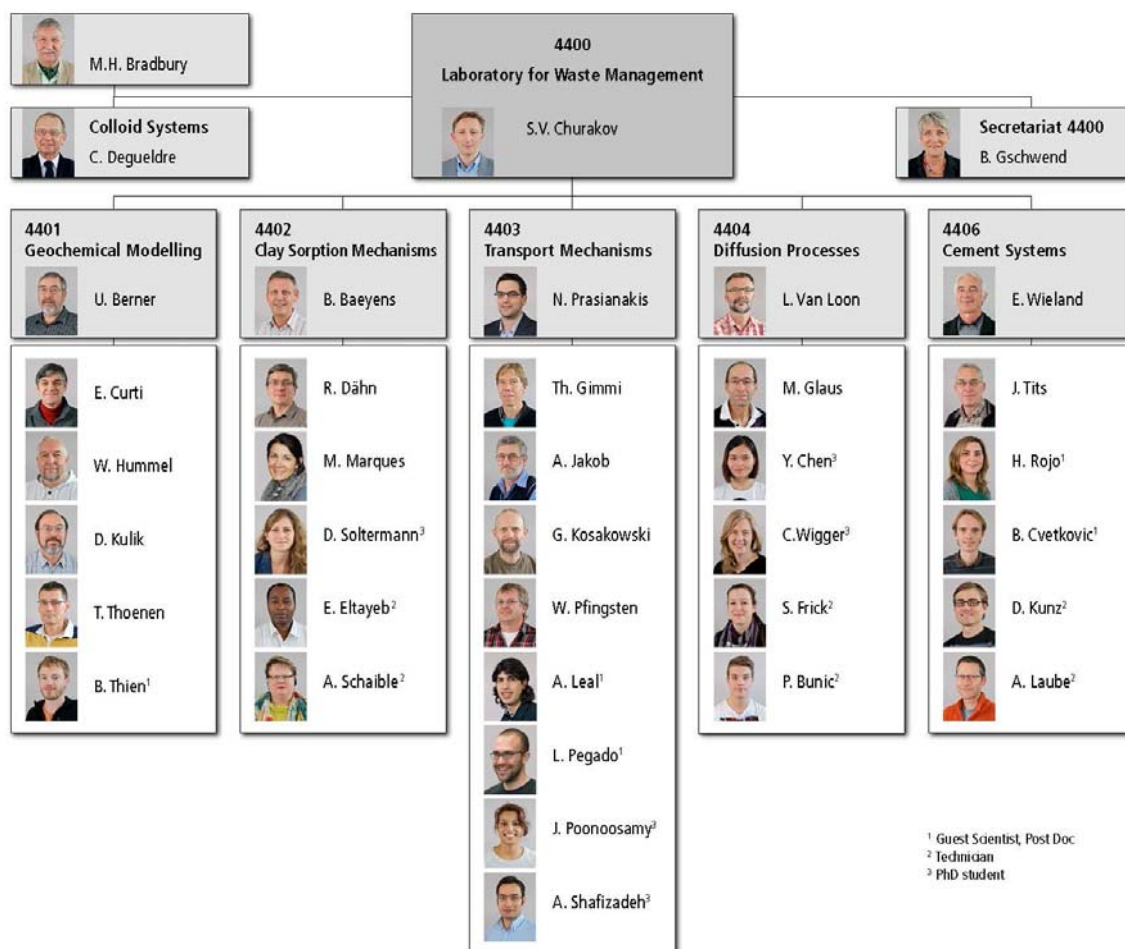
properties of the pore network and ion-/water-surface interactions. Influence of pore size, and clay particle orientation distributions were studied using molecular simulations, pore scale modelling and quasi-elastic neutron scattering. Combining simulations and experiments, it was possible to explain the nature of scale and time dependent water mobility measured by quasi-elastic scattering experiments in clays. The developed modelling approach provides a potential basis for upscaling molecular diffusion processes of water and ions from pore to laboratory and field scales.

The benchmarking of transport codes against experimental data is necessary to support the credibility of numerical simulations. In this context, the evolution of porosity in natural and artificial media, and the associated changes in transport parameters, is of major interest for many natural and engineered systems. In the framework of a PhD project supported by Nagra, a 2D reactive transport experiment has been set up, in which the changes in transport properties of the media were induced by

dissolution of strontium and precipitation of barium sulfate. This dissolution-precipitation reaction leads to porosity decrease at the reaction front and consequent changes in the flow field of the adjectively injected fluid. This experiment was successfully modelled with the OpenGeoSys-GEM coupled code.

LES further participates in the "Colloid Formation and Migration (CFM)" project conducted at the Grimsel Test Site, in the framework of Phase VI of the research program, which was extended and shall continue through 2016-2018. Currently, the work was focused on the long-term in-situ test, which includes installation of a doped clay source to monitor the generated/eroded colloids in the surrounding groundwater. Offsite colloid measurements were conducted at PSI using a single-particle counter (SPC). The colloid concentrations are also measured in the field using a mobile laser-induced breakdown detection (LIBD). The general trends in the LIBD and SPC data are in good agreement.

LES Organigram 2014



¹ Guest Scientist, Post Doc
² Technician
³ PhD student

2 GEOCHEMICAL MODELLING

U. Berner, E. Curti, D. Kulik, W. Hummel, T. Thoenen, B. Thien (post doc)

2.1 Overview

In 2014, as was already the case in precedent years, a substantial part of the Geochemical modelling group's work was dedicated to the ongoing work for the Swiss Sectoral Plan for Deep Geological Disposal. At this final stage of the second phase of the Sectoral Plan work of several co-workers concentrated on finalizing the reports and on revising the reports according to comments of external reviewers. Some reports were presented to the regulatory bodies and related committees in form of oral presentations. In several cases requests from Nagra led to short notice studies on Sectoral Plan related additional work.

The research topic conducted by group members in 2014 includes studies of early release of nuclides from spent fuel matrices, recent developments in solid solution aqueous solution equilibria for cement phases, critical assessment of thermodynamic properties and solubility of selected safety relevant nuclides and benchmarking of geochemical models by simulations of water-rock interactions in hydrothermal systems.

2.2 Activities in support of the Sectoral Plan

2.2.1 PSI/Nagra Chemical Thermodynamic Database 12/07

The update of the Nagra/PSI Chemical Thermodynamic Database 01/01 (Nagra/PSI TDB 01/01, HUMMEL et al. 2002) to the PSI/Nagra Chemical Thermodynamic Database 12/07 (PSI/Nagra TDB 12/07) has finally been completed with accomplishment of the comprehensive documentation. The update was started in 2008 to support the safety assessments for Stages 1 and 2 of the SGT and data selection was completed in 2009 with the release of the electronic versions for GEMS-PSI and PHRREQC.

The present update is mainly based on the OECD NEA's book series on Chemical Thermodynamics and the volumes concerning Ni (GAMSJÄGER et al. 2005), Se (OLIN et al. 2005), Zr (BROWN et al. 2005), Th (RAND et al. 2008), and the update of the previous volumes on U, Np, Pu, Am and Tc (GUILLAUMONT et al. 2003) have all been considered. In addition, thermochemical data for silicon compounds and complexes have been the subject of an extensive in-house review (see below). All other data contained in the Nagra/PSI TDB 01/01 have been accepted

without any change. Thus, all data concerning Al, Eu, Pd and Sn that were the subject of in-house reviews during the preparation of the Nagra/PSI TDB 01/01 remain unchanged.

During documentation, special emphasis was put on the SIT ion interaction coefficients, which were not explicitly included in the Nagra/PSI TDB 01/01. The entire documentation of the PSI/Nagra TDB 12/07 can be downloaded from <http://www.psi.ch/les/database> and the electronic version is distributed with the current version of GEMS3 (<http://gems.web.psi.ch>).

2.2.2 Critical assessment of silicate species

Within the scope of the update of the Nagra/PSI TDB 01/01 to the PSI/Nagra TDB 12/07 thermochemical data for silicon compounds and complexes have been the subjects of an extensive in-house review (HUMMEL 2014). A graphical summary of aqueous species finally included in the PSI/Nagra TDB 12/07 is shown in Table 2.1.

The monomeric aqueous silica species are well established and cover the entire pH range of interest for modelling in aquatic chemistry. The experimentally determined solubility of amorphous silica, $\text{SiO}_2(\text{am})$, can be reproduced sufficiently well up to pH 11.0 by including a single polymeric silica species, $\text{Si}_4\text{O}_8(\text{OH})_4^{4-}$, in the model (HUMMEL 2014).

Aqueous metal silicate complexes of the type $\text{MSiO}(\text{OH})_3^{(n-1)}$ are known for a number of metal cations M^{n+} (Table 2.1). However, most of them have been studied in acidic solutions at $\text{pH} < 5.0$ and their range of predominance generally is restricted to $\text{pH} < 7.0$.

Aqueous metal silicate complexes of the type $\text{MSiO}_2(\text{OH})_2^{(n-2)}$, predominating in the neutral pH range (5.0–9.0), have been reported for Ca^{2+} and Mg^{2+} (SANTSCHI & SCHINDLER 1974), and PuO_2^{2+} (YUSOV & FEDOSEEV 2003). However, the species $\text{PuO}_2\text{SiO}_2(\text{OH})_2(\text{aq})$, as well as $\text{NpO}_2\text{SiO}_2(\text{OH})_2(\text{aq})$ claimed to be found in alkaline solutions (pH 10.5–12.0) (SHILOV et al. 2004), are included as "placeholders" (supplemental data) only in our TDB as the reported evidence for their formation is contradictory and needs confirmation. The species $\text{Th}(\text{OH})_3(\text{SiO}(\text{OH})_3)_3^{2-}$ has been proposed (RAI et al. 2008) to interpret a solubility study of $\text{ThO}_2(\text{am})$ in alkaline silica solutions (pH 10.0 – 13.3). This species also needs confirmation

Table 2.1: Aqueous silica species and metal silicate complexes included in the PSI/Nagra TDB 12/07. The positions of the formulae indicate the pH range of their experimental determination and the green background their supposed predominance. Species with supplemental data are in italics, strikethrough indicates removal of the species from the TDB.

	acidic pH < 5	neutral 5 – 9	alkaline 9 – 13	hyperalkaline > 13
H ⁺	Si(OH) ₄ (aq)		SiO(OH) ₃ ⁻	SiO ₂ (OH) ₂ ²⁻
			Si ₄ O ₈ (OH) ₄ ⁴⁻	
Ca ²⁺	CaSiO(OH) ₃ ⁺	CaSiO ₂ (OH) ₂ (aq)		
Mg ²⁺	MgSiO(OH) ₃ ⁺	MgSiO ₂ (OH) ₂ (aq)		
Fe ²⁺				
Ni ²⁺	<i>NiSiO(OH)₃⁺</i>			
Al ³⁺	AlSiO(OH) ₃ ²⁺		Al(OH)₃SiO(OH)₃⁻	AlSiO ₃ (OH) ₄ ³⁻
Fe ³⁺	FeSiO(OH) ₃ ²⁺			
Eu ³⁺	EuSiO(OH) ₃ ²⁺			
Np ³⁺	<i>NpSiO(OH)₃²⁺</i>			
Pu ³⁺	<i>PuSiO(OH)₃²⁺</i>			
Am ³⁺	AmSiO(OH) ₃ ²⁺			
Cm ³⁺	CmSiO(OH) ₃ ²⁺			
Th ⁴⁺			<i>Th(OH)₃(SiO(OH)₃)₃²⁻</i>	
U ⁴⁺				
Np ⁴⁺	<i>NpSiO(OH)₃³⁺</i>			
Pu ⁴⁺	<i>PuSiO(OH)₃³⁺</i>			
NpO ₂ ⁺	<i>NpO₂SiO(OH)₃(aq)</i>			
PuO ₂ ⁺				
UO ₂ ²⁺	UO ₂ SiO(OH) ₃ ⁺			
NpO ₂ ²⁺	<i>NpO₂SiO(OH)₃⁺</i>		<i>NpO₂SiO₂(OH)₂(aq)</i>	
PuO ₂ ²⁺	<i>PuO₂SiO(OH)₃⁺</i>	<i>PuO₂SiO₂(OH)₂(aq)</i>		

The fate of the species Al(OH)₃SiO(OH)₃⁻ is a special case. The first study of aluminium silicate complexation by potentiometric titrations in the alkaline region, 9.0 < pH < 13.0, was mentioned by POKROVSKI et al. (1998). In this extended abstract the authors claimed to be able to interpret their (not yet published) experimental data in terms of formation of the species Al(OH)₃SiO(OH)₃⁻. Hence, we decided to include this complex in the previous version of our data base (Nagra/PSI TDB 01/01) as guidelines for modellers. To the best of our knowledge, the potentiometric data and their interpretation mentioned in the extended abstract (POKROVSKI et al. 1998) have never been published as a full paper.

In a later paper from the same group about a Raman spectroscopic study (GOUT et al. 2000), the authors never mention Al(OH)₃SiO(OH)₃⁻ explicitly, but in their section basic pH (≈ 12.5) they state that the complex SiAlO₃(OH)₄³⁻ (predominant at pH > 13.0) is minor in these solutions and, therefore, cannot

account for the observed amounts of complexes including Al and Si. Thus, the important quantities of complexed Al and Si at pH 12.5 must be due to the formation of other complexes, between SiO(OH)₃⁻ and SiO₂(OH)₂²⁻ and Al(OH)₄⁻. However, it was impossible to derive the stoichiometry and charge of these complexes from our measurements, because the amounts of complexed and free Al and Si do not show any regular dependence on component concentrations. This strongly suggests the formation of several, likely polymerized, Al – Si species. In this statement they implicitly retract the complex Al(OH)₃SiO(OH)₃⁻ and its associated stability constant published in their extended abstract (POKROVSKI et al. 1998). Consequently, we removed this complex and its stability constant from our data base. Presently, no other complexes are known that could replace this complex.

In summary, the complex AlSiO(OH)₃²⁺ is fairly well established in acidic solutions, but as it predominates

at pH < 5.0 it is of little importance for groundwater modelling. The complex $\text{SiAlO}_3(\text{OH})_4^{3-}$ was identified in "ultra-basic solutions" at pH about 14.0 (GOUT et al. 2000); it may hardly be of any importance in environmental modelling. In neutral to basic solutions there is qualitative evidence of polynuclear Al – Si complexes but no quantitative data are available.

2.2.3 Solubility of chemotoxic elements

There are several elements which have no safety relevant radioactive isotopes, but may have important consequences when considering chemotoxic aspects of repositories for radioactive wastes. Such elements were not considered in the corresponding "solubility"

reports for stage 2 of the SGT (BERNER 2014a, 2014b), but can also become relevant for the safety assessment due to sorption competition with radionuclides. Based on the calculated reference porewater characteristics provided in BERNER (2013) the solubility of chromium, manganese, copper, zinc and cadmium was estimated in cement environments (high pH) and in clay environments (neutral pH) for cadmium. Missing thermodynamic data were taken from KOZAWA et al. (1966) (Mn), POWELL et al. (2011) (Cd), COLÁS et al. (2007) (Cr, Zn). Thermodynamic data for Zn are sparse and were therefore estimated in analogy to Fe(II) from LEMIRE et al. (2013).

Table 2.2: Estimated solubilities for potentially chemotoxic elements in high pH environments and in clay environments (Cd).

Total element solubilities in [$\text{mol}\cdot\text{kg}^{-1}$]	Cr	Mn	Cu	Zn	Cd
Cementitious environment pH 12.5	$1.9\cdot 10^{-6}$	$6.1\cdot 10^{-5}$	$8.0\cdot 10^{-6}$	not limited	$2.0\cdot 10^{-6}$
Clay environment pH 7.3					$1.3\cdot 10^{-5}$

2.3 FIRST-Nuclides project

2.3.1 Introduction

This project was already announced in the last years report, but only very few data were reported. In the meantime, substantial progress was made and a summary of results is provided in this report.

The European collaborative project FIRST-Nuclides aims at understanding and quantifying the early release of radionuclides from Spent Fuel (SF) subject to aqueous corrosion in a geological repository, the so-called Instant Release Fraction (IRF). Two PSI laboratories (LES and Hot Laboratory) are involved in two major tasks of this project. The first task consists in the set-up and implementation of leaching experiments on high-burnup SF and cladding samples from the Gösgen and Leibstadt nuclear power plants, using a 19 mM NaCl - 1 mM NaHCO_3 (pH ~ 7.4) leaching solution, as agreed by all project partners.

The second task, for which LES has the leadership, deals with the chemical state and spatial distribution of fission products in SF using micro X-ray absorption/fluorescence spectroscopy. The focus is on ^{79}Se , a low fission yield but dose-determining nuclide in safety analyses of radioactive waste disposal sites. During reactor operation, Se fission products could migrate to grain boundaries and fuel/cladding gaps. After canister breaching and

water ingress in a geological repository, oxidizing conditions could be established at the fuel surface due to α -radiolysis of water. Under oxidizing conditions, selenium forms soluble, poorly adsorbed anionic species ($\text{Se}^{\text{IV}}\text{O}_3^{2-}$ and $\text{Se}^{\text{VI}}\text{O}_4^{2-}$), which can be readily mobilized in aqueous environments. In contrast, Se(0) and Se(-II) are sparingly soluble forms of selenium and are not expected to contribute significantly to the IRF. Previous leaching experiments on Leibstadt SF failed to reveal the presence of Se in the aqueous phase, in spite of several months leaching and quite sensitive analytical techniques (JOHNSON et al. 2012). Therefore, it is currently not clear whether ^{79}Se has to be considered as IRF contributor.

The main objective of the spectroscopic measurements carried out within FIRST-Nuclides is to determine the primary oxidation state and atomic-scale coordination of Se in selected non-leached UO_2 SF samples, in order to understand whether Se fission products would be mobilized or not by aqueous leaching. The results obtained on dispersed micro-particles of UO_2 SF from the Leibstadt boiling water reactor (burnup 79 GWd/tU) have been briefly documented in the annual report 2013.

Previous studies have shown that release of radionuclides from SF under geologic disposal conditions is controlled by two mechanisms: (a) the

rapid release of soluble fission products, mainly long-lived radioisotopes of Cs, I, Cl as well as ^{14}C , and (b) the release of actinides and fission products due to slow dissolution of the UO_2 matrix. In the long-term safety assessment terminology, the rapid release is often referred to as IRF and is thought to include contributions from the fuel/cladding gap and from soluble nuclides segregated at fuel grain boundaries accessible to water.

The IRF is a critical parameter in safety assessment, which however cannot be easily quantified due to the scarcity of experimental data. A main objective of FIRST-Nuclides is to fill this gap by providing new IRF data from high burnup UO_2 and MOX fuel irradiated in different Pressurized Water Reactor (PWR) or Boiling Water Reactor (BWR) reactors in Europe by means of aqueous leaching experiments. PSI selected a BWR fuel rod from the Leibstadt nuclear power plant (NPP) and a PWR fuel rod from the Gösigen NPP for investigations within this project.

At the time of this reporting, sampling and analyses

of leaching solutions are far from being complete. A detail reporting on the results of these experiments will therefore be provided in the next annual report.

Here, we report on the progress made in the evaluation of the aforementioned data, as well as on new measurements carried out this year on two SF micro samples from the Swedish Oskarshamn-3 boiling water reactor. These measurements were carried out at the microXAS beamline (SLS). In contrast to the Leibstadt SF, these samples were prepared as polished chips using Focussed Ion Beam (FIB) milling, which greatly improved the quality of the fluorescence signal and even allowed to record absorption spectra approaching Extended X-ray Absorption fine Structure (EXAFS) quality. One sample (CEN) was taken from the center of the pellet, whereas the second one (RIM) originates from the periphery of the same pellet and includes the outer pellet boundary (Fig. 2.1). Both samples were prepared at Studsvik Nuclear AB and shipped to PSI. Part of the transport costs were covered by a TALISMAN grant.

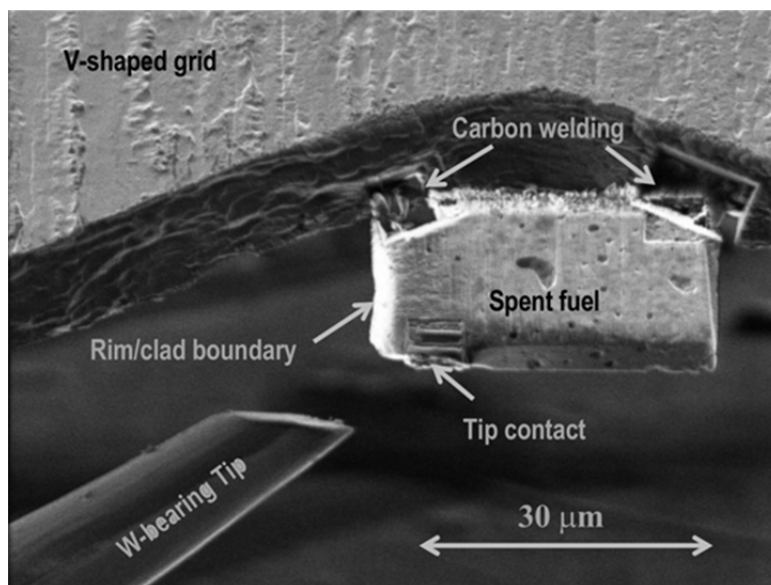


Fig. 2.1: FIB Sample (RIM) from the Oskarshamn-3 spent UO_2 fuel used for XANES measurements (courtesy Studsvik Nuclear AB).

2.3.2 X-ray spectroscopy

The comparison of the spectra obtained on spent fuel samples with those of Se reference compounds having different oxidation states (-II, -I, 0, IV and VI, see Fig. 2.2) suggests that selenium may occur in the fuel as Se(-II) (selenide). The similarity to the $\text{ZnSe}(-\text{II})$ and $\text{Na}_2\text{Se}(-\text{II})$ spectra is striking. However, Fig. 2.2 also suggests that the spent fuel X-ray Absorption Near Edge Spectroscopy (XANES) spectra could also be reconstructed through linear

combinations fits (LCF) of the Se(0) and Se(IV) O_2 reference spectra, whereas contributions from the $\text{Na}_2\text{Se}(\text{VI})\text{O}_4$ spectrum can be excluded. A quantitative LCF analysis confirmed this anticipation and acceptable best fits were obtained for about 50% - 50% combinations of the two components. The XANES data are thus not conclusive and suggest that the Se may occur in the studied SNF either as a mixture of Se(0) and Se(IV) or entirely as Se(-II).

However, the occurrence of two distinct Se species,

Se(0) and Se(IV), at almost constant ratio over the entire surface of six SF samples from two different reactors (Oskarshamn-3 and Leibstadt) would be an unlikely coincidence. The striking similarity of all recorded Se-K XANES spectra (a total of about 30 distinct locations of few μm^2 were probed on six different samples) rather points to a unique chemical state of Se, favouring the former interpretation.

Because of the very low yield of Se fission products in reactors operated with thermal neutrons, selenium is a trace component (about 100 ppm total Se) in SNF. Formation of a solid solution with UO_2 should therefore be considered. The existence of a large number of stable U(IV) selenide compounds such as USe_2 suggests that stable Se(-II) – U(IV) bonds may form in UO_2 SF via substitution of O(-II) or of interstitial sites by Se(-II).

In order to test this hypothesis, theoretical calculations of Se-K XANES absorption spectra have been carried out using the FDMNES code (JOLY 2001) with the support of the FitIt software (SMOLENTSEV & SOLDATOV 2007) which allows for geometrical optimization of the spectra. The results of the theoretical analysis are illustrated in Fig. 2.3, which shows the best fit of a single spectrum from Leibstadt SNF, and Fig. 2.4, which pictures the optimized Se-U-O cluster corresponding to the best fit. The fitted Se-U distance is close to those

determined by X-ray diffraction for USe_2 compounds. Attempts to fit the SNF XANES spectra assuming replacement of U(IV) by Se(IV) failed, due to the unavoidable absorption white line characterizing Se(IV) absorption at the K-edge. These results therefore provide a strong indication in favour of Se(-II) for O(-II) substitution in the UO_2 lattice.

The improved fluorescence intensity obtained from the FIB samples allowed us to record, at a particularly favourable location, an absorption spectrum over several hundred eV, allowing a two-shell EXAFS analysis up to $k \sim 6 \text{ \AA}^{-1}$. In spite of very high Debye-Waller factors (σ^2) indicating a large degree of structural disorder, the results (Table 2.3 and Fig. 2.4) are in fair agreement with the geometrical optimization of XANES spectra. The derived U-Se distances are identical within the uncertainties to those derived from the XANES fit and agree with crystal chemical data for uranium selenides.

In summary, the accumulated data converge in supporting the hypothesis that selenium is incorporated within the UO_2 structure in oxygen sites. In order to provide a final test for this hypothesis, it is foreseen to complete the measurements by recording XANES spectra of well-characterized uranium selenides.

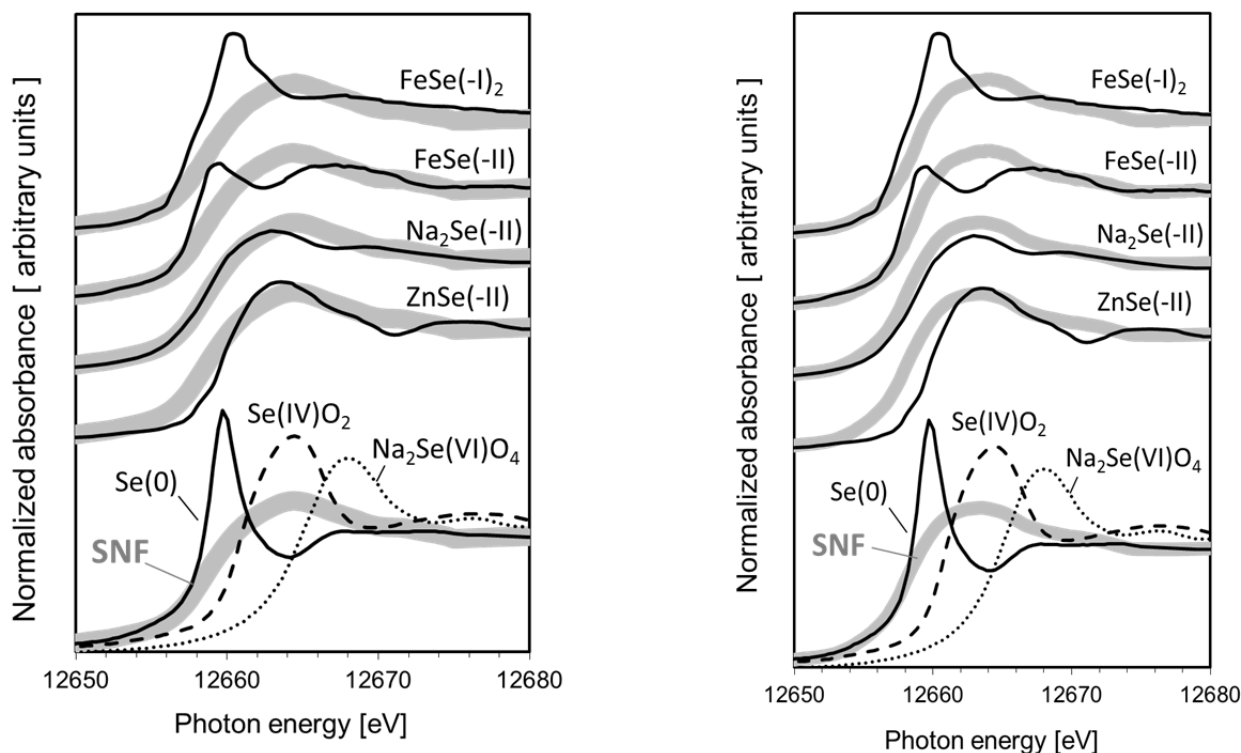


Fig. 2.2: Envelopes of Se K-edge μ -XANES obtained from all spectra collected on Leibstadt (left) and on Oskarshamn-3 (right) samples (SF, grey bands) compared with the spectra of reference compounds (black lines). The SF spectra envelopes are repeated for clarity in the stacked plot.

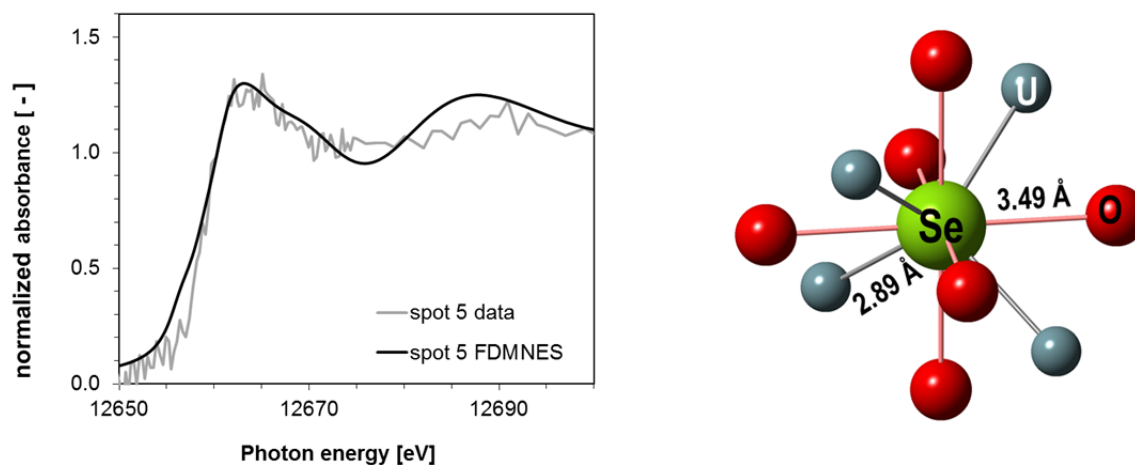


Fig. 2.3: Fit of an experimental Se K-edge micro-XANES spectrum from Leibstadt SF left and corresponding optimized geometry right.

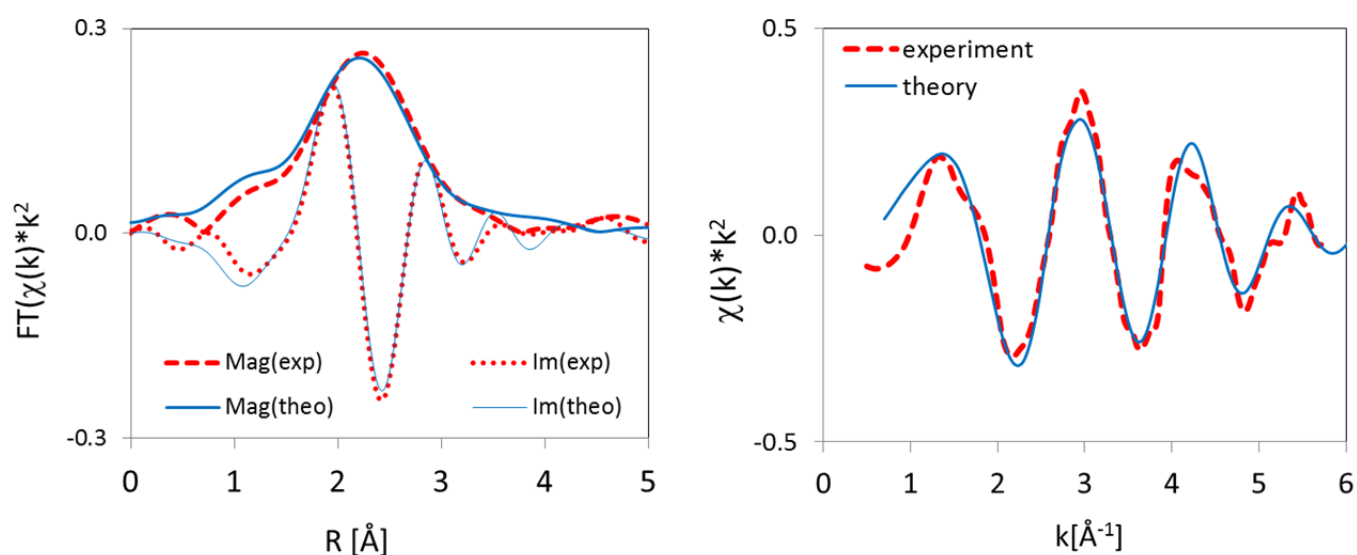


Fig. 2.4: Se K-edge EXAFS fit of a microspot probed on a SF sample from the Oskarshamn-3 reactor (RIM sample). Left: fit of the Fourier transformed spectrum (magnitude and imaginary part). Right: Back-transformed experimental and fitted spectra. The fit parameters are listed in Table 2.3.

Table 2.3: EXAFS fit parameters derived for the absorption spectrum of a single micro spot from the RIM SF sample. Fixed parameters are shown in italics; fitted parameters are in bold face.

Se-U			Se-O			ΔE_0 (eV)	S_0^2
<i>CN</i>	R (Å)	σ^2 (Å²)	<i>CN</i>	R (Å)	σ^2 (Å²)		
<i>4</i>	2.88 ± 0.05	0.029 ± 0.014	<i>6</i>	2.98 ± 0.14	0.042 ± 0.031	1.64 ± 3.05	0.91

2.4 Thermodynamic databases and GEM software

The R&D work in Gibbs Energy Minimisation Software (for) Thermodynamic Modelling Project (GEMS TM: <http://gems.web.psi.ch>) was focused on the GEMSFITS code, as well as on extensions in GEM-Selektor and GEMS3K codes (TSolMod library) to improve multi-site models of mixing in solid solutions by adding reciprocal non-ideality terms.

The GEMSFITS code package (MIRON et al. 2014) is an innovative tool for fitting parameters of chemical thermodynamic models against experimental data in an internally consistent way, and for performing various inverse-modelling tasks (e.g. geothermometry). This has many applications for more accurate and robust modelling of complex multicomponent-multiphase geochemical systems. The new code is more general and has a much broader scope than its earlier prototype (HINGERL et al. 2014) aimed at fitting interaction parameters of thermodynamic activity models only. The GEMSFITS code is coupled with the GEMS3K chemical solver (KULIK et al. 2013) – a Gibbs energy minimization kernel of GEM Software that, in turn, includes the TSolMod library (WAGNER et al. 2012) of equations of state and activity models of solution phases (fluid mixtures, aqueous solutions, solid solutions etc.). For the parameter fitting, GEMSFITS uses a robust open-source NLOpt (<http://ab-initio.mit.edu/wiki/index.php/NLOpt>) library for nonlinear optimization, providing easy selection between several algorithms (global, local, gradient-based). Statistical evaluation of results is performed by calculating summary statistics (e.g. sensitivities of measured data and parameters, correlation coefficients, and the parameter confidence intervals estimated by the Monte Carlo method).

GEMSFITS codes can import, manage and query extensive sets of experimental data stored in data base files in the industry-winning NoSQL BSON format (<http://ejdb.org>; <http://bsonspec.org/>; <http://www.json.org/>). Due to the flexibility of NoSQL, many types of experimental data can be inserted, describing various experimental properties such as (but not limited to): bulk chemical composition, volume, temperature and pressure of experimental systems, measured phase properties (e.g. solubility data, contents of elements in solid

solutions), measured phase properties (e.g. density, osmotic coefficients, pH, activities/fugacities of elements).

The GEMSFITS is equipped with a graphical user interface (GUI) that allows creating a project for fitting tasks, managing the experimental data base, running the fitting task, and analysing the results. In a project, any number of fitting tasks (variants) can be created, edited (in JSON format), and stored in the data base. Multiple parameters can be fitted simultaneously against selected experimental properties, along with several options for data weighting, parameter bounds and constraints, and statistical methods. Results (parameters, sensitivity data, and statistics) can be stored in the data base, viewed and plotted on XY plots using the GUI.

2.5 Solid solution – aqueous solution systems

Detailed understanding of the incorporation of aluminium and alkali in Calcium Silicatehydrates (C-S-H) is important for improving chemical thermodynamic predictions of composition and alteration of hydrated cements. However, the experimental data on solubility and sorption in C-(A)-S-H-(N)-(K) system long remained incomplete and sometimes controversial. In recent years, systematic experimental studies on the uptake of aluminium, alkali and anions on C-S-H composition and water uptake have been carried out in several European laboratories (L'HOPITAL 2014). The obtained systematic datasets need to be translated into a consistent thermodynamic framework. We aim at a structurally consistent multi-site solid solution model for C-S-H that will integrate not only the alkali- and aluminium uptake, but also its effects on volume and density, as well as the influence of moderate temperature changes (7 to 80 °C).

Our new multi-site solid solution model, CASHNK, takes advantage of the presently available understanding of C-S-H tobermorite-like structure, extending and refining earlier solid solution models (KULIK & KERSTEN 2001; LOTHENBACH & WINNEFELD 2006; KULIK 2011; MYERS et al. 2014). The spectroscopic data (L'HOPITAL 2014; RENAUDIN et al. 2009) and MD/MC simulations (PEGADO et al. 2014) suggest that in C-S-H structure (Fig. 2.5, Table 2.4) substitutions may simultaneously occur within three different sublattice sites.

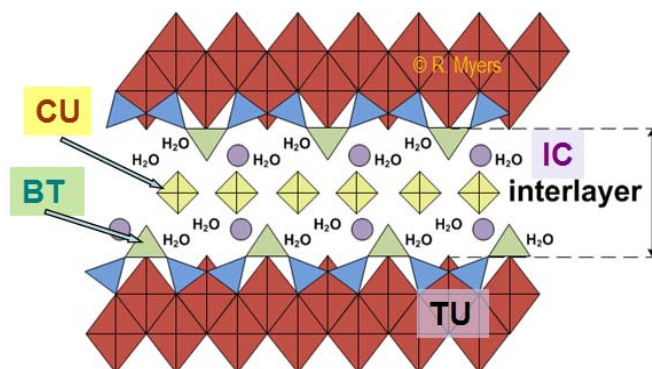


Fig. 2.5: Structural sites (sublattices) of C-S-H.

Table 2.4: Sites and substituting moieties defining the CASHNK solid solution model.

Sublattices (sites):	TU (tobermorite dimeric unit)		IC (interlayer ion exchange)		BT (bridging tetrahedral unit)		CU (additional Ca unit)	
Moieties (species); their one-letter codes	$\text{Ca}_2\text{Si}_2\text{O}_5(\text{OH})_4$	T	$(\text{H}_3\text{O})_2$	H	SiO_2	S	Va	v
			CaH_2O	C	Va	v	$\text{Ca}(\text{OH})_2$	C
			$\text{AlOH}(\text{H}_2\text{O})_2$	A	AlOOH	A	AlOOH	A
			$(\text{NaH}_2\text{O})_2$	N				
			$(\text{KH}_2\text{O})_2$	K				

Va (v) denotes vacancy (different moieties on different sublattices). Charges on IC moieties (+2) and on TU unit (-2) are not shown because they cancel out in any CASHNK compound. The number of H_2O molecules in IC moieties is chosen to conform to the data on density and water content in C-S-H at 25 % r.h. (MULLER et al. 2013).

As seen in Table 2.4, the SiO_2 moiety can only be substituted in BT sites, whereas Ca can be substituted in IC and CU sites, and Al – in BT, IC and CU sites. Vacancies in the BT sublattice define the defect-tobermorite structure. All possible end members can be generated by combining one moiety for each sublattice (45 end members in total, including 8 for C-S-H without Al, Na and K; 27 for C-A-S-H). For easier identification, each moiety is coded with one letter (Table 2.4). For instance, the least-calcium-rich end member with $\text{Ca}/\text{Si} = 0.67$ is THSv, $\{(\text{H}_3\text{O})_2\}$: $\{\text{SiO}_2\}$: $\{\text{Va}\}$: $[\text{Ca}_2\text{Si}_2\text{O}_5(\text{OH})_4]$. In this formula sublattices with substitutions are separated by colons, and moieties are taken in braces. The T moiety is the same for all end members and, for this reason, it is kept at the end of the end-member compound formula. The THSv compound formally has the infinite "dreierketten" chain length CL (as any other compound with S or A moiety in the BT sublattice). Any compound with a vacancy in BT sublattice has

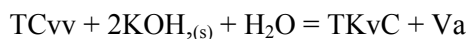
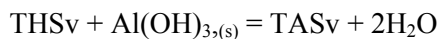
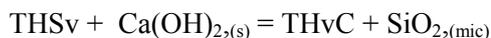
$CL = 2$. The mean chain length can be estimated from dimeric end member mole fractions x_{j2} (KULIK 2011):

$$\langle CL \rangle = \frac{3}{\sum_{j2} x_{j2}} - 1$$

The resulting CASHNK multi-site solid solution model is flexible, structurally plausible, and can be rigorously described using the Compound Energy Formalism (HILLERT 2001) with the thermodynamic properties computed using the GEM software. The difficulty is that such a multi-site model requires many end members, most of which do not exist in pure state, and probably many site interaction parameters. This necessitates (i) the systematic prediction of initial thermodynamic properties of end members from their composition, and (ii) the usage of an advanced GEM input parameter optimization tool such as the GEMSFITS code (MIRON et al. 2014).

The initial thermodynamic dataset for 45 end members of the CASHNK model, consistent with the PSI-Nagra and Cemdata TDBs, was generated as follows. Two end members – THSv and TCvv – were selected as reference compounds, with standard thermodynamic properties at 1 bar, 25 °C obtained,

respectively, by upscaling those of TobH and T2C end-members of the CSH3T solid solution model (KULIK 2011) without the gel-water content. Standard properties of other end member compounds were derived from exchange reactions like



and so on, assuming zero effects of reaction ($\Delta_r G^0=0$, $\Delta_r S^0=0$, $\Delta_r Cp^0=0$, $\Delta_r V^0=0$), and all zero standard properties of vacancy Va. Properties of the following compounds were used: from Cemdata and PSI-Nagra data bases - $\text{Ca}(\text{OH})_{2,(s)}$ – portlandite; $\text{Al}(\text{OH})_{3,(s)}$ – gibbsite; H_2O – water; from (WAGMAN et al. 1982): solid $\text{KOH}_{,(s)}$ and $\text{NaOH}_{,(s)}$; by simultaneous adjustment to typical low-Ca C-S-H solubility data $[\text{Ca}]=1.6 \cdot 10^{-3}$ M and $[\text{Si}]=3.8 \cdot 10^{-3}$ M: THSv and $\text{SiO}_{2,(mic)}$ – microcrystalline silica. Calculations were performed using the ReacDC module of GEM-Selektor v.3.2.

Next, trial calculations of C-S-H solubility were performed in the aqueous solid solution sub-system, at Ca/Si ratios of 0.5, 1.0 and 1.7 using, for the first run, the reciprocal terms in the sublattice mixing models after SUNDMAN & ÅGREN 1981. It turned out that these reciprocal non-ideality terms are quite significant and should not be ignored.

A multi-site solid solution with two or more sublattices and two or more moieties substituted on each sublattice is called *reciprocal*. The term *reciprocal* can be understood using the simplest solid solution phase $\{\text{A,B}\}\{\text{X,Y}\}$ (e.g. WOOD & NICHOLLS 1978; HILLERT 2001). All possible compositions can be represented on a ‘composition square’ made of end members AX, BX, AY, BY. However, only three of them are needed to describe any bulk composition of this phase. For instance, the center of the square can be obtained by mixing equal amounts of either AX and BY or AY and BX, hence the name ‘reciprocal’. Any three of four end members can be declared as ‘independent’, while the remaining one will be ‘dependent’ because all its properties can be obtained from those of ‘independent’ end members and that of a reciprocal reaction



with a standard molar Gibbs energy effect

$$\Delta_{rr} G^0 = G^0_{\text{AX}} + G^0_{\text{BY}} - G^0_{\text{AY}} - G^0_{\text{BX}}$$

The chemical potential of the j-th end-member is

$$\mu_j = G^0_j + RT \ln x_j + RT \ln \lambda_j + RT \ln f_j + RT \ln \gamma_j$$

where $\ln x_j$ is the mole fraction; f_j is the activity coefficient due to excess Gibbs energy; $\ln \lambda_j = \ln a_j^{(con)} - \ln x_j$; $a_j^{(con)}$ is the ideal part of activity related to the configurational entropy (PRICE 1985); and γ_j is the reciprocal activity coefficient, which is unity (ideal behaviour) for all end members if and only if $\Delta_{rr} G^0 = 0$ for all possible reciprocal reactions.

For the above example of $\{\text{A,B}\}\{\text{X,Y}\}$ solid solution, one can derive [WOOD & NICHOLLS 1978]

$$RT \ln \gamma_{\text{AX}} = -y_{\text{B}} y_{\text{Y}} \Delta_{\pi} G^0 \quad RT \ln \gamma_{\text{BY}} = -y_{\text{A}} y_{\text{X}} \Delta_{\pi} G^0$$

$$RT \ln \gamma_{\text{AY}} = +y_{\text{B}} y_{\text{X}} \Delta_{\pi} G^0 \quad RT \ln \gamma_{\text{BX}} = +y_{\text{A}} y_{\text{Y}} \Delta_{\pi} G^0$$

where y_{A} , y_{B} are the site fractions of A or B on the first sublattice, and y_{X} , y_{Y} that of X or Y on the second sublattice (they can be easily computed from end-member mole fractions). From the above equations, reciprocal non-ideality terms appear to reflect the energies of interaction upon simultaneous substitutions in two sublattices. This formalism of reciprocal reactions can be extended for the case when more than two moieties substitute on each of two sublattices; the number of end members and especially reciprocal reactions dramatically increases in such cases.

It is difficult to impossible to apply reciprocal reactions to solid solutions with simultaneous substitutions in three or more sublattices. Fortunately, SUNDMAN & ÅGREN (1981) suggested a method for computing reciprocal activity coefficient terms in this general case. We have implemented this method in TSolMod library in addition to calculation of configurational terms and substitution interaction terms implemented earlier. Now, the GEMS3K code can compute all terms in chemical potentials of end members, and, thus, rigorously models very complex mixing in solid solutions like the CASHNK. Accordingly, all input parameters (G^0 values of end members, interaction parameters) can be optimized using the GEMSFITS code in their multiplicity.

As an example, GEM-Selektor screenshots on Figs. 2.6, 2.7, 2.8 show results of trial GEM calculations in a C-S-H system with zero excess Gibbs energy interaction parameters.

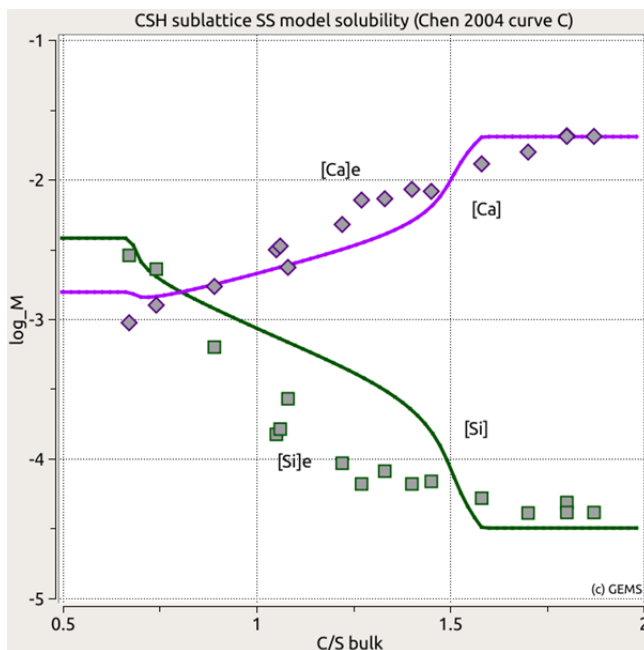
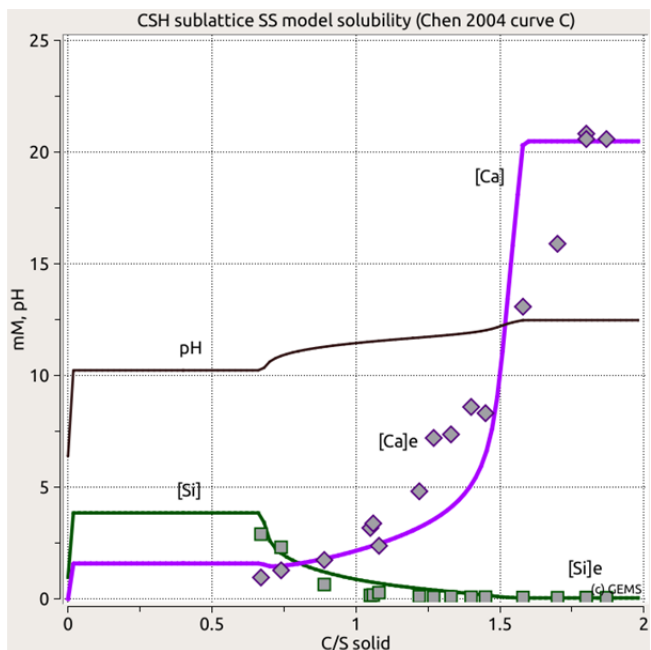


Fig. 2.6: Modelled C-S-H solubility against data from CHEN et al. (2004), Curve C (diamonds and squares): in millimolar (left) and \log_{10} molarity (right) scales.

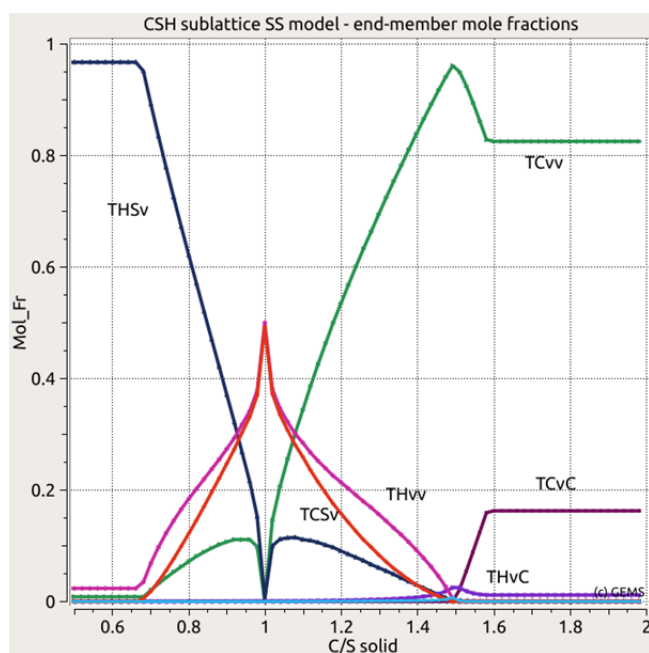
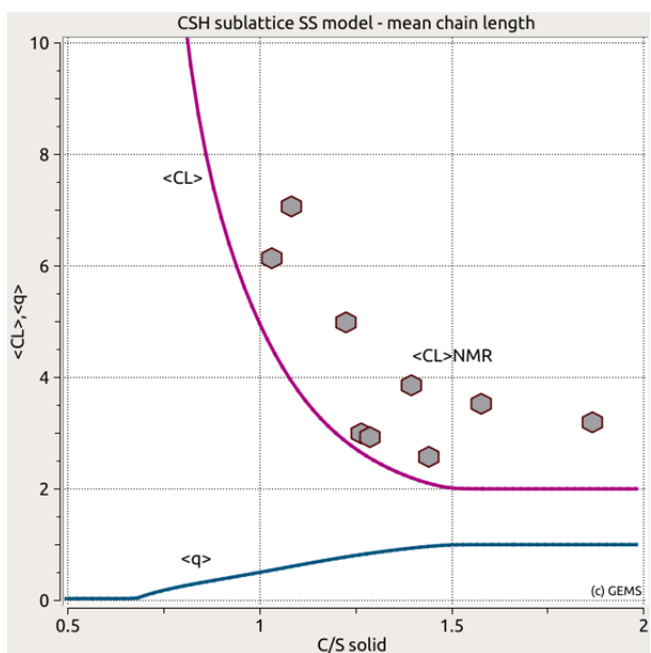


Fig. 2.7: Left: simulated mean chain length $\langle CL \rangle$ and fraction of dimers $\langle q \rangle$ against the data from CHEN et al. (2004, Fig. 7 therein). Right: mole fractions of end members in C-S-H sublattice model.

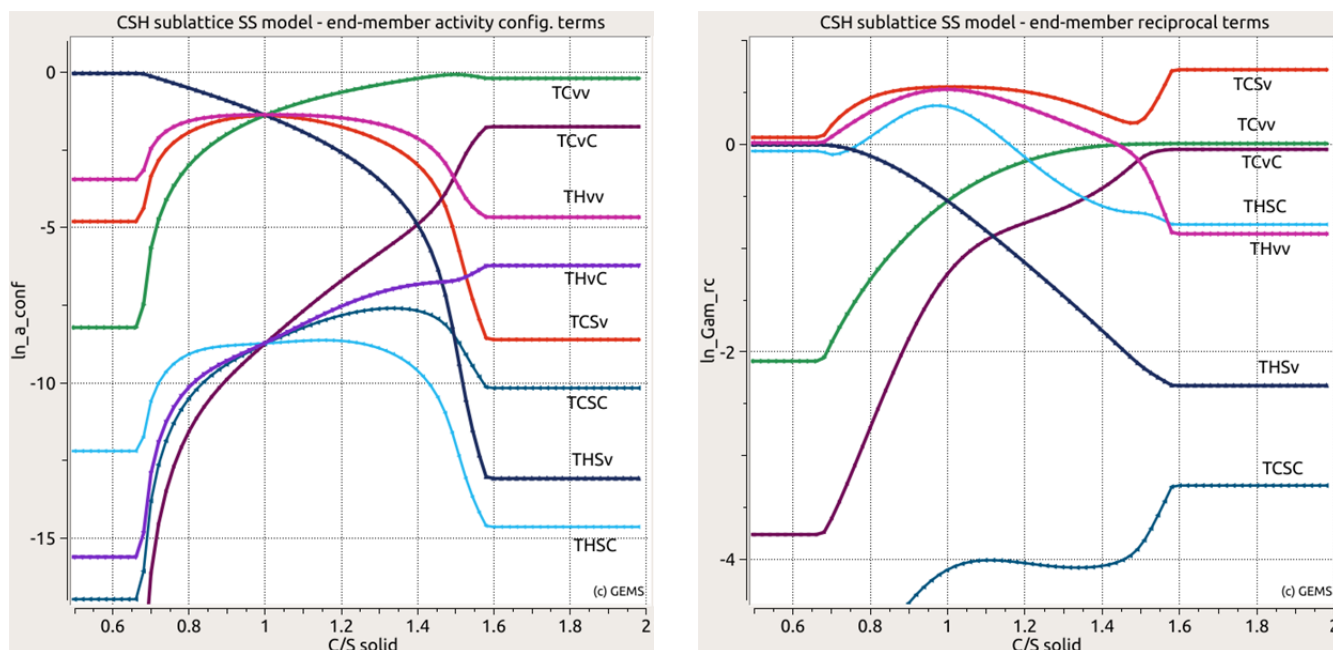


Fig. 2.8: CSH sublattice solid solution model: Configurational activity terms $\ln x_j + \ln \lambda_j$ (left); reciprocal non-ideality terms $\ln \gamma_j$ (right).

These plots show that, even without fine-tuned excess interaction parameters, the model correctly reproduces the congruence point (where the $[\text{Ca}]/[\text{Si}]$ ratio in solution equals the Ca/Si ratio in the solid), dissolved $[\text{Si}]$ in presence of portlandite (Fig. 2.6), and the $\langle \text{CL} \rangle$ trend (Fig. 2.7). $\langle \text{CL} \rangle$ can be adjusted by changing G° values of dimeric end members (e.g. TCvv, TCvC) relative to that of other end members. This also has an impact on configurational and reciprocal activity terms (Fig. 2.8), and on variations of end member mole fractions (Fig. 2.7), which very well reproduce the ordered, relatively stable pentameric C-S-H compound ($\langle \text{CL} \rangle = 5$) at $\text{Ca}/\text{Si} = 1$.

2.6 Water-rock interactions in Icelandic hydrothermal systems

This study is part of the integrative research project Sinergia COTHERM that is aimed at improving our understanding of the sub-surface processes in magmatically driven natural geothermal systems. The concepts developed in this study are directly feasible for most of the water-rock interaction problems, including simulations of in situ conditions in geological waste repositories.

The subsurface stratigraphy of Iceland mainly consists in a succession of basalt bed layers (compact basalt with low porosity and permeability) which are rather fresh, and hyaloclastite layers (with high porosity and permeability, made of tiny glassy fragments) which are completely altered (MARKS et al. 2010). The parameters influencing the mineralogical evolutions in these systems were accessed using a simplified geochemical reactive transport model.

Calculations were performed for basalt flow and hyaloclastite, different water compositions, volcanic gas contents, and various temperatures and pressures. The results indicate that the initial porosity is the key factor to control the evolution of hydrothermal systems. During the transformation of protolith into secondary minerals, the total volume of solids increases, up to complete clogging of the basalt bed systems (Fig. 2.9), whereas the volume does not significantly change for hyaloclastites. This explains why compact basalts are observed to be rather fresh: there is no alteration without water flow. Consequently, hyaloclastites can be completely altered.

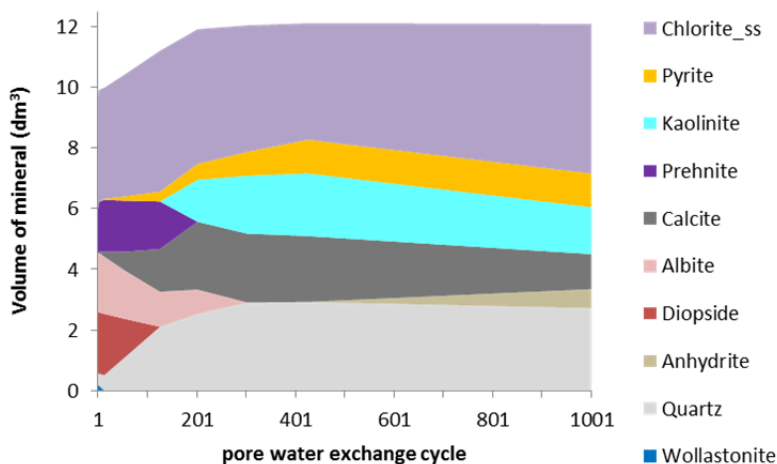


Fig. 2.9: Evolution of mineral volume as a function of reaction progress, for a 10% initial porosity basalt altered in fresh water with addition of H_2S and CO_2 gases, at $250^\circ C$ and 25 MPa. The initial volume of protolith is 9 dm^3 ; the maximum volume of the system is 10 dm^3 . When the total mineral volume exceeds the limit of 10 dm^3 , the system is considered to be completely clogged.

2.7 References

BERNER U. (2013)

Abschätzung der Löslichkeit von Kupfer in Zement- und Bentonitreferenzwässern. PSI Technical Report AN-44-12-10, Paul Scherrer Institute, Villigen, Switzerland.

BERNER U. (2014a)

Solubility of radionuclides in a bentonite environment for provisional safety analyses for SGT-E2. Nagra Techn. Rep. NTB 14-06 (in press).

BERNER U. (2014b)

Solubility of radionuclides in a concrete environment for provisional safety analyses for SGT-E2. Nagra Techn. Rep. NTB 14-07 (in press).

BROWN P.L., CURTI E., GRAMBOW B. (2005)

Chemical Thermodynamics of Zirconium. Chemical Thermodynamics Vol. 8, Elsevier, Amsterdam, Netherlands, 512 pp.

CHEN J.J., THOMAS J.J., TAYLOR H.F.W., JENNINGS H.M. (2004)

Solubility and structure of calcium silicate hydrate. Cement Concr. Res. 34, 1499-1519.

COLÀS E., MONTOYA V., GAONA X., DOMÈNECH C., GRIVÉ M., DURO L. (2007)

Development of ThermoChimie data base. Version 6 update, ANDRA report D.R.0ENQ.07.001, 362pp.

GAMJSJÄGER H., BUGAJSKI J., GAJDA T., LEMIRE R.J., PREIS W. (2005)

Chemical Thermodynamics of Nickel. Chemical Thermodynamics Vol. 6, Elsevier, Amsterdam, Netherlands, 617 pp.

GOUT R., POKROVSKI G.S., SCHOTT J., ZWICK A. (2000)

Raman spectroscopic study of aluminum silicate complexes at $20^\circ C$ in basic solutions. J. Solution Chem. 29, 1173-1185.

GUILLAUMONT R., FANGHÄNEL T., FUGER J., GRENTHE I., NECK V., PALMER D.A., RAND M.A. (2003)

Update on the Chemical Thermodynamics of Uranium, Neptunium, Plutonium, Americium and Technetium. Chemical Thermodynamics Vol. 5, Elsevier, Amsterdam, Netherlands, 763 pp.

HILLERT M. (2001)

The compound energy formalism. J. Alloys Compd. 320, 161-176.

HINGERL F.F., KOSAKOWSKI G., WAGNER T., KULIK D.A., DRIESNER T. (2014)

GEMSFIT: a generic fitting tool for geochemical activity models. Computat. Geosci. 18, 227-242.

HUMMEL W. (2014)

The PSI/Nagra chemical thermodynamic database 12/07 (Update of the Nagra/PSI TDB 01/01): Data selection for silicon. PSI Technical Report TM-44-12-05, Paul Scherrer Institute, Villigen, Switzerland, 40 pp.

- HUMMEL W., BERNER U., CURTI E., PEARSON F.J., THOENEN T. (2002)
Nagra/PSI Chemical Thermodynamic Data Base 01/01. Nagra Technical Report NTB 02-16, Nagra, Wetingen, Switzerland, and Universal Publishers, Parkland, Florida, 565 pp.
- JOHNSON L., GÜNTHER-LEOPOLD I., KOBLER WALDIS J.B., LINDER H.P., LOW J., CUI D., EKEROTH E., SPAHIU K., EVINS L.Z. (2012)
Rapid aqueous release of fission products from high burn-up LWR fuel: Experimental results and correlations with fission gas release. *J. Nucl. Mat.* 420, 54–62.
- JOLY Y. (2001)
X-ray absorption near-edge structure calculations beyond the muffin-tin approximation. *Phys. Rev. B* 63, 125120-1–125120-10.
- KARPOV I.K., CHUDNENKO K.V., KULIK D.A., AVCHENKO O.V., BYCHINSKII V.A. (2001)
Minimization of Gibbs free energy in geochemical systems by convex programming. *Geochem. Internat.* 39, 1108-1119.
- KOZAWA A., KALNOKI-KIS T., YEAGER F. (1966)
Solubilities of Mn(II) and Mn(III) Ions in concentrated alkaline solutions. *J. Electrochem. Soc.* 113/5, 405-409.
- KULIK D.A. (2011)
Improving the structural consistency of C-S-H solid solution thermodynamic models. *Cement Concr. Res.* 41, 477-495.
- KULIK D.A., KERSTEN M. (2001)
Aqueous solubility diagrams for cementitious waste stabilization systems: 2. End-member stoichiometries of ideal calcium silicate hydrate solid solutions. *J. Am. Ceram. Soc.* 84, 3017-3026.
- KULIK D.A., WAGNER T., DMYTRIEVA S.V., KOSAKOWSKI G., HINGERL F.F., CHUDNENKO K.V., BERNER U. (2013)
GEM-Selektor geochemical modelling package: revised algorithm and GEMS3K numerical kernel for coupled simulation codes. *Computat. Geosci.* 17, 1-24.
- L'HOPITAL E. (2014)
Aluminium and alkali uptake in calcium silicate hydrates (C-S-H), PhD Thesis. EPFL, Oct. 2, 2014.
- LEMIRE R.J., BERNER U., MUSIKAS C., PALMER D.A., TAYLOR P., TOCHIYAMA O. (2013)
Chemical Thermodynamics of Iron. *Chemical Thermodynamics Vol. 13a. NEA OECD*, 1082 pp.
- LOTHENBACH B., WINNEFELD F. (2006)
Thermodynamic modelling of the hydration of Portland cement. *Cement Concr. Res.* 36, 209-226.
- MARKS N., SCHIFFMAN P., ZIERENBERG R.A., FRANNON H., FRIDLEIFSSON G.O. (2010)
Hydrothermal alteration in the Reykjanes geothermal system: Insights from Iceland deep drilling program well RN-17. *J. Volcan. Geoth. Res.* 189, 172-190.
- MIRON G.D., KULIK D.A., DMYTRIEVA S.V., WAGNER T. (2014)
GEMSfits: Code package for optimization of geochemical model parameters and inverse modelling. *Appl. Geochem.* (in press).
- MULLER A.C.A., SCRIVENER K.L., GAJEWICZ A.M., McDONALD P.J. (2013)
Use of bench-top NMR to measure the density, composition and desorption isotherm of C-S-H in cement paste. *Microporous Mesoporous Mater.* 178, 99-103.
- MYERS R.J., BERNAL S.A., PROVIS J.L. (2014)
A thermodynamic model for C-(N-)A-S-H gel: CNASH_{ss} derivation and validation. *Cement Concr. Res.* 66, 27-47.
- OLIN Å., NOLÄNG G., OSADCHII E., ÖHMAN L.-O., ROSÉN E. (2005)
Chemical Thermodynamics of Selenium. *Chemical Thermodynamics Vol. 7*, Elsevier, Amsterdam, Netherlands, 851 pp.
- PEGADO L., LABBEZ C., CHURAKOV S.V. (2014)
Mechanism of aluminium incorporation into C-S-H from ab initio calculations. *J. Mater. Chem. A2*, 3477- 3483.
- POKROVSKI G.S., SCHOTT J., SALVI S., GOUT R., KUBICKI J.D. (1998)
Structure and stability of aluminum-silica complexes in neutral to basic solutions. Experimental study and molecular orbital calculations. *Mineralog. Magazine* 62A, 1194-1195.
- POWELL K.J., BROWN P.L., BYRNE R.H., GAJDA T., HEFTER G., LEUZ A.-K., SJÖBERG S., WANNER H. (2011)
Chemical speciation of environmentally significant metals with inorganic ligands. Part 4: The Cd²⁺ + OH⁻, Cl⁻, CO₃²⁻, SO₄²⁻, and PO₄³⁻ systems (IUPAC Technical Report). *Pure Appl. Chem.* 83/5, 1163–1214.
- PRICE J.G. (1985)
Ideal site mixing in solid solutions, with an application to two-feldspar geothermometry. *Amer. Mineral.* 70, 696-701.

- RAI D., YUI M., MOORE D.A., LUMETTA G.J., ROSSO K.M., XIA Y., FELMY A.R., SKOMURSKI F. N. (2008) Thermodynamic model for ThO₂(am) solubility in alkaline silica solutions. *J. Solution Chem.* 37, 1725-1746.
- RAND M., FUGER J., GRENTHE I., NECK V., RAI D. (2008) Chemical Thermodynamics of Thorium. *Chemical Thermodynamics Vol. 11*, OECD NEA, Paris, France, 900 pp.
- RENAUDIN G., RUSSIAS J., LEROUX F., CAU-DIT-COUMES C., FRIZON F. (2009) Structural characterization of C-S-H and C-A-S-H samples - Part II: Local environment investigated by spectroscopic analyses. *J. Solid State Chem.* 182, 3320-3329.
- SANTSCHI P.H., SCHINDLER P.W. (1974) Complex formation in the ternary systems Ca^{II}-H₄SiO₄-H₂O and Mg^{II}-H₄SiO₄-H₂O. *J. Chem. Soc. Dalton Trans.*, 181-184.
- SHILOV V.P., FEDOSEEV A.M., YUSOV A.B., DELEGARD C.H. (2004) Behaviour of Np(VII, VI, V) in silicate solutions. *Radiochemistry*, 46, 574-577 (translated from *Radiokhimiya* 46 (2004) 527-530).
- SMOLENTSEV G., SOLDATOV A.V. (2007) FitIt: New software to extract structural information on the basis of XANES fitting. *Comp. Matter. Sci.* 39, 569-574.
- SUNDMAN B., ÅGREN J. (1981) A regular solution model for phases with several components and sublattices, suitable for computer applications. *J. Phys. Chem. Solids* 42, 297-301.
- WAGMAN D.D., EVANS W.H., PARKER V.B. (1982) The NBS tables of chemical thermodynamic properties. Selected values for inorganic and C1 and C2 organic substances in SI units. *J. Phys. Chem. Ref. Data* 11, Suppl. 2.
- WAGNER T., KULIK D.A., HINGERL F.F., DMYTRIEVA S.V. (2012) GEM-Selektor geochemical modelling package: TSolMod library and data interface for multicomponent phase models. *Can. Mineral.* 50, 1173-1195.
- WOOD B.J., NICHOLLS J. (1978) The thermodynamic properties of reciprocal solid solutions. *Contrib. Mineral. Petrol.* 66, 389-400.
- YUSOV A.B., FEDOSEEV A. M. (2003) Reaction of Plutonium(VI) with orthosilicic acid Si(OH)₄. *Russ. J. Coord. Chem.* 29, 582-590 (translated from *Koordinatsionnaya Khimiya*, 29 (2003) 623-634).

3 TRANSPORT MECHANISMS

N.I. Prasianakis, S.V. Churakov, Th. Gimmi, A. Jakob, G. Kosakowski, W. Pfingsten, A. Leal (post doc), L. Pegado (guest scientist), J. Poonoosamy (PhD student), A. Shafizadeh (PhD student), S. Meng (Master student)

3.1 Overview

In 2014, the main research activities of the Transport Mechanism Group were related to the Sectoral Plan for Deep Geological Disposal (SGT). The main target was on providing documentation for the Stage 2 of the SGT. The report on the geochemical evolution of the low- and intermediate-level waste (L/ILW) near field was finalized this year (KOSAKOWSKI et al. 2014). Therein, the spatial and temporal geochemical evolution of the cementitious near field, and the interactions with the technical barriers and the surrounding rock have been described. The processes that occur in the Engineered Gas Transport System (EGTS), the evolution of mineralogy and porosity has been assessed with the help of state-of-the-art coupled reactive transport models. (KOSAKOWSKI & SMITH 2014, KOSAKOWSKI & WATANABE 2014). Group members have also provided significant contribution to the report on the evolution of the near field of a HLW repository (BRADBURY et al. 2014).

The group members coordinate the sampling and current modelling of the DR-A field experiment in the Mont Terri Underground Rock Laboratory. The experiment investigates the effects of chemical perturbations in the porewater on ion's transport in Opalinus Clay. The online sampling phase was finalized in November 2013 and field installation was overcored. Several samples have been studied in detail, and the obtained profile data measured in this field experiment will be used in transport modelling and simulations.

Mineralogical and porosity changes at cement–clay interface are further investigated at a micrometer scale within the CROSS-department (NUM-NES) PhD project partially supported by NAGRA and PSI Director's reserve (project title: "Evolution of cement-clay interfaces", Amir Shafizadeh). Changes in porosity at different reaction intervals are monitored by neutron imaging at the ICON facility at PSI. In the reporting year, new diffusion experiments with heavy water (D₂O) were performed on aged and fresh samples with the aim to assess the changes in the transport properties at the cement-clay interface.

Within the nuclear Master project "*Modelling Radionuclide Transport in Clay for a Radial Symmetric Experimental Set-up – Extension and Application of MCOTAC*", (Shuo Meng), the multispecies reactive transport code MCOTAC has been extended for modelling set-ups with radial

symmetry, commonly found in laboratory experiments. The updated code has been validated using the commercial software COMSOL Multiphysics and has been applied in modelling laboratory through diffusion experiments. The new model benefits from the 2SPNE SC/CE sorption model and SIT ionic strength correction implemented in MCOTAC.

Atomistic simulations and spectroscopic studies are applied in order to deepen the fundamental understanding of radionuclide's transport and sorption mechanisms. More specific, in collaboration with the University of Surrey (UK), molecular dynamics simulations were applied to predict nuclear magnetic resonance (NMR) relaxation parameters, which in turn paves the way to better interpretation of experimental data and understanding of water transport and porosity distribution in C-S-H (BHATT et al. 2014). Further, ion sorption by C-S-H phases has been modelled using a multi-scale modelling approach aiming at refining a thermodynamic model for ion sorption at the level of a single C-S-H particle. Two milestones have been already reached (PEGADO et al. 2014 & CHURAKOV et al. 2014b). Significant progress has been made with respect to the upscaling of diffusion transport coefficients from molecular to laboratory scales. The scale dependent diffusion of water in montmorillonite has been assessed combining molecular dynamics, random walk simulations and neutron scattering measurements (CHURAKOV et al. 2014a). This multi-scale modelling approach was further applied to investigate the relation between pore structure and sample-scale diffusion coefficients.

The benchmarking and verification of reactive transport coupled codes is an on-going activity in the Transport Mechanisms Group. An experimental benchmark for reactive transport in granular porous media has been set-up, analyzed and modelled within the PhD project (project title: "Experimental benchmark for the verification and validation of reactive transport codes", Jenna Poonoosamy) supported by NAGRA. The flow path and porosity changes in the reacting porous media have been analyzed with several microscopy techniques. These experiments were modelled using the OpenGeoSys-GEM coupled code and the major experimental features were reproduced (POONOOSAMY et al. 2014). Finally, the co-operation with the Center for Environmental Research, UFZ Leipzig in the area of

reactive transport (OpenGeoSys-GEM) was strengthened and resulted in a joint publication (KOSAKOWSKI & WATANABE 2014).

A new Postdoc researcher (Dr. A. Leal) joined the group in September 2014. His project will focus on improving stability and robustness of geochemical solvers (e.g. GEMS) with an overarching aim to speed up the reactive transport simulation used for the assessment of the in situ conditions in the repository.

The new group leader (Dr. N.I. Prasianakis) joined the group in October 2014. His expertise in state of the art algorithms (e.g. Lattice Boltzmann Method), as well as in modelling and simulation of detailed 3D reactive transport phenomena in porous media, will strengthen the group's competencies in the area of multi-scale reactive transport simulations.

3.2 Activities in support of the Sectoral Plan

3.2.1 Geochemical evolution of the L/ILW near field

The report on the geochemical evolution of the L/ILW near field was finalized this year (KOSAKOWSKI et al. (2014)). It summarizes the spatial and temporal geochemical evolution of the cementitious near field, the interactions with the technical barriers and the surrounding host rock, and defines the reference states for the sorption and solubility data bases in the cementitious near field. The report is based on literature reviews, geochemical batch calculations and mass balance estimates, as well as 1D reactive transport calculations.

The description of cement degradation in the near field is consistent with that in previous studies. It is expected that the degradation of the cementitious near field will occur in several phases:

- a) the first phase of cement degradation, which will persist only for a short period of time, is related to the hydration of clinker minerals where the porewater has a pH of 13 or even higher as a consequence of the high content of dissolved alkali hydroxides,
- b) the second phase is determined by a constant pH of 12.5, buffered by the equilibrium with portlandite. The alkali concentration is reduced by mineral reactions and/or solute transport,
- c) the third phase is characterized by the complete dissolution of portlandite. The pore water is in equilibrium with C-S-H which gives rise to a pH value near 11 or even lower. The Ca/Si ratio of C-S-H will change towards lower values,

- d) in a very late phase the formation of carbonates, clays or zeolites will cause the pH to drop to near neutral values.

The spatial and temporal occurrence of the cement degradation phases is governed by several coupled externally and internally induced processes. The most important ones are considered to be the interactions with the host rock, the interactions with waste, the degradation of cement minerals by alkali-silica-aggregate reactions and by cement carbonation. The development of saturation is of vital importance for many processes. Saturation is governed by the interplay of groundwater ingress from the host rock and by gas production due to anoxic corrosion of metals and the degradation of organic waste presumably by methanogenesis. Full or partial desaturation of the emplacement caverns, of the adjacent host rock or of the technical barriers in the access tunnels will reduce or even prevent the transport of dissolved species and therefore significantly impede chemical reactions.

The diffusive and advective exchange of porewater between the cementitious near field and the host rocks gives rise to mineral reactions and changes of the porewater pH. Mineral reactions at the interface have been investigated with the help of numerical models. The clay minerals of the host rock are dissolved and transformed into secondary minerals (e.g. zeolites) up to a distance of a few dm in 100'000 years (period under review for performance assessment of a L/ILW deep geological repository). For the case of higher water fluxes in the host rock this zone extends possibly up to 1 m over the same time frame. Beyond this transition zone and further into the host rock, a zone will develop with an elevated pH of 8-9, but without significant mineralogical changes. This zone extends a few meters into the host rock in the case of a diffusive transport regime, whereas in the downstream direction it may reach more than thousand meters in the case of higher water fluxes and very low host rock porosities. For a diffusion dominated regime the portlandite in the cementitious near field will be dissolved up to a distance of 2 m from the near field-host rock interface. In the region where portlandite dissolution occurred, the concrete porewater pH will drop to values corresponding to the third phase of the cement degradation. In the case of higher water fluxes from single facial units of the host rock into the caverns the portlandite dissolution front may extend a further few meters downstream in 100'000 years, while in the portlandite-depleted region all the cement minerals will completely degrade with time. Selected results were already published last year in KOSAKOWSKI & BERNER (2013).

3.2.2 Interface Evolution in the engineered Gas Transport System (EGTS)

The Engineered Gas Transport System (EGTS) is a backfill and sealing system that allows the controlled discharge of gases produced due to metal corrosion and the degradation of organics in low level and long-lived intermediate level waste repositories. The evolution of mineralogy and porosity of such a system has been assessed with the help of state-of-the-art coupled reactive transport models. This year, the results were summarized in a report (KOSAKOWSKI & SMITH 2014) and selected results were published in a research article (KOSAKOWSKI & WATANABE 2014). Fig. 3.1 shows the major processes that take place in a reference EGTS design after 100'000 years. In a diffusive transport regime dissolution/precipitation fronts evolve in the concrete and the sand/bentonite compartments separated by a

10 m layer of limestone gravel (calcite with trace amounts of other clay minerals). At the concrete side portlandite is progressively dissolved and some further ettringite and small amounts of calcite are formed. At the sand/bentonite side, montmorillonite and quartz are progressively replaced by zeolites and minor amounts of hydromagnetite and hydrotalcite, due to the high-pH front (OH^-) originating from the concrete. The silica released from the dissolution of the quartz sand, clay and zeolite minerals diffuse into the transition layer and mix with calcium diffusion out of the concrete. This triggers the precipitation of C-S-H phases near but not directly at the interface to concrete resp. sand/bentonite. For this particular layout, the precipitation is spread along the transition layer. Distinct accumulation of precipitates at the interfaces, which would clog the porosity, is not observed.

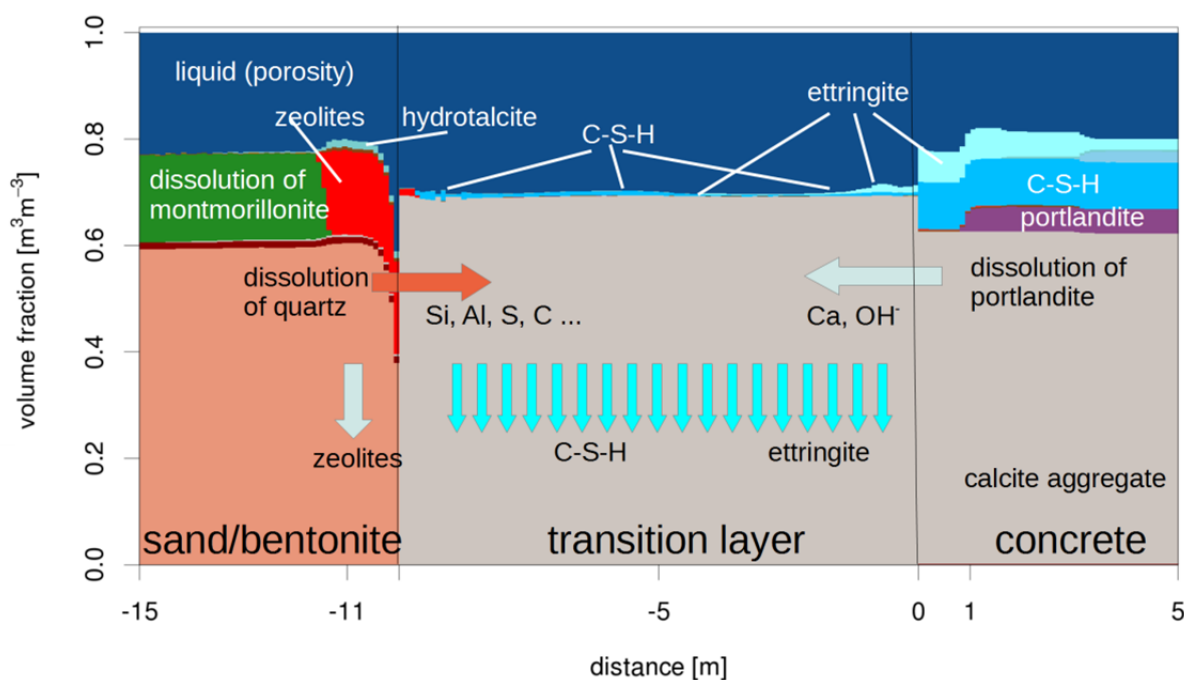


Fig. 3.1: Schematic illustration of major processes in an EGTS where concrete and sand/bentonite compartments are separated by a 10 m layer of limestone gravel (calcite with trace amounts of other clay minerals) after 100'000 years (from KOSAKOWSKI & SMITH 2014).

3.2.3 Influence of a low-pH liner on the near field of a HLW repository

In Switzerland the geological storage in the Opalinus Clay formation is the preferred option for the disposal of spent fuel (SF) and high-level radioactive waste (HLW). The waste will be encapsulated in steel canisters and emplaced into long tunnels that are backfilled with bentonite. Due to uncertainties in the depth of the repository and the associated stress state, a concrete liner might be used for support of emplacement tunnels.

Numerical reactive transport calculations were carried out to investigate the influence of a concrete liner on the adjacent barrier materials, namely bentonite and Opalinus Clay. The geochemical set-up was tailored to the specific materials foreseen in the Swiss repository concept, namely MX-80 bentonite, low-pH concrete (ESDRED) and Opalinus Clay. The calculations provide information on the extent of pH fronts, on the sequence and extent of mineral phase transformations, and on porosity changes cement-clay interfaces. The alteration depth into the bentonite due to the interaction with the concrete liner (assumed to be 15 cm thick) is likely to be much

less than 13 cm over a one million year time scale, with the main reaction products being clays (illite), hydroxides, carbonates, calcium silicate hydrates, and aluminosilicates. The swelling pressure and the sorption capacity in this region will be reduced, but not to zero. Part of the results was published in BERNER et al. (2013).

3.2.4 DR-A field experiment in the Mont Terri Underground Rock Laboratory

The DR-A field experiment in the Mont Terri Underground Rock Laboratory was overcored in November 2013. This experiment aims at investigating the effects of a high ionic strength perturbation, including a strong increase of K concentrations, on the diffusion and retention properties of Cs and other ions. After retrieving the core with the interval region (diameter of 30 cm), subsamples in radial direction, parallel to bedding, were prepared. Three profiles were taken with a resolution of 1 cm to measure the radioactive tracers HTO and ^{60}Co (^{85}Sr was no longer detectable) as well as the anions Cl, I and Br. From adjacent samples, two profiles with the same resolution were taken to obtain the total content of the main ions. Additional profiles were taken with a resolution of about 3 mm to obtain better-resolved ^{60}Co profiles. Finally, intact pieces with a size of several centimeters were sampled to obtain the Cs distribution around the interval. The preliminary data compilation indicates that the concentration profiles of the HTO, ^{60}Co , Cl, I, Br and of the main ions per bulk mass of rock generally follow the expected trends. Some deviations, however, occur, such as an unexpected decrease of HTO concentrations towards the borehole interface, or lower concentrations of sorbing cations in the upper part of the interval, where no porous filter was installed. The decrease of some concentrations towards the borehole is probably related to a dilution that occurred during the overcoring. Ca and Mg contents decreased, and K contents increased near the borehole, as a result of cation exchange reactions induced by the high ionic strength perturbation. These data are consistent with the observed concentrations in the circulated interval solution. Transport modelling including the profile data has just started.

3.2.5 Multispecies random walk simulations in radial symmetry – model concept, benchmark and application to HTO, ^{22}Na and ^{36}Cl diffusion in clay

The modelling of radionuclide transport in clay can be often simplified by taking into account the radial symmetry of the laboratory experimental set-up or for example the cylindrical shape of the underground nuclear waste storage installations. Particularly, if the complex geochemical system is described by a large number of species and the chemical (sorption) reactions and minerals have to be considered, the one-dimensional simulations in radial geometry allow the modelling and simulation of the radionuclide migration in reasonable computational time. Therefore an extension of the multispecies reactive transport code MCOTAC (PFINGSTEN 1996, 2002, 2011) to applications with radial symmetry has been performed within the nuclear master project "Modelling Radionuclide Transport in Clay for a Radial Symmetric Experimental Set-up – Extension and Application of MCOTAC" by Shuo Meng. The advantage of the random walk approach over other numerical schemes is that negative species concentrations are excluded during transport calculations. Negative species concentrations can generate numerical instabilities when transport and geochemical equilibrium-kinetic modules are directly coupled. No direct procedure available to describe the one-dimensional random walk of particles in radial symmetry is available. Therefore, the two-dimensional random walk set-up was applied (PFINGSTEN 2002) but the calculations of chemical equilibrium were reduced to a single radial coordinate reducing memory allocation and saving computational time.

In order to verify this new random walk approach for radial symmetry, MCOTAC radial symmetrical calculations for single species diffusion in clay were compared with results from COMSOL Multiphysics calculations (Fig. 3.2). The agreement is very good proving correctness of the MCOTAC algorithm for reactive transport in radial symmetry.

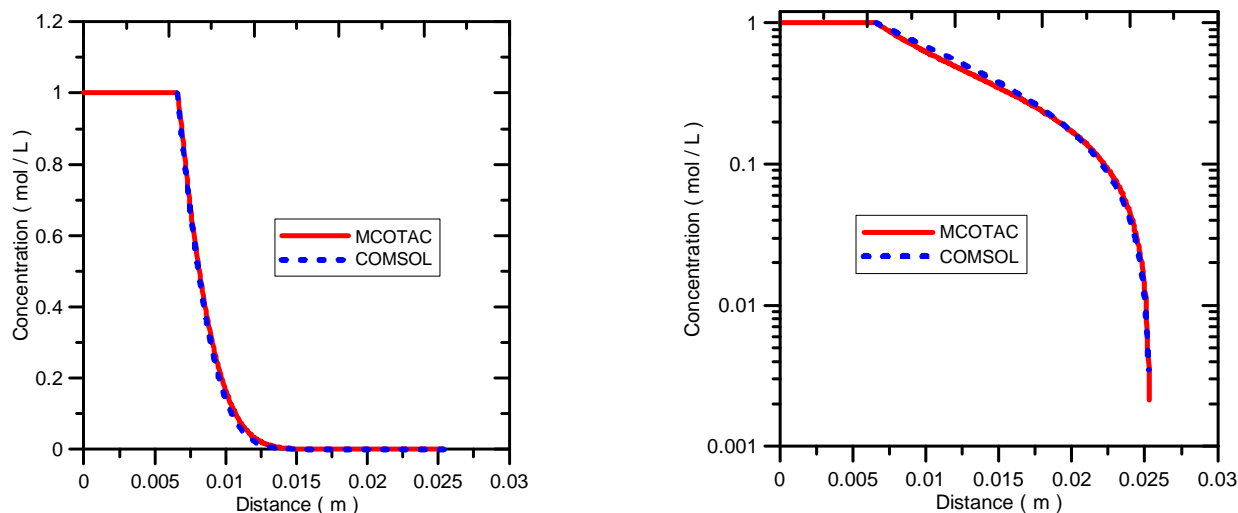


Fig. 3.2: Comparison of MCOTAC and COMSOL profiles for a well-defined set-up. Calculation of single species diffusion into a cylindrical clay sample is plotted at 0.058 days (left) and 2.443 days (right).

The new model was applied to laboratory through diffusion experiments with HTO, ^{22}Na and ^{36}Cl tracers (VAN LOON et al., 2004), taking full account of the individual transport parameters of filters and sample. Moreover a time-decreasing tracer concentration in the high concentration reservoir due to tracer diffusion from the reservoir was considered.

Two HTO diffusion experiments with different high-concentration-reservoir volumes were reported by VAN LOON et al. (2004). The larger reservoir volume resulted in smaller variation of the HTO concentration thus mimicking a constant concentration boundary. Modelling this experiment with the new more detailed set-up allowed considering different porosities and diffusion coefficients for the filters and sample, and a slight decrease in HTO concentration in the high concentration reservoir. In this modelling, the same best fit parameters as reported in the literature were obtained. The results that were obtained using the new set-up in the case of the small reservoir volume (where the HTO concentration decreased remarkably) were also in agreement with the literature where identical transport parameters for filter and sample have been used.

The situation was different in the diffusion experiment with sorbing ^{22}Na . Using the more detailed model set-up different best fit parameters for D_e and K_d (Fig. 3.3) were obtained. This can be explained by the fact that the effects of a) the no-sorption of ^{22}Na on the filters and b) the sorption of ^{22}Na on the clay sample, due to different porosity and diffusion coefficients for the filters and sample, cannot be modelled using the same mean transport parameters identical for both. For the diffusion experiment with ^{36}Cl slightly different fit parameters were obtained as well.

After comparing the results of the simplified model approach and the more detailed model approach, it is concluded that it is essential to take into account all the experimental details in the modelling in order to deduce more accurately the sample transport parameters, as for example was done in JAKOB et al. (2009). However, in some cases both the simple and the detailed model set-ups may result in the same best fit parameters (e.g. HTO diffusion experiment).

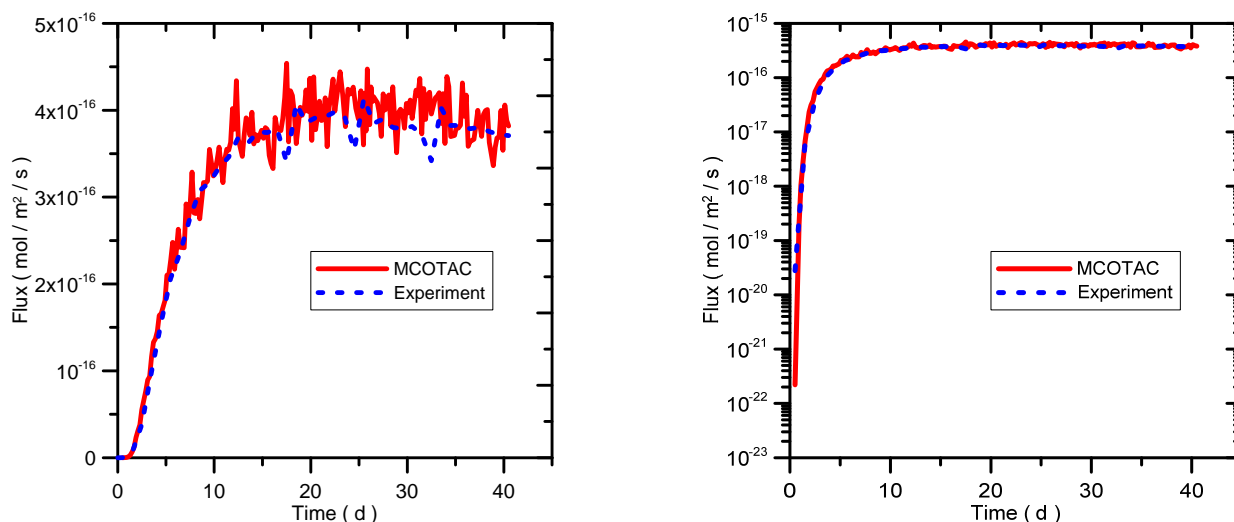


Fig. 3.3: Measured (experiment) and calculated (simulation) flux for radial ^{22}Na diffusion through a clay sample.

3.2.6 Uncertainty propagation of the Linear-Free-Energy-Relationship sorption parameters when applied in reactive transport calculations

For safety assessments of high level radioactive waste repositories in deep geological formations, the understanding of radionuclide sorption is of major importance. So far, calculations for safety assessments use a simple K_d approach to calculate individual radionuclide retardation. These K_d approaches are successfully supported by much more sophisticated sorption models that include several sorption reactions on mineral surfaces, ion exchange reactions, etc. for which not all sorption model

parameters could be measured up to now. BRADBURY & BAEYENS (1997) developed a sophisticated sorption model for cations on clay minerals. They also suggested a Linear Free Energy Relationship (LFER) used to calculate surface complexation constants for cations on minerals. These constants were deduced from hydrolysis constants for cations where a lot of experimental data are available. The derivation of the LFER is accompanied by an uncertainty regarding the calculated values of the surface complexation constants, given in the following equations (BRADBURY & BAEYENS 2005) for strong and weak sites in the case of Na-montmorillonite:

$$\text{Strong sites: } \log^S K_{(x-1)} = 8.1 \pm 0.3 + (0.90 \pm 0.02) \log^{OH} K_x \quad (3.1)$$

$$\text{Weak sites: } \log^{W1} K_{(x-1)} = 6.2 \pm 0.8 + (0.98 \pm 0.09) \log^{OH} K_x \quad (3.2)$$

An analysis of the propagation of this uncertainty is necessary when using this data in reactive transport calculations. This analysis was carried out with the reactive transport code MCOTAC (PFINGSTEN 1996, 2002, 2011) for Ni(II) migration through compacted bentonite as an example of bivalent metal migrating through Na-montmorillonite. Two different bentonite types (MX-80 and FEBEX) were studied taking into consideration sorption competition of Ni(II) and Fe(II). This increases the uncertainty space since the surface complexation constants for Ni(II) and Fe(II) are involved in the reactive transport calculation for the Ni(II) migration. The geochemical system set-up consists of a water-saturated Na-montmorillonite with a porewater composition according to NAGRA (2002), where at one side at $x=0$ m Ni(II) leaches into the Na-montmorillonite at constant (solubility

limited) concentration. Ni(II) breakthrough is calculated at $x=0.6$ m, which corresponds to about a foreseen thickness of a bentonite buffer around waste containing steel containers in a high level repository. Sorption competition causes a reduction in the sorption of Ni(II), and consequently its faster migration.

In Fig. 3.4 Ni(II) breakthrough curves are shown using the maximum, reference and minimum values of the surface complexation constants calculated according to the LFER (Eqs. 3.1 and 3.2). Comparison of the breakthrough curves shows that the bandwidth of the surface complexation constants transfers to a relative spread of the breakthrough curves within a range of several hundreds of years (range of 700 years at the concentration breakthrough level of 10^{-7} M at time = 700 years).

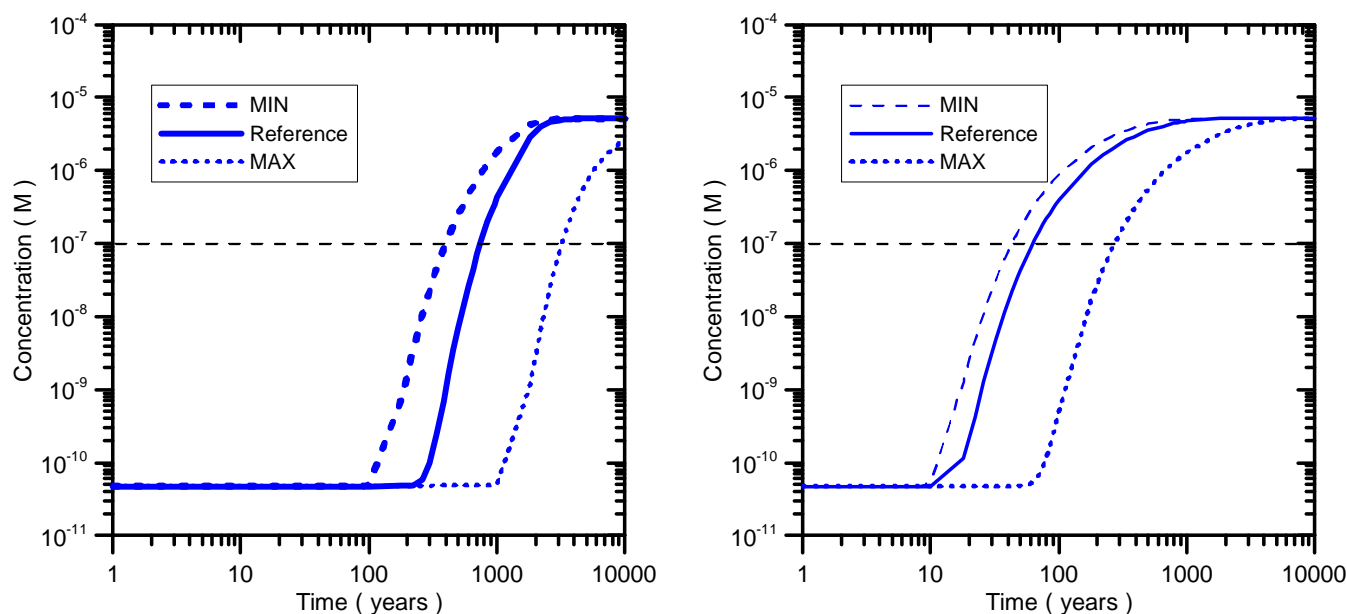


Fig. 3.4: Ni(II) breakthrough curves at $x=0.6$ m into the MX-80 bentonite calculated for the LFER uncertainty range with MCOTAC. Ni(II) level is 10^{-5} M; (left) no sorption competition with Fe(II) is assumed; (right) sorption competition with Fe(II) is assumed.

For the case where sorption competition with Fe(II) was considered, the increase of the uncertainty space due to the incorporation of the Fe(II) surface complexation constants leads to an increased relative spreading of the calculated Ni(II) breakthrough curves (range of 300 years at the concentration breakthrough level of 10^{-7} M at time = 60 years). This is explained by the fact that Ni(II) breakthrough takes place at earlier times.

This, apparently straightforward, analysis demonstrates the propagation of the uncertainty inherent to the sorption constants derived based on the LFER when applied to reactive transport calculations. For the bentonite backfill of a deep geological repository, the calculated uncertainties for Ni(II) breakthrough comprise several hundreds of years, which is apparently not of high significance compared to other processes. More important is to account the other relevant phenomena such as sorption competition with Fe(II). In addition, the uncertainty of values for the surface complexation constants calculated using the LFER should be considered when modelling the diffusion of radionuclides in laboratory experiments. In this case, the uncertainty of the sorption parameter affects directly the determination of the diffusion coefficient.

3.2.7 Experimental observation of porosity change at a cement-clay interface

In the project "Evolution of cement-clay interfaces" (PhD student Amir Shafizadeh) a heavy water (D_2O) diffusion experiment on a) two fresh interfaces (1 day old), and b) an aged one (273 days old) were

performed to explain the observed changes in water content at several cement-clay interfaces detected by neutron radiographs (Progress Report 2013),

The propagation of the D_2O front, resolved in time and space, across the interface was measured using cold neutrons at the ICON facility of SINQ, PSI. The D_2O was introduced from the cement side, to diffuse into the porewater (H_2O) which is present in the cement and clay pore space. The difference in neutron scattering properties of these two types of water (D_2O vs H_2O) makes possible the observation of the spatially resolved dynamics of the D_2O diffusion. The acquired radiographs were geometrically aligned and the black- and white-spots due to γ -radiation as well as the pixel failures were filtered out (gamma filter). The images were further corrected for dark current (image with closed shutter), for spatial heterogeneity of the beam and the detector (open beam correction), and for average beam intensity (dose correction with internal standard). Finally, the post-processed images, which were obtained at different times, were normalized using a reference image in order to obtain the transmission images.

Diffusion through the fresh interface samples occurred according to the original diffusion parameters of these materials, as expected. In contrast, a sharp change in D_2O concentration is observed at the interface of the aged sample (Fig. 3.5). This can be explained by porosity changes at the interface, and reduced diffusive flux of D_2O through the interface.

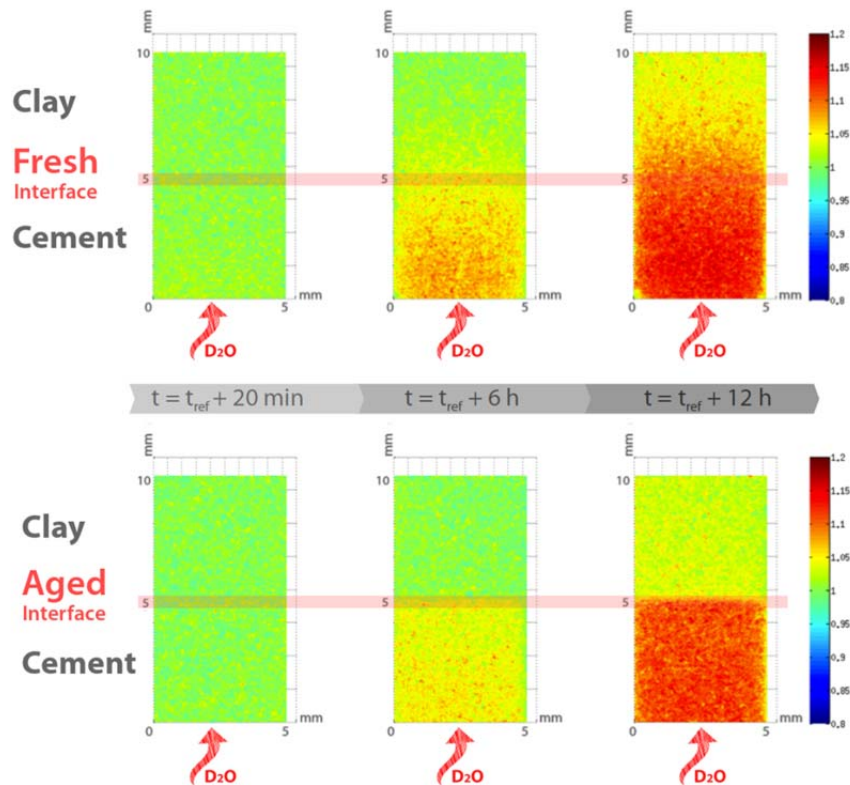


Fig. 3.5: Selected time series of transmission images of D_2O diffusion (normalized to t_{ref}) across an aged interface (lower set of plots) and a fresh one (upper set of plots) measured using a neutron beam. Higher values (in red) indicate higher D_2O to H_2O ratio relative to t_{ref} . The D_2O was introduced to the cement part of the sample (bottom).

3.3 Fundamental understanding of transport and sorption mechanisms

3.3.1 Water transport in cement revealed by NMR relaxometry and molecular simulations

Calcium silicate hydrates (C-S-H) are complex nanoporous materials which are responsible for the retention of radionuclides and water transport in cement. Nuclear magnetic resonance (NMR) relaxation experimentation is an effective technique for probing the dynamics of proton spins in porous media but interpretation requires the application of appropriate spin diffusion models. In collaboration with the University of Surrey (UK) within TRANSCEND FP7 Marie Curie ITN, molecular simulations were applied to predict NMR relaxation parameters using a dipolar spin-spin correlation function. Water dynamics was modeled for the interlayer (slit pore) and an external 1 nm sized pores (gel pore) in tobermorite. Diffusion in the slit pores occurs largely through discrete site hopping. While the 2D diffusion coefficient in the gel pore was of the same order of magnitude as in bulk water, it was more than two orders of magnitude smaller in the slit pores. The NMR relaxation parameters obtained in

simulations helps to improve interpretation of NMR measurement in cement and obtain better knowledge on the exchange rate of water between gel and slit pores as well as to characterize pore size distribution in C-S-H.

3.3.2 Multi-scale molecular modelling of ion sorption by C-S-H phases

During 2014, the post-doc project "Thermodynamic equilibrium in C(-A)-S-H (Calcium-(Aluminium)-Silicate-Hydrate) from molecular simulations" (L. Pegado), a subproject of the SNF-funded Sinergia project "Stable phase composition in novel cementitious materials: C(-A)-S-H", has been continued through the project "A thermodynamic model for C-S-H/C-A-S-H from a bottom-up approach". The latter is financed mainly by NANOCEM, the Industrial-Academic Research Network on Cement and Concrete. By means of multi-scale molecular modelling, the goal is to refine a thermodynamic model for ion sorption by C-S-H at the level of a single C-S-H/C-A-S-H particle. The result can be used to support and provide input to macroscopic phenomenological thermodynamic models. The microscopic, single-particle model will incorporate a description of surface charge formation,

equilibrium with bulk electrolyte solutions, Si/Al substitution and silicate chain polymerization. Two milestones have been already reached during the reporting period:

- The mechanism of Al incorporation into C-S-H at low Ca to Si ratio has been addressed through large-scale ab initio calculations, showing that having Al in bridging tetrahedra is the thermodynamically favored state (PEGADO et. al. 2014).
- Ion sorption equilibrium in C-S-H was modeled through titrating Grand Canonical Monte Carlo (GCMC) simulations at the level of the Primitive Model of electrolytes but employing pK_a's for surface -OH groups previously calculated from ab initio molecular dynamics (AIMD). The model was found to satisfactorily reproduce available experimental data (Fig. 3.6). In particular, the charge-reversal of C-S-H particles, observed for high electrostatic coupling, is well reproduced (CHURAKOV et. al. 2014b).

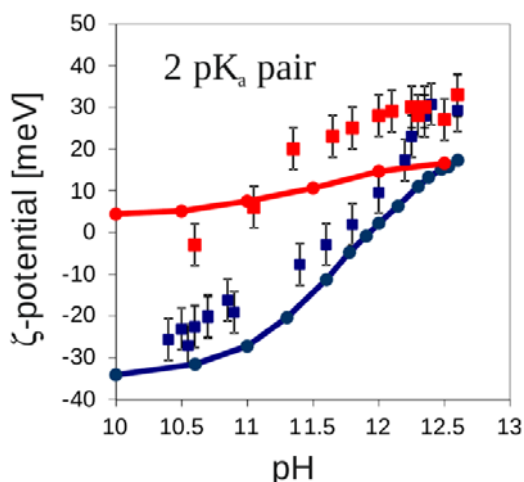


Fig. 3.6: Simulation (lines, blind prediction) and experimental (symbols) results for the zeta-potential of C-S-H particle dispersions in equilibrium with solutions of either $\text{Ca}(\text{OH})_2$ alone (blue) or a mixture of $\text{Ca}(\text{OH})_2$ and CaCl_2 (red) with a constant concentration of Ca^{2+} (20 mM).

Moreover, the calibration of classical polarizable force fields for $\text{Si}(\text{OH})_4$ and $\text{Si}(\text{OH})_3\text{O}^-$ in aqueous solution has been completed. It has been achieved by comparing with the water structure around a single molecule as obtained from first principles molecular dynamics simulations. It is now possible to calculate effective potentials (PMF's - Potentials of Mean Force) between different ions and relevant surface

groups in C-S-H from classical atomistic molecular dynamics simulations. The PMF's will be used further, in coarse-grained GCMC simulations of ion sorption to incorporate ion specific and solvent effects into the current models.

3.3.3 Up-scaling of diffusion coefficients: Scale dependent mobility of aqueous species

No single experimental or modelling technique provides data that allow a description of transport processes in clays and clay minerals at all relevant scales. Accordingly, several complementary approaches have to be combined to understand and explain the interplay between transport relevant phenomena. Molecular dynamics simulations (MD) were applied to investigate the mobility of water in the interlayer of montmorillonite, and to estimate the influence of mineral surfaces and interlayer ions on the water diffusion. Random walk (RW) simulations based on a simplified representation of pore space in montmorillonite were used to understand the effect of the arrangement of particles on the meso- to macroscopic diffusivity of water. In this way, the scale dependent diffusion of water in montmorillonite was evaluated (CHURAKOV et al. 2014a). According to the MD simulations, at very short timescales water dynamics has the characteristic features of an oscillatory motion in the cage formed by neighbors in the first coordination shell. At slightly larger, but still short times (~ 10 -100 ps) the limited width of the interlayer leads to a decreasing diffusion coefficient perpendicular to the interlayers and thus to locally anisotropic diffusion (Fig. 3.7). The RW simulations for an idealized sample map consisting of hexagon montmorillonite particles (Fig. 3.8) show also a decrease of the diffusion coefficients at early times, and then a further decrease at a normalized time T_h that corresponds to a diffusion distance equal to the typical length of the particles (or the length of individual pores). Such a detailed understanding of transport processes is needed for the correct interpretation of experimental data. It is thus expected that experimental diffusion coefficients depend on the timescales of the measurement. This was verified with QENS (Quasi Elastic Neutron Scattering) measurements of aqueous diffusion in montmorillonite with two pseudo-layers of water. The experiments were performed at four significantly different energy resolutions, that is, at four different observation times (Fig. 3.9). At observation times of 160 ps, local diffusion cannot be well described with an isotropic 3D diffusion model, but has features of a local 2D motion.

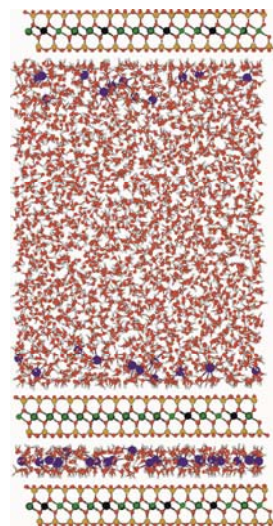
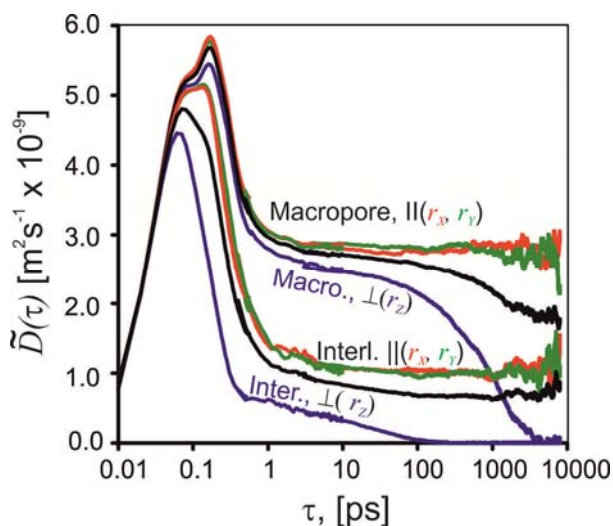


Fig. 3.7: Left: Scale dependent diffusion coefficients of water parallel (||) and perpendicular (⊥) to a basal montmorillonite plane obtained for an interlayer with two pseudo-layers of water (~0.5 nm thick) and a larger pore (macropore, ~6 nm thick). The black curves represent the orientation-averaged diffusion coefficients for the interlayer and the macropore. Right: Snapshot of the simulated system. Na-ions are blue, oxygen atoms are red, hydrogen atoms are white, silica atoms are brown, aluminum atoms are green and magnesium atoms are black.

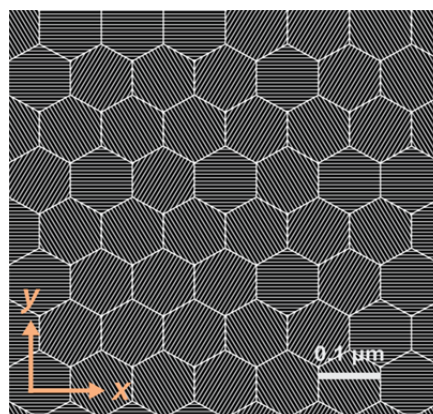
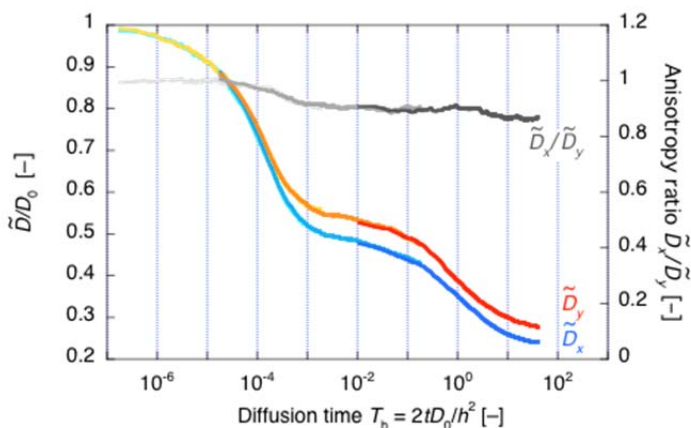


Fig. 3.8: Time evolution of normalized diffusion coefficients of water (left) derived from RW simulations for an idealized pore map consisting of hexagonal particles (right) with randomly oriented interlayers separated by interparticle pores with the same width as the interlayer pores. Results for three independent simulations for different time ranges are shown with increasing color saturation. At a diffusion time $T_h = 1$, a particle has diffused a distance h , where h is the width of a hexagon (0.1 micrometer).

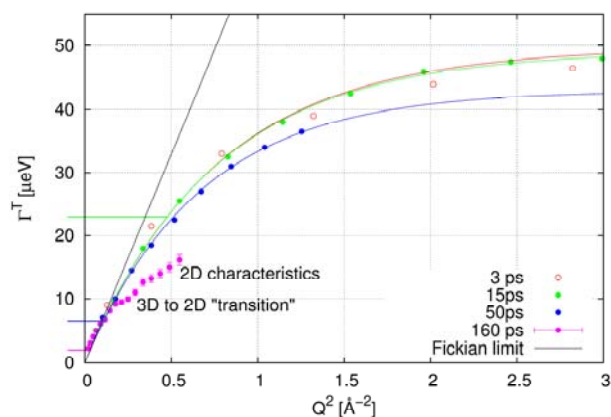


Fig. 3.9: Line broadening Γ^T (HWHM, half width at half maximum of peak) due to translational diffusion of water molecules in montmorillonite with two pseudo layers of water measured by QENS with different observation times. The data are fitted with a jump diffusion model. The horizontal markers on the y axis show the different instrument resolutions. All data points obtained for the observation time 3 ps are below the instrument resolution. The most important feature observed at the longest observation time (160 ps) is the reduced line width at high Q values. This feature is indicative for the transition from local 3D to apparent 2D diffusive motion of water in the interlayer.

3.3.4 Up-scaling of diffusion coefficients: Influence of interparticle pore width distribution

Random Walk simulations are well suited to investigate the relation between pore structure and sample-scale diffusion coefficients. For that purpose, a series of large clay structure maps (16'000 by 16'000 pixels) were modelled with a previously developed algorithm (TYAGI et al. 2013). The 2D structure maps had the same types of montmorillonite particles, but differed in their interparticle pore size distributions. The mean interparticle pore width was in all cases 3 nm, but the coefficient of variation of the width distribution was varied from 1.5 (rather uniform widths) to 12 (very broad distribution). A part of two sample maps and the resulting sample-scale diffusion coefficients are shown in Fig. 3.10. A broad interparticle pore width distribution leads to a lower sample-scale diffusion coefficient, i.e. a larger tortuosity, compared to a narrow distribution.

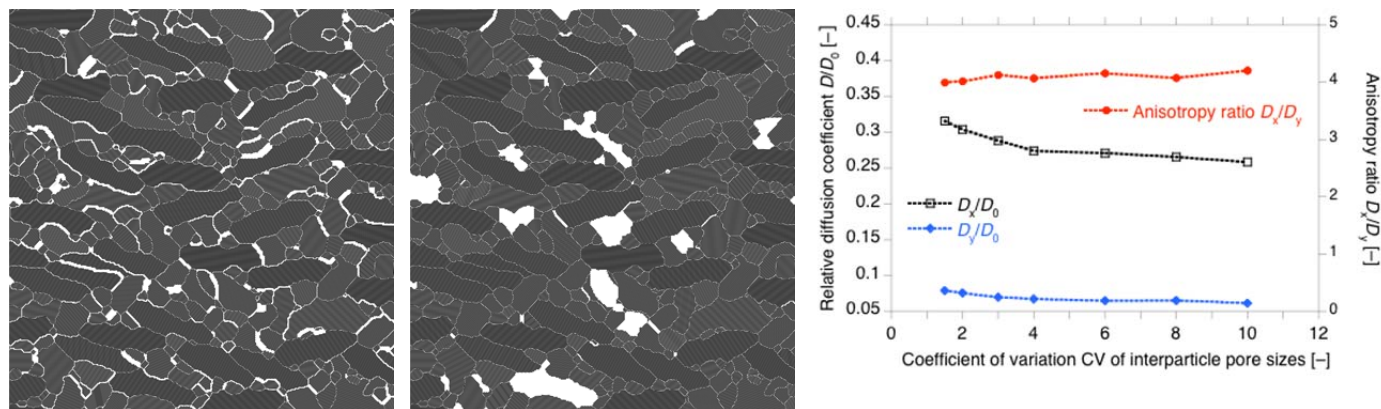


Fig. 3.10: Left: A small part (1/16) of the clay structure maps with a CV of the interparticle pore width distribution of 2 and of 10. Right: Sample-scale diffusion coefficients in x and y direction, normalized by the local water diffusion coefficient D_0 , and the corresponding anisotropy ratio obtained for different coefficients of variation of the interparticle pore width distribution.

3.4 Benchmarking and validation of coupled codes

3.4.1 Cooperation with Centre for Environmental Research, Leipzig

In 2014, the co-operation with the Helmholtz Centre for Environmental Research (UFZ, Leipzig, Germany), in the field of reactive transport, was concentrated on the application of the coupled code OpenGeoSys-GEM and on the evaluation of multiphase- and multicomponent-problems. The most recent cooperation is related to the modelling of the humidity transport and consumption of water in waste packages which is tightly coupled not only to liquid saturation, but also to several geochemical processes (metal corrosion, carbonation, internal degradation, degradation of organic wastes).

At the UFZ the next generation of the multi-physics code OpenGeoSys solver (OGS6) is under development. OGS6 will improve the usability of the user interface and the quality of the underlying code, in order to simplify code maintenance and make it easier to add user-specific modules. In addition OGS6 is specifically designed to run on HPC (High Performance Computers). Currently there are intense discussions how to migrate the existing OGS-GEM coupling to OGS6. Such a new coupling would profit from better scalability on HPC systems and from the new modular structure, which makes it much easier to tailor the coupling to specific applications.

The contacts between PhD students of both institutions were further fostered. Additionally, a joint journal publication on the latest OpenGeoSys-GEM version was published (KOSAKOWSKI & WATANABE 2014).

3.4.2 Experimental benchmarks for the verification and validation of reactive transport codes

The changes of the porosity in a porous medium due to mineral alteration processes, and the associated change of transport parameters influence the evolution of natural or engineered underground disposal systems. In the framework of a PhD project partially supported by Nagra (J. Poonoosamy), and for the validation and benchmarking of numerical codes, experiments along the line of the ones proposed by TROTIGNON et al. (2005) & COCHEPIN et al. (2008) have been conducted. The aim was to use a simple chemical set-up, and to design a

reproducible and fast to conduct experiment, including several process couplings: advective-diffusive transport of solutes, effect of liquid phase density on advective transport, kinetically controlled dissolution/precipitation reactions causing porosity changes.

A transparent quasi 2D tank with dimensions 0.1 m by 0.1 m (Fig. 3.11) with thickness of 0.01 m was filled with a granular porous media (SiO_2). A 0.01 m thick reactive layer of celestite (SrSO_4) was placed in the middle of the tank. The reactive layer was composed by a mixture of small and large celestite grains. A highly concentrated solution of barium chloride (BaCl_2) was injected at a steady rate. Once the barium-rich solution reaches the reactive layer, the celestite dissolves and nearly pure barite (BaSO_4) precipitates. Due to larger molar volume of barite compared to celestite, its precipitation in the reactive media is likely to cause porosity decrease. During the course of the experiment, changes in flow field (monitored by dye tracer test) were observed, suggesting local permeability changes. Post mortem analysis of the reactive layer by micro X-ray diffraction (μ -XRD) and microscopy techniques (Fig. 3.12) suggest that large celestite grain were passivated by a barite layer. Nanocrystalline grains of barite replacing small celestite grains precipitate in the pore space, cementing the larger celestite crystals and in some cases disjoint the pore space locally.

The experiments were modelled using the reactive transport code OpenGeosys-GEM (SHAO et al. 2009, KOSAKOWSKI & WATANABE 2013) and the major experimental features of the experiment were successfully reproduced (POONOOSAMY et al. 2014).

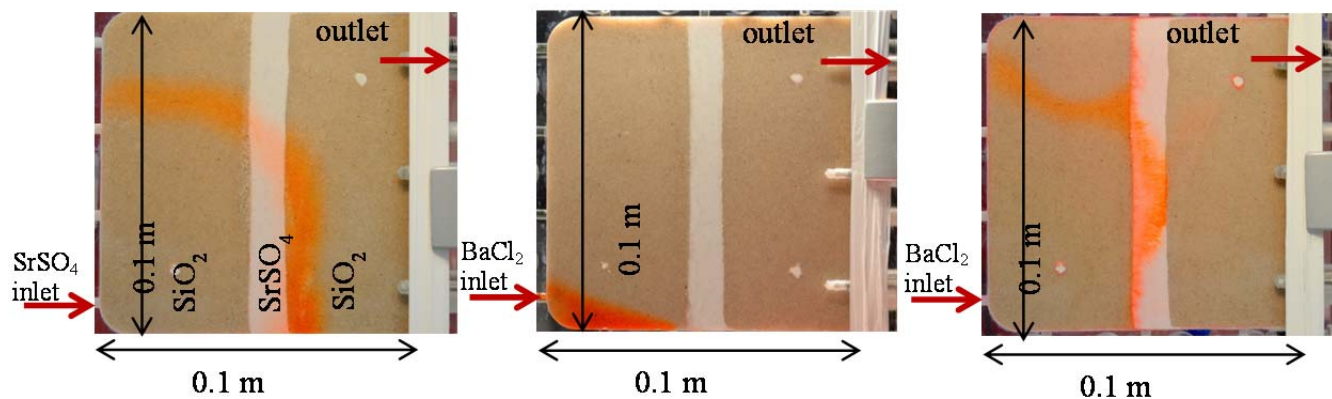


Fig. 3.11: Dye tracer profile profiles (from left to right) of transport experiment with no chemical reaction, reactive transport experiment with a density effect due to injection of a barium chloride and reactive transport experiment after porosity decrease.

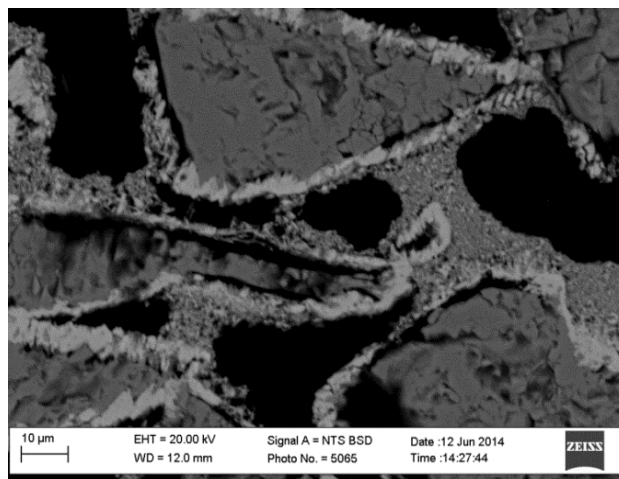
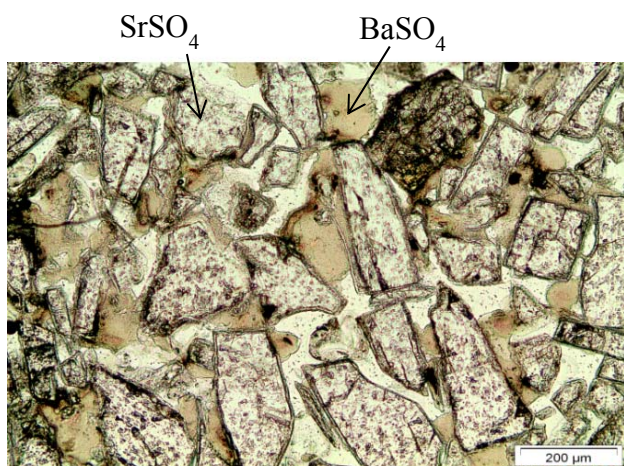


Fig. 3.12: Microscopic view of cross sectional area of the celestite region. Left: optical microscope, Right: scanning electron microscope (an image using Back Scattered Electrons).

3.5 References

- BERNER U., KULIK D.A., KOSAKOWSKI G. (2013)
Geochemical impact of a low-pH cement liner on the near field of a repository for spent fuel and high-level radioactive waste. *Phys. Chem. Earth* 64, 46–56.
- BRADBURY M. H., BAEYENS B. (1997)
A mechanistic description of Ni and Zn sorption on Na-montmorillonite Part II: modelling. *J. of Contam. Hydrol.* 27(3-4): 223-248.
- BRADBURY M. H., BAEYENS B. (2005)
Modelling the sorption of Mn(II), Co(II), Ni(II), Zn(II), Cd(II), Eu(III), Am(III), Sn(IV), Th(IV), Np(V) and U(VI) on montmorillonite: Linear free energy relationships and estimates of surface binding constants for some selected heavy metals and actinides. *Geochim. Cosmochim. Acta* 69(4): 875-892.
- CHURAKOV S.V., GIMMI T., UNRUH T., VAN LOON L.R., JURANYI F. (2014a)
Resolving diffusion in clay minerals at different timescales: Combination of experimental and modelling approaches. *Appl. Clay Sci.* 96, 36-44.
- CHURAKOV S.V., LABBEZ C, PEGADO L., SULPIZI M. (2014b)
Intrinsic acidity of surface sites in calcium-silicate-hydrates and its implication to their electrokinetic properties. *J. of Phys. Chem. C*, 118, 11752.
- COCHEPIN B., BILDSTEIN O., STEEFEL C., LAGNEAU V., VAN DER LEE J. (2008)
Approaches to modelling coupled flow and reaction in a 2D cementation experiment. *Adv. Water Res.*, 31, 1540-1551.

- ENRESA (2002)
Full-scale engineered barriers experiment for a deep geological repository for high level radioactive waste in crystalline host rock. Final Report. Madrid, Spain.
- HUMMEL W. (2009)
Ionic strength corrections and estimation of SIT ion interaction coefficients. PSI internal report TM-44-09-01, Paul Scherrer Institut, 5232 Villigen PSI, Switzerland.
- JAKOB, A., PFINGSTEN, W., VAN LOON, L. (2009)
Effects of sorption competition on caesium diffusion through compacted argillaceous rock. *Geochimica et Cosmochimica Acta* 73(9): 2441-2456.
- KOSAKOWSKI G., BERNER U. (2013)
The evolution of clay rock/cement interfaces in a cementitious repository for low- and intermediate level radioactive waste. *Phys. Chem. Earth* 64, 65–86.
- KOSAKOWSKI G., BERNER U., WIELAND E., GLAUS M.A., DEGUELDRE C. (2014)
Geochemical evolution of the L/ILW near field. Nagra Technical Report NTB 14-11, Wetingen, Switzerland, Nagra.
- KOSAKOWSKI G., SMITH P. (2014)
Long-term evolution of the engineered gas transport system. Nagra Arbeitsberichte NAB 14-16, Nagra, Wetingen Switzerland.
- KOSAKOWSKI G., & WATANABE N. (2014)
OpenGeoSys-Gem: A numerical tool for calculating geochemical and porosity changes in saturated and partially saturated media. *Physics and Chemistry of the Earth* 70-71, 138-149
- NAGRA (2002)
Project Opalinus Clay: Safety Report. Demonstration of Disposal Feasibility for Spent Fuel, Vitriified High-level Waste and Long-lived Intermediate-level Waste. Nagra Technical Report NTB 02-05. Wetingen, Switzerland.
- PEGADO L., LABBEZ C, CHURAKOV S.V. (2014)
Mechanism of aluminium incorporation in C-S-H from ab initio calculations. *Journal of Materials Chemistry A*, 2, 3477
- PFINGSTEN W. (1996)
Efficient modelling of reactive transport phenomena by a multispecies random walk coupled to chemical equilibrium. *Nuclear Technology* 116(2): 208-221.
- PFINGSTEN W. (2002)
Experimental and modelling indications for self-sealing of a cementitious L&ILW repository by calcite precipitation. *Nuclear Technology* 140(1): 63-82.
- PFINGSTEN W., BRADBURY M.H., BAEYENS B. (2011)
The influence of Fe(II) competition on the sorption and migration of Ni(ii) in MX-80 bentonite. *Applied Geochemistry* 26(8), 1414-1422.
- POONOOSAMY J., KOSAKOWSKI G., VAN LOON L., MÄDER U. (2014)
Dissolution-precipitation process in tank experiments for testing numerical models for reactive transport calculations (in preparation).
- SHAO H., DMYTRIEVA S., KOLDITZ O., KULIK D., PFINGSTEN D., KOSAKOWSKI G. (2009)
Modelling reactive transport in non-ideal aqueous–solid solution system. *Applied Geochemistry*, 24(7), 1287–1300.
- THOENEN T. (2012)
SIT data base for NaCl solutions. Priv. comm.
- TROTIGNON L., DIDOT A., BILDSTEIN O., LAGNEAU V., MARGERIT Y. (2005)
Design of a 2D cementation experiment in porous medium using numerical simulation. *Oil & Gas Science and Technology - Rev. IFP*, 60, 307-318.
- TYAGI M., GIMMI T., CHURAKOV S.V. (2013)
Multi-scale micro-structure generation strategy for up-scaling transport in clays. Submitted. *Advances in Water Resources*, 59, 181–195, DOI: 10.1016/j.advwatres.2013.06.002 .
- VAN LOON L.R., SOLER J.M., MUELLER W., BRADBURY M.H. (2004)
Anisotropic diffusion in layered argillaceous rocks: A case study with Opalinus Clay. *Environ. Sci. Technol.* 38, 5721-5728.
- COMSOL Multiphysics:
<http://www.comsol.com>
- NANOCEM research network:
<http://www.nanocem.org>

4 CLAY SORPTION MECHANISMS

B. Baeyens, R. Dähn, M. Marques Fernandes, A. Schaible, E. Eltayeb, D. Soltermann (PhD student)

4.1 Overview

Several activities in the framework of Stage 2 of the Sectoral Plan for Deep Geological Disposal (SGT-E2) have been completed in 2014. This work comprised of the following topics.

- As input for the provisional safety analyses for SGT-E2, sorption data bases (SDBs) for the different host rocks (Opalinus Clay, 'Brauner Dogger', Effingen Member, Helvetic Marl), the underlying confining units, and MX-80 bentonite were finalised (BAEYENS et al. 2014a). This report also evaluates the influence of a high pH plume on the SDBs.
- Sorption isotherm measurements on the potential host rocks (BAEYENS et al. 2014b) have been completed. Data sets on Helvetic Marl and 'Brauner Dogger' and Effingen Member with low clay contents have been included in addition to the data for Opalinus Clay. The experimental results were compared to blind predictions calculated using the same methodology developed to derive the sorption values given in the SDBs.

Mechanistic sorption studies on clay minerals are ongoing activities. These include:

- The Swiss-Hungarian co-operation project (Swiss Contribution) entitled "*Development of a macro- and microscopic approach to investigate the geochemistry of radioactive waste disposal systems*" has finished in September this year. The project aimed at validation of sorption modelling approach on the two argillaceous rocks, namely Boda Clay and Opalinus Clay.
- The PhD thesis entitled "*Ferrous iron uptake mechanisms at the montmorillonite-water interface under anoxic and electrochemically reduced conditions*" has been successfully completed. The defense took place on 10 July 2014 at the ETH Zürich. The results of this PhD study were reported in four papers published in the journal "Environmental Science & Technology". Two of these, dealing with the Fe(II) interaction and modelling on natural Fe bearing montmorillonites, were published this year (SOLTERMANN et al. 2014a,b).

Mechanism of sorption processes and spectroscopic studies

- The Swiss National Foundation (SNF) has approved a new PhD project entitled "*Detailed understanding of metal adsorption on clay minerals obtained by combining atomistic simulations and X-ray absorption spectroscopy*". The project is expected to start early 2015.
- The 7th Actinide XAS workshop (AnXAS 2014) was held from 20th to the 22nd of May 2014 at Schloss Böttstein.

4.2 Activities in support of the Sectoral Plan

In the first phase of the Sectoral Plan for Deep Geological Repositories, Nagra proposed six siting regions for low- and intermediate-level (L/ILW) and three siting regions for high-level (HLW) radioactive waste (NAGRA 2008). Provisional safety analyses for all siting regions are applied for site evaluation in Stage 2 of SGT. The host rocks considered are all classified as argillaceous rocks in which diffusion is the dominant transport mechanism for released radionuclides. A state-of-the-art sorption database is one of the key parameter sets needed for quantitative evaluation of radionuclide retardation in the host rocks and the bentonite buffer.

Sorption data bases for the argillaceous rocks (Opalinus Clay, 'Brauner Dogger', Effingen Member and Helvetic Marls), underlying confining units and bentonite under a wide range of porewater and mineralogical compositions were developed by BAEYENS et al. (2014a). The methodology was based on sorption edge measurements data for illite and montmorillonite, the assumption that 2:1 type clay minerals are the dominant sorbents, and so-called conversion factors which take into account the clay content of the argillaceous rocks and radionuclide speciation in the different porewaters. All of the host rocks selected by Nagra, i.e. Opalinus Clay, 'Brauner Dogger', Effingen Member and Helvetic Marls, and, MX-80 bentonite, contain significant fractions of 2:1 clay minerals such as illite, illite-smectite mixed layers and montmorillonite.

Since the methodology used for generating sorption values for SDBs is relatively new, its extensive validation is needed. A series of sorption isotherms for representative radionuclides were measured under realistic chemical conditions on potential host rocks and compared with model-based calculations for

trace concentrations. Co(II) and Ni(II) were chosen as being representative for divalent transition metals, Eu(III) for lanthanides and trivalent actinides, and Th(IV) for tetravalent actinides. Sorption isotherms for U(VI) were also measured. In total, 53 sorption isotherms with the elements Cs(I), Co(II), Ni(II), Eu(III), Th(IV) and U(VI) on Opalinus Clay, 'Brauner Dogger', Effingen Member, Helvetic Marls and MX-80 bentonite have been measured (BAEYENS et al. 2014b). The agreement between measured and calculated R_d values for each rock type and the associated water chemistries was used as the measure of the model performance.

"Measured R_d values" at trace concentrations are plotted against the calculated R_d values in Fig. 4.1. The continuous line represents a 1:1 correspondence between the measured and calculated sorption values. Points falling below this line indicate under predicted

values whereas those above the line indicate over predicted values. The dashed lines encompass almost all of the measured data and illustrate that the maximum difference between the calculated and measured R_d values is generally at most a factor of ± 6 , i.e. ± 0.8 log units. Based on this, it is concluded that the methodology applied to derive sorption values in the SDBs for a wide range of host rock mineralogy and water chemistry combinations has a high degree of reliability and captures the sorption in real systems within the uncertainty bounds given.

From the information presented here, and previous studies (BRADBURY & BAEYENS 2010, 2011), there is now a substantial body of evidence which strongly supports the approach and methodology for developing SDBs for argillaceous rocks and bentonite as applied in BAEYENS et al. (2014a).

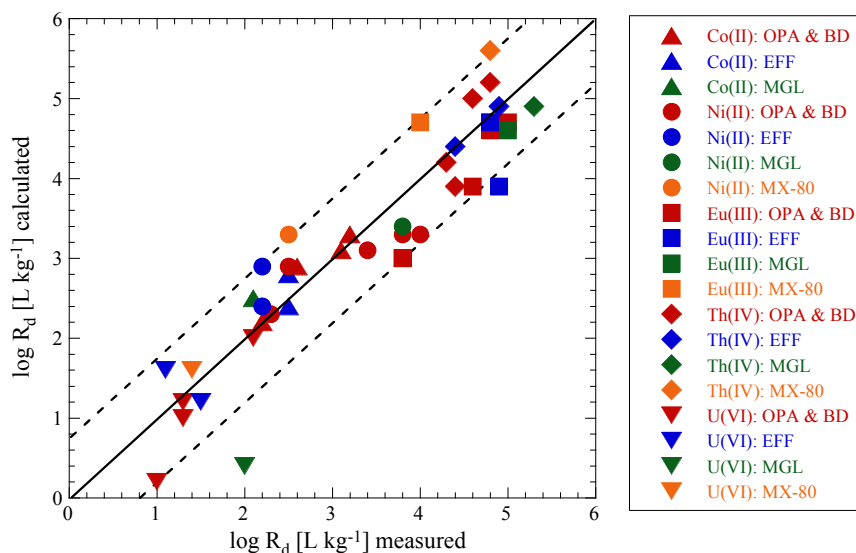


Fig. 4.1: Comparison of measured and calculated R_d at trace concentrations for Co(II), Ni(II), Eu(III), Th(IV) and U(VI) on Opalinus Clay (OPA), 'Brauner Dogger' (BD), Effingen Member (EFF), Helvetic Marls (MGL) and MX-80 bentonite (MX-80). The broken lines represent a band width of ± 0.8 log units.

4.3 Mechanistic sorption modelling

4.3.1 Sorption modelling of Eu, Th and UO₂ on Opalinus Clay and Boda Clay

In the framework of the Swiss Contribution agreement to the development of new EU-Members states (Schweizer Erweiterungsbeitrag) a cooperation project entitled "Development of a macro- and microscopic approach to investigate the geochemistry of radioactive waste disposal systems" has been set up between PSI/LES and the Hungarian Academy of Sciences, Centre for Energy Research (Budapest). The project started on 15 October 2010 and ended on 14 September 2014. The objectives were to make specific contributions to the safety

assessment of future radioactive waste repositories through a mechanistic understanding of relevant retention processes, and to provide the necessary models and data bases. These microscopic investigations were strongly linked to macroscopic studies and geochemical modelling.

An important aim of this project was to validate the hypothesis upon which the "bottom-up" approach for argillaceous rocks is based i.e. that the uptake of radionuclides in such complex systems is controlled by sorption on 2:1 type clay minerals. Fig. 4.2 summarizes the results for Eu, Th and UO₂ on the argillaceous rocks Ib-4 540 (Boda Clay) and SLA-938 (Opalinus Clay). Blind predictions were made by applying the 2SPNE SC/CE sorption model

developed for illite (BRADBURY & BAEYENS 2009), scaled to the 2:1 clays content, and, taking into account the aqueous speciation of the radionuclides in the porewaters. The methodology is illustrated in Fig. 4.2 where the broken red curves are the calculated sorption isotherm for pure illite in a 0.1 M NaClO₄ background electrolyte at the pH of the corresponding porewater. The broken blue lines are the calculated isotherms linearly scaled to the 2:1 clay content of Boda Clay and Opalinus Clay. The black solid lines are the blind predictions taking into account the aqueous speciation of the radionuclides in the porewater.

The Eu sorption isotherms on both rocks are under predicted by ~ 0.5 to 0.8 log units over the entire Eu(III) concentration range investigated. Since both porewaters are in equilibrium with atmospheric CO₂ partial pressure, the formation of Eu(III) carbonate surface complexes might increase the sorption.

However, at present such data are not available for illite. For Th and UO₂ the blind predictions fit very well the experimental data, the modelled curves for both elements on Boda Clay and Opalinus Clay lie within the experimental error bars.

Contrary to the expectations, other minerals present in Boda Clay, such as the zeolite analcime with its high cation exchange capacity (~ 4.5 eq·kg⁻¹ (GSA RESOURCES 2000)) and hematite, apparently do not contribute to the uptake of the studied elements. Despite the differences in the mineralogies and porewater chemistries of the studied argillaceous rocks, the approach described the uptake behaviour of the various metal ions on both systems quite well, confirming the reliability and robustness of the "bottom-up" approach and the parameters of the sorption models. The results of the wet chemistry studies and sorption modelling have been submitted to Applied Geochemistry (MARQUES FERNANDES et al. 2014). The manuscript is currently under review.

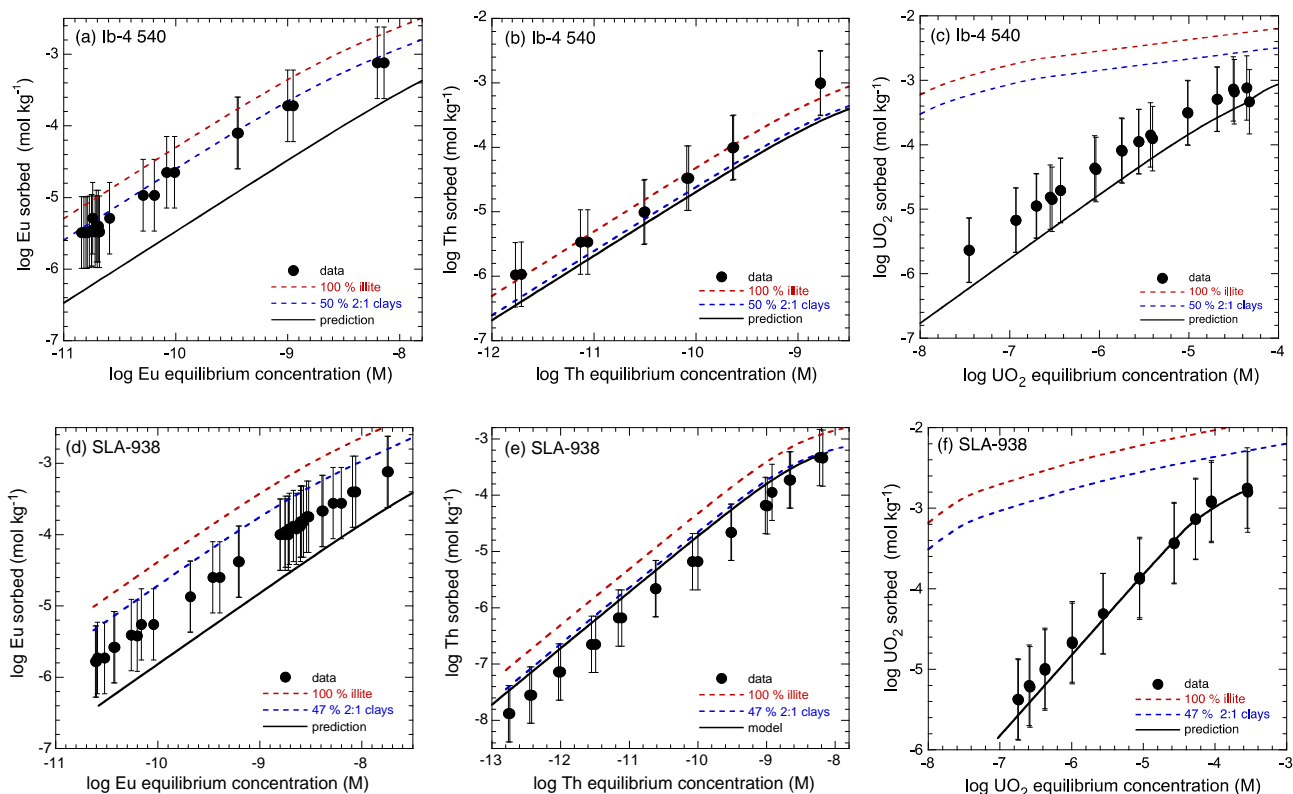


Fig. 4.2: Sorption isotherms of (a) Eu, (b) Th and (c) UO₂ on Boda Clay (Ib-4 540) and (d) Eu, (e) Th and (f) UO₂ on Opalinus Clay (SLA-938). Experimental results (symbols) and modelling (continuous line) using the "bottom-up" approach. The broken lines are the sorption on pure illite (red) and those scaled for the content of the 2:1 type clays (blue) in 0.1 M NaClO₄ background electrolyte at pH 7.7 (Boda Clay) and 7.9 (Opalinus Clay) (see text for details).

4.3.2 Fe(II) uptake on natural montmorillonites: Macroscopic and spectroscopic characterization and surface complexation modelling (PhD project)

The PhD project of Daniela Soltermann entitled "*The influence of Fe(II) on clay properties, the sorption of Fe(II) on clays and competitive sorption investigations: a combined macroscopic and microscopic study*" (SNF Grant 200021-129947) focused on the understanding of the uptake of Fe(II) on natural iron bearing clay minerals combining wet chemistry studies and spectroscopic investigations. Sorption edges and isotherms were measured under anoxic conditions on a synthetic iron free montmorillonite (IFM) and two natural Fe-bearing smectites, i.e. STx and SWy having different structural Fe contents of 0.5 and 2.9 wt. %, respectively. The Fe(II) uptake as a function of Fe(II) concentration (isotherm) at pH 6.2 in 0.1 M NaClO₄ is shown in Fig. 4.3. The batch experiments clearly indicate that the uptake of Fe(II) on the Fe(III)-rich montmorillonite (SWy) is much more pronounced than on the low Fe-bearing (STx) and iron free (IFM) clays.

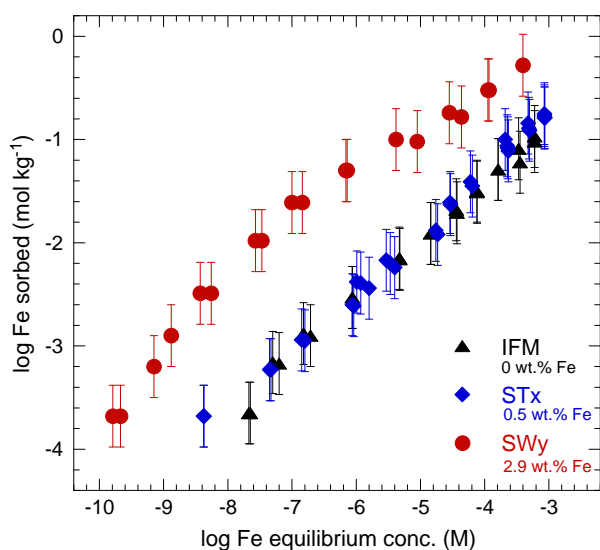


Fig. 4.3: Sorption isotherm data of Fe(II) on SWy, STx and synthetic IFM in 0.1 M NaClO₄ at pH 6.2.

Mössbauer spectroscopy analysis revealed that on Fe(III)-rich SWy at pH 6.2 nearly all the sorbed Fe(II) was oxidized to surface-bound Fe(III). In addition, the formation of secondary Fe(III) precipitates was observed at higher Fe(II) equilibrium concentrations. On Fe(III)-low STx montmorillonite the sorbed Fe is predominantly present as Fe(II). These results are illustrated in Fig. 4.4 (a-d). ⁵⁷Fe Mössbauer spectroscopy was also performed on ⁵⁶Fe loaded clays to probe the oxidation state of structural iron upon sorption of

Fe(II). The observed reduction of structural Fe(III) in SWy and STx unambiguously evidences the role of structural Fe(III) as an e⁻ acceptor (see Fig. 4.4 (e) and f).

These results provided compelling evidence that Fe(II) uptake behaviour on clay minerals are strongly correlated to the redox properties of the structural Fe. The improved understanding of the redox interactions between sorbed Fe(II) and clay minerals gained in this study was essential for developing the model for Fe(II) sorption on natural montmorillonites.

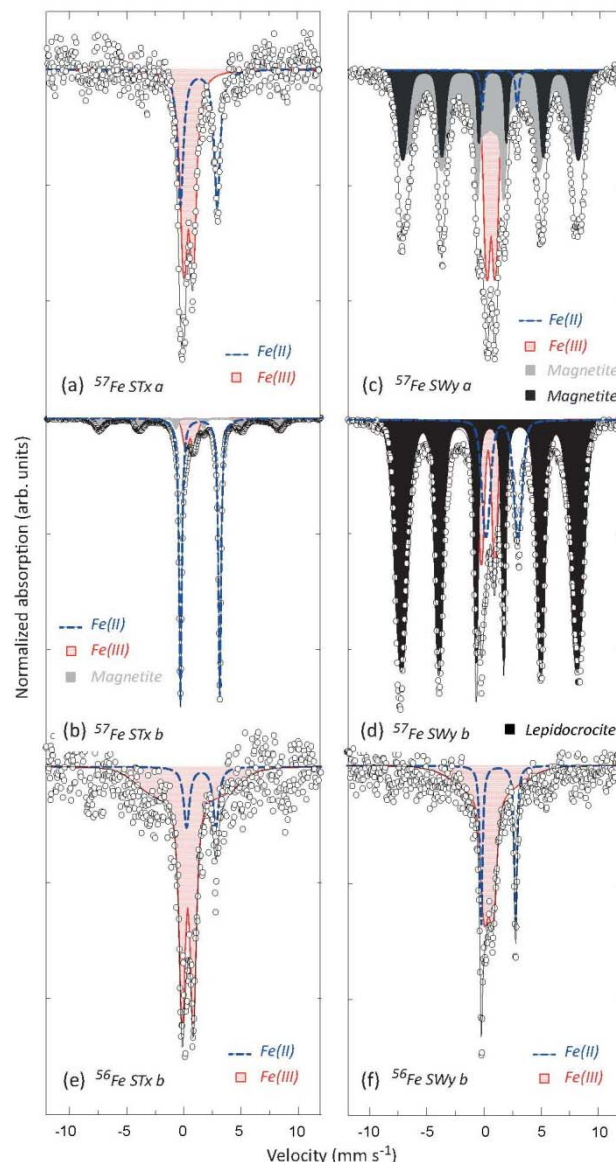


Fig. 4.4: Mössbauer spectra of STx (a,b) and SWy (c,d) reacted with ⁵⁷Fe(II) at ⁵⁷Fe loadings of (a) 9.5 mmol kg⁻¹, (b) 39.8 mmol kg⁻¹, (c) 49.0 mmol kg⁻¹ and (d) 128.8 mmol kg⁻¹. The corresponding Mössbauer spectra of STx and SWy reacted with invisible ⁵⁶Fe(II) shown in figures (e) and (f).

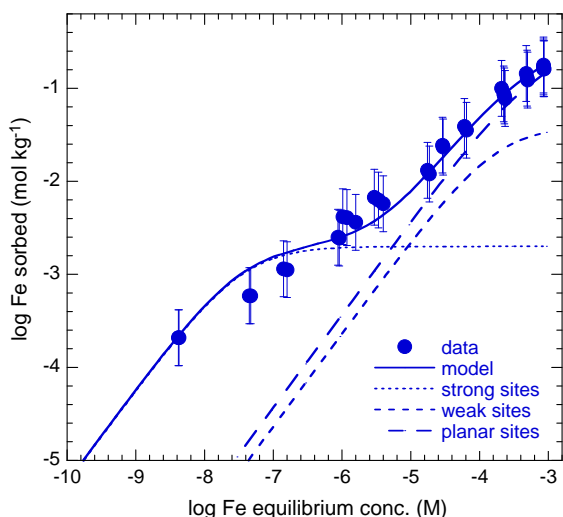
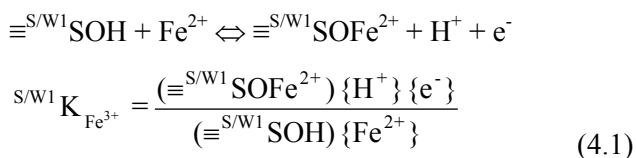


Fig. 4.5: Fe(II) sorption isotherm on STx at pH 6.2 in 0.1 M NaClO₄. The continuous line is the best-fit curve obtained using the 2SPNE SC/CE sorption model. The contributions of the Fe(II) surface species to the overall sorption are illustrated by the different broken curves.

The sorption of Fe(II) on the synthetic iron free and the Fe poor montmorillonite (STx) could be modelled with the 2SPNE SC/CE sorption model (BRADBURY & BAEYENS 1997) and the parameters given in Table 4.1. No electron transfer process needed to be considered (Fig. 4.5).

In contrary, for the sorption modelling on the Fe rich SWy montmorillonite under anoxic conditions an additional reaction involving oxidation of the surface bound ferrous iron was needed to be included in the existing sorption model. The overall surface complexation reaction with the corresponding surface complexation constant for this process is given in Eq. 4.1.



where () represent concentrations and {} activities.

To perform redox calculations and account for the redox state of the solutions, the common convention of the electron activity, $pe = -\log\{\text{e}^-\}$, was used. The results of the modelling are illustrated in Fig. 4.6 for the sorption isotherm measured at pH 6.2 using the parameters given in Table 4.1.

Table 4.1: Surface complexation constants and selectivity coefficient used in the 2SPNE SC/CE sorption model for montmorillonite (SOLTERMANN et al. 2014b).

Surface complexation reaction	$\log K_{SC}$	
	STx	SWy
$\equiv^S\text{SOH} + \text{Fe}^{2+} \leftrightarrow \equiv^S\text{SOFe}^+ + \text{H}^+$	1.7	1.7
$\equiv^{W1}\text{SOH} + \text{Fe}^{2+} \leftrightarrow \equiv^{W1}\text{SOFe}^+ + \text{H}^+$	-2.0	-2.0
$\equiv^S\text{SOH} + \text{Fe}^{2+} \leftrightarrow \equiv^S\text{SOFe}^{2+} + \text{H}^+ + \text{e}^-$	-	-1.7
$\equiv^{W1}\text{SOH} + \text{Fe}^{2+} \leftrightarrow \equiv^{W1}\text{SOFe}^{2+} + \text{H}^+ + \text{e}^-$	-	-3.8

Cation exchange reaction	$\log K_c$	
	STx-1	SWy-2
$2\text{Na}^+\text{-clay} + \text{Fe}^{2+} \leftrightarrow \text{Fe}^{2+}\text{-clay} + 2\text{Na}^+$	0.8 ± 0.3	0.8 ± 0.3

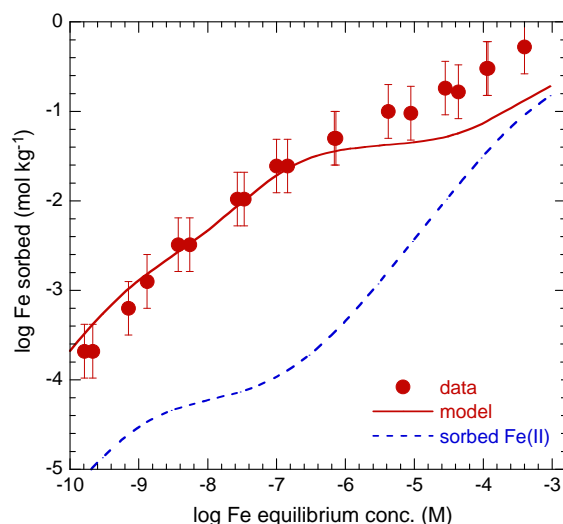


Fig. 4.6: Fe(II) sorption on SWy montmorillonite at pH 6.2 in 0.1 M NaClO₄. The continuous line is the best-fit curve obtained using the 2SPNE SC/CE sorption model. The contributions of the Fe(II) surface species to the overall sorption is illustrated by the dashed blue line. The data points at Fe concentration above $5 \cdot 10^{-6} \text{M}$ indicates a region of probable precipitation of ferric iron phases (see Mössbauer).

Fe(II) sorption experiments on STx and SWy were also carried out under electrochemically reducing conditions ($E_h = -0.64 \text{ V/SHE}$). The results of these measurements were in agreement with the model prediction for reducing conditions and thus validated the extended sorption model for Fe(II) over a wide range of redox conditions ($-0.64 \text{ V} \leq E_h \leq +0.28 \text{ V}$) and Fe(II) equilibrium concentrations.

As an example of its application the sorption model presented here was applied to the bentonite near field concept of a Swiss high-level radioactive waste repository. The near field is reducing ($E_h \sim -0.20$ V at pH 7.8) and the porewater contains relatively high Fe(II) concentrations, ca. 10^{-5} M (saturation with siderite). Because of potential competitive sorption effects, it is important to understand what the dominant iron surface complexes are. The sorption model predicted that the iron sorbed on the montmorillonite surface will be predominantly present as Fe(II) and therefore competitive sorption with divalent radionuclides in the radioactive waste repository is to be expected. Clearly, similar calculations can be applied to natural and other engineered environmental systems to assess the influence of competitive sorption effects between iron and divalent transition metals on their mobility and bioavailability.

4.4 XAS related activities

4.4.1 SNF project

In the PhD project "*Detailed understanding of metal adsorption on clay minerals obtained by combining atomistic simulations and X-ray absorption spectroscopy*" funded by the SNF an innovative approach for the systematic improvement of the simulations results of EXAFS data and their comparison with the experiments will be developed. The aim of this study is to explain at an atomistic scale the retention mechanism of environmentally relevant elements, covering various oxidation states from III to VI on most common clay minerals, montmorillonite and illite, combining molecular simulations and spectroscopic measurements.

4.4.2 AnXAS 2014

The 7th Actinide XAS workshop (AnXAS 2014) was held from 20th to the 22nd of May 2014 at Schloss Böttstein with more than 60 participants. Actinide XAS is a series of international workshops which focus on the basic- and applied research of radioactive materials using synchrotron-based techniques. A total of 40 oral and 20 posters contributions presented at the workshop covered topics such as: Solution and Coordination Chemistry of the Actinides, Actinides in Environmental and Life Sciences, Solid State Chemistry and Physics of the Actinides, Theoretical and Modelling Tools, Facility Reports and Upcoming Techniques. During the poster session at the Swiss Light Source the participants had the opportunity to visit the various XAS beamlines, and especially the microXAS beamline, which allows the measurements of radioactive samples. The next Actinide XAS

workshop will be organized by the University of Manchester and held at the Diamond Light Source in 2016.



Fig. 4.7: Participants of the 7th Actinide XAS workshop (AnXAS 2014) at Schloss Böttstein.

4.5 References

- BAEYENS B., THOENEN T., BRADBURY M.H., MARQUES FERNANDES M. (2014a)
Sorption data bases for the host rocks and lower confining units and bentonite for provisional safety analyses for SGT-E2. Nagra Tech. Rep. NTB 12-04.
- BAEYENS B., MARQUES FERNANDES M., BRADBURY M.H. (2014b)
Comparison between host rock and bentonite sorption measurements and predictions using the SDB approach applied in the provisional safety analyses for SGT-E2. Nagra Tech. Rep. NTB 12-05.
- BRADBURY, M. H., BAEYENS, B. (1997)
A mechanistic description of Ni and Zn sorption on Na- montmorillonite. 2. Modelling. J. Contam. Hydrol. 27, 223-248.
- BRADBURY M. H., BAEYENS B. (2009)
Sorption modelling on illite. Part I: Titration measurements and the sorption of Ni, Co, Eu and Sn. Geochim. Cosmochim. Acta 73, 990-1003.
- BRADBURY M.H., BAEYENS B. (2010)
Comparison of the reference Opalinus Clay and MX-80 bentonite sorption data bases used in the Entsorgungsnachweis with sorption data bases predicted from sorption measurements on illite and montmorillonite. PSI Bericht Nr. 10-09 and Nagra Techn. Report NTB 09-07.
- BRADBURY M.H., BAEYENS B. (2011)
Predictive sorption modelling of Ni(II), Co(II), Eu(III), Th(IV) and U(VI) on MX-80 bentonite and Opalinus Clay: A "bottom-up" approach. Appl. Clay Sci. 52, 27-33.
- GSA RESOURCES (2000)
Cation-exchange capacity of zeolites. Cation-exchange: <http://www.gsaresources.com>

MARQUES FERNANDES M., VER N., BAEYENS B. (2014)

Application of the "bottom-up" approach for the predictive modelling of sorption isotherms on Hungarian Boda Clay and Swiss Opalinus Clay. Submitted to Appl. Geochem.

NAGRA (2008)

Begründung der Abfallzuteilung, der Barrierensysteme und der Anforderungen an die Geologie. Bericht zur Sicherheit und technischen Machbarkeit. Nagra Tech. Rep. NTB 08-05.

SOLTERMANN D., MARQUES FERNANDES M., BAEYENS B., DÄHN R., JOSHI P.A, SCHEINOST A.C, GORSKI C.A. (2014a)

Fe(II) Uptake on natural montmorillonites. I. Macroscopic and spectroscopic characterization. Environ. Sci. Technol. 48, 8688- 8697.

SOLTERMANN D., BAEYENS B., BRADBURY M.H, MARQUES FERNANDES M. (2014b)

Fe(II) Uptake on natural montmorillonites. II. Surface complexation modelling. Environ. Sci. Technol. 48, 8698-8705.

5 CEMENT SYSTEMS

E. Wieland, J. Tits, A. Laube, D. Kunz, B. Cvetković (post doc), H. Rojo Sanz (guest scientist)

5.1 Overview

Cementitious materials are an important component of the engineered barrier in the deep geological repositories for low-level and short-lived intermediate-level (L/ILW) and long-lived intermediate-level (ILW) radioactive wastes in Switzerland. The group "Cement Systems" carries out research on the long-term behaviour of safety relevant waste components in the cementitious near field, such as organic materials and ^{14}C bearing compounds formed in the course of the anoxic corrosion of irradiated steel, and on radionuclide-cement interactions with the aim of filling gaps in the existing cement sorption data base (SDB) used in performance assessment (PA).

In 2014 the group was responsible for the preparation of the final versions of the cement SDB (WIELAND 2014). This report is a part of the documentation for the Stage 2 of the SGT. Furthermore, a first draft of a report on the geochemical evolution of heterogeneities in the cementitious near field is currently being prepared. The SGT related experimental research programme focussed on: i) determination of the low molecular weight (LMW) organics produced during the anoxic corrosion of steel, ii) development of compound-specific ^{14}C AMS (accelerator mass spectrometry), iii) measurements of the chemical stability of acetic acid under the hyper-alkaline conditions of a cement-based near field, and iv) sorption mechanism studies within redox-sensitive, dose-determining Se(IV/-II) anions in hardened cement paste (HCP) and individual cement phases.

The studies on the release of LMW organic compounds during the anoxic corrosion of non-activated steel and the development of an analytical method sensitive enough for the determination of ^{14}C bearing compounds formed during the corrosion of activated steel are partially financed by Swissnuclear (Project title: *"Investigation on the chemical speciation of ^{14}C released from activated steel"*) and by the 7th EU Framework Programme project CAST (Carbon Source Term). In 2014 specific tasks within this project have been developed in co-operation with Prof. G. Schlotterbeck (Institute for Chemistry and Bioanalytics (ICB), University of Applied Sciences Northwestern Switzerland (FHNW), Muttenz, Switzerland) and PD Dr. S. Szidat (Department of Chemistry and Biochemistry, University of Bern, Switzerland).

The investigations of Se uptake mechanisms by cementitious materials under reducing conditions are partially financed by the German Federal Ministry of Education and Research in the framework of the Verbundprojekt "Immorad" (Grundlegende Untersuchungen zur Immobilisierung langlebiger Radionuklide durch die Wechselwirkung mit endlagerrelevanten Sekundärphasen; coordinator: Dr. Th. Schäfer (KIT-INE)). The project is carried out in collaboration with Dr. A.C. Scheinost (Rossendorf (ROBL) beamline at the ESRF).

5.2 Activities in support of the Sectoral Plan

A multi-barrier concept is foreseen to ensure the safe disposal of L/ILW and ILW in cement-based deep geological repositories (NAGRA 2002). The engineered barrier is composed of the waste matrix, the waste-containing steel drums, the emplacement containers for the steel drums, the backfill material used to fill vaults within the emplacement containers, and between emplacement containers and the liner. A report is currently being prepared with the aim of assessing the barrier function of the waste-containing steel drums by considering the reactivity of the waste materials inside waste packages (WIELAND et al. 2014). The waste sorts selected for the study are considered to be representative of waste packages to be emplaced in the L/ILW caverns: i) a resin-containing bitumized waste package, ii) a cemented waste package, and iii) resin-containing waste embedded in polystyrene. Information on the materials encapsulated in the waste packages is available from MIRAM (NAGRA 2008). The chemical processes considered are: i) anoxic metal corrosion due to the presence of steel, ii) degradation of organic waste materials present in the waste and/or used as embedding matrix (e.g. bitumen), and iii) dissolution of gravel used to make the waste-solidifying concrete. The kinetics of these processes was assessed based on information available in the literature. Mass balance calculations were carried out to determine the amount of water available in the waste packages because all the above-mentioned chemical processes consume water. The results show that the amount of water limits the extent of reaction of the materials in the waste packages.

In particular, the cemented waste matrices and the resin-containing waste embedded in polystyrene are more reactive than the resin-containing bitumized waste matrices due to a factor 10 higher amount of water.

5.3 Speciation and fate of organic compounds in the cementitious near field

5.3.1 ¹⁴C project

Carbon-14 containing LMW organic compounds are expected to form in the course of the anoxic corrosion of activated steel, in particular hydrocarbons such as methane, ethane etc., and oxidized hydrocarbons, such as alcohols, aldehydes, carboxylic acids (WIELAND & HUMMEL 2014). These ¹⁴C bearing compounds could be major contributors to the peak dose released from an L/ILW repository. Although the ¹⁴C inventory associated with activated steel in the repository is well known, the chemical speciation of the ¹⁴C liberated during corrosion of steel under repository relevant conditions is poorly known. The Swissnuclear financed ¹⁴C project aims at filling this knowledge gap and involves a corrosion experiment with activated steel. In 2014, the series of batch-type experiments with non-activated steel powders was brought to an end. The development of the experimental set-up for the corrosion experiment with activated steel was continued and first steps towards the development of the compound-specific ¹⁴C AMS technique required to detect ¹⁴C containing compounds at very low concentrations have been undertaken.

5.3.1.1 Identification and quantification of organic compounds released during iron corrosion

Additional series of corrosion experiments with reaction time up to 35 days were performed in neutral and alkaline solutions with the aim of completing the studies started in 2013 (LES PROGRESS REPORT 2013). The corrosion experiments were carried out using iron powders from two different manufacturers, i.e. Sigma Aldrich and BASF, which had been pre-treated according to a procedure reported in the literature (DENG et al. 1997). Gas chromatography (GC) coupled with mass spectrometry (MS) for volatile LMW organics and high performance ion exclusion chromatography (HPIEC) coupled with MS were applied to identify and quantify the organic compounds. The gas phase analysis was developed in collaboration with the Institute for Chemistry and Bioanalytics at the University of Applied Sciences Northwestern Switzerland (ICB/FHNW).

Table 5.1 summarises the organic compounds that were identified in the corrosion experiments along with all compounds that have been reported in the literature (WIELAND & HUMMEL 2014). The organic

compounds expected to be produced during steel and iron corrosion, respectively, can be divided into three groups: a) gaseous (alkanes/alkenes) b) volatile (alcohols/aldehydes), and c) aqueous compounds (carboxylic acids/carbonate). All these corrosion-derived products are LMW organic compounds with ≤ 5 carbon atoms. Most of the compounds that had been reported in the literature were detected in the in-house corrosion experiments. Nevertheless, some compounds, such as butylene, pentene, propanoate and butonate could not be observed. The formation of small amounts of carbonate could not be checked due to the presence of carbonate in the neutral and alkaline solutions.

5.3.1.2 Source of oxidized hydrocarbons during the anoxic corrosion of iron

The time-dependent corrosion experiments with iron powders show 1) a fast formation of organic compounds within the first day, and 2) a large difference in the concentrations of organic compounds determined in the experiments with pre-treated and untreated iron powders (see LES PROGRESS REPORT 2013). Corrosion experiments were carried out in 2014 with the aim of identifying the process responsible for the rapid formation of organic compounds in the initial stage of iron corrosion. To this end, the solution of iron-containing samples was subsequently replaced with fresh solution after 3 (exchange I), 6 (exchange II), 9 (exchange III) and 49 days (exchange IV) of reaction time (Fig. 5.1). The experiments were carried out with the HCl pre-treated BASF iron powder and in an artificial cement pore water (ACW) with pH = 12.5 (portlandite-saturated solution). Note that similar observations were made in experiments with pre-treated Sigma iron powder.

Fig. 5.1 shows that the concentrations of all organic compounds dropped to a very low level close to the limit of detection already after the first replacement of the solution after 3 days reaction time. The concentrations stayed very low after the exchanges II and III (3 days reaction time in between). Even a long period of 40 days reaction between exchange III and exchange IV did not significantly increase the concentrations of the organic compounds. This shows that two stages in the corrosion process with clearly different corrosion rates can be distinguished. Contact of a solution with the iron powder gives rise to fast release of all organic compounds, i.e. gaseous, volatile and dissolved species, in the initial stage.

Table 5.1: Carbon species expected to be formed as a result of steel corrosion as reported in literature (**bold plus regular font style**) and subsequently identified at PSI in corrosion experiments with non-activated iron powders (**bold**).

Alkane/alkene	Alcohols/aldehydes	Carboxylic acids	Carbonate
Methane (CH ₄)	Methanol (CH ₃ OH)	Formate (HCOO ⁻)	CO ₂
Ethane (C ₂ H ₆)	Ethanol (C ₂ H ₅ OH)	Acetate (CH ₃ COO ⁻)	CO ₃ ²⁻
Ethene (C ₂ H ₄)	Formaldehyde (CH ₂ O)	Propanoate (C ₂ H ₅ COO ⁻)	(CO)
Propane (C ₃ H ₈)	Acetaldehyde (C ₂ H ₄ O)	Butanoate (C ₃ H ₇ COO ⁻)	
Propene (C ₃ H ₆)	Propionaldehyde (C ₃ H ₆ O)	Malonate (CH ₂ (COO ⁻) ₂)	
Butane (C ₄ H ₁₀)		Oxalate (C ₂ O ₄ ²⁻)	
Butylene (C ₄ H ₈)			
Pentene (C ₅ H ₁₀)			

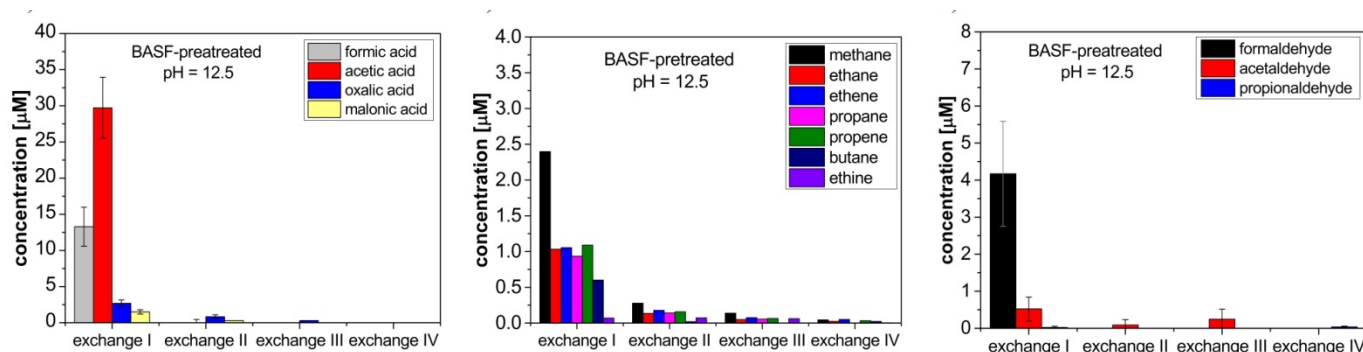


Fig. 5.1: Concentrations of carboxylic acids (left), gaseous hydrocarbons (middle) and aldehydes (right) as a function of solution replacements (see text).

In the long run, however, small but measurable concentrations are only observed for the gaseous compounds while the concentrations of the oxidized hydrocarbons (i.e. alcohols, aldehydes, carboxylic acids) are close to the detection limit, indicating either no formation or formation at very low rates. Hence, our results support the idea of very slow corrosion of iron under hyper-alkaline conditions.

Reducing conditions should prevail in the corrosion samples (iron powders in contact with degassed, "oxygen-free" solution) as residual oxygen is expected to be consumed in the early stage of the corrosion process. Therefore, the formation of reduced hydrocarbons under the experimental conditions is expected to occur in the long run while the formation of oxidized hydrocarbons cannot be ruled out in the early stage due to the presence of residual oxygen. Two possible scenarios for the fast formation of oxidized hydrocarbons in the initial stage of the corrosion process can thus be envisaged: 1) the oxidized hydrocarbons (dissolved carbon

species) are generated during the pre-treatment of the iron powders (HCl wash in air) and instantaneously released to solution, or 2) the oxidized hydrocarbons are formed rapidly and simultaneously with the reduced, gaseous compounds due to the presence of residual oxygen in solution. To prove one against the other hypothesis, a series of batch-type experiments were carried using the same solution, i.e. a solution prepared by equilibrating Milli-Q water with a calcium silicate hydrate (C-S-H) phase with Ca:Si (C:S) ratio = 0.8 (resulting pH = 11.5), which was injected subsequently into different vials containing pre-treated iron powder. The iron suspensions were then equilibrated for 3 days. Note that residual oxygen that could be potentially present in the solution at very low concentration in the source solution should be consumed in the first sample (exchange I) while complete absence of oxygen is expected in the subsequent samples (exchanges II and III). The results from this experiment are shown in Fig. 5.2 for carboxylates.

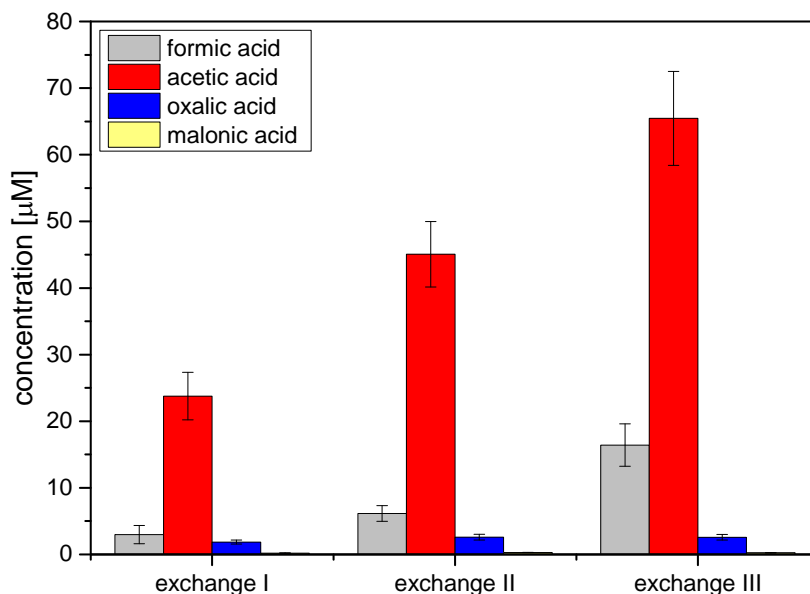


Fig. 5.2: Concentrations of carboxylic acids as a function of subsequent solution-powder exchanges ($pH = 11.5$).

The linear increase in the concentrations of the detectable carboxylates, i.e. formic, acetic and malonic acids, indicates that these compounds did not form due to the oxidation of carbon by residual oxygen but rather they had been formed as a result of the pre-treatment process. This finding is in agreement with the first hypothesis. The compounds are instantaneously released from the surface of the pre-treated iron powder upon contact with the solution. Note that the concentrations of alcohols and aldehydes are below the detection limit in this experiment. The results suggest that oxidized hydrocarbons present in the course of the anoxic corrosion of iron are not products of the corrosion process but rather the consequence of a sample pre-treatment, i.e. whether they had been subjected to oxidizing conditions (e.g. acid wash, storage in air etc.).

5.3.1.3 Coupling HPIEC with accelerator mass spectrometry (AMS) for compound-specific ^{14}C analysis

Preliminary calculations showed that the concentrations of ^{14}C bearing organic compounds expected to be formed in the planned corrosion experiments with the available activated steel sample (SCHUMANN et al. 2014) are extremely low. Estimates based on corrosion rates under alkaline conditions (50 nm y^{-1}), the known surface area and activity of the irradiated steel sample (1 g material with a surface area of $\sim 1 \text{ cm}^2 \text{ g}^{-1}$ and $\sim 18 \text{ kBq g}^{-1}$ ^{14}C (SCHUMANN et al. 2014) revealed that the ^{14}C production rate corresponds to $\sim 3 \cdot 10^{-15} \text{ mol L}^{-1} \text{ d}^{-1}$. The ^{14}C concentration is further reduced because a chromatographic fractionation into single ^{14}C bearing

compounds will be applied prior to ^{14}C determination. Detection of very low ^{14}C concentrations requires an extremely sensitive ^{14}C analytical method. To this end, a compound-specific ^{14}C AMS method is currently being developed, which requires the coupling of standard separation techniques (GC, HPIEC) with ^{14}C detection by AMS.

The first steps towards the development of compound-specific ^{14}C detection have been undertaken in the last year. Recovery of the chromatographic fractionation and the dynamic range of the AMS were determined. The simplified flow chart shown in Fig. 5.3 illustrates the approach currently being developed for ^{14}C bearing carboxylates by coupling chromatographic separation to ^{14}C AMS detection. After the chromatographic separation of the carboxylates, the different species have to be collected in separate fractions, transferred to the AMS system and oxidized to inject ^{14}C as $^{14}\text{CO}_2$. Several aspects have to be considered in conjunction with the AMS measurements, in particular the required concentrations of ^{12}C , ^{14}C and the ratio of $^{14}\text{C}/^{12}\text{C}$. The procedure for sample preparation was analysed by conducting theoretical calculations in connection with the required $^{14}\text{C}/^{12}\text{C}$ ratio for ^{14}C AMS. The calculations show that the compound-specific ^{14}C AMS approach should be feasible for the ^{14}C activities expected in the planned corrosion experiment with activated steel (see above). The ^{14}C AMS measurements will be carried out using the MICADAS (MIni CARbon DAting System) at the Laboratory for Environmental and Radiochemistry at the University of Bern, Switzerland (Fig. 5.3).

In 2014, also the chromatographic separation of the carboxylic acids and fractionation of the samples was optimised and quantified. Standard solutions of formic, acetic, oxalic, valeric and malonic acids with known concentrations were injected into the HPIEC to optimise the fractionation parameters and to determine the recovery. Recoveries ranging from 95 to 110 % were obtained for the different compounds, thus confirming the efficiency and reproducibility of fractionation using HPIEC.

First measurements using ^{14}C AMS were carried out with the aim of testing the detection limit and the dynamic range for the specific task. Note that the ^{14}C content can be expressed in terms of the fraction

modern carbon ($F^{14}\text{C}$), which is defined by $F^{14}\text{C} = {}^{14}\text{C}/({}^{12}\text{C} \cdot 10^{-12})$.

The background signal created by chromatographic fractionation determines the lower detection limit, whereas the upper limit of detection is determined by the AMS. A background signal of $0.06 F^{14}\text{C}$ was determined for samples prepared in the HOTLAB at PSI. Additional samples with defined ^{14}C activities were analysed which showed that the content of ^{14}C should be less than $100 F^{14}\text{C}$ to avoid overloading of the analytical device. This provides analytical constraints as only the dynamic range between $0.06 - 100 F^{14}\text{C}$ is available for compound-specific ^{14}C analysis.

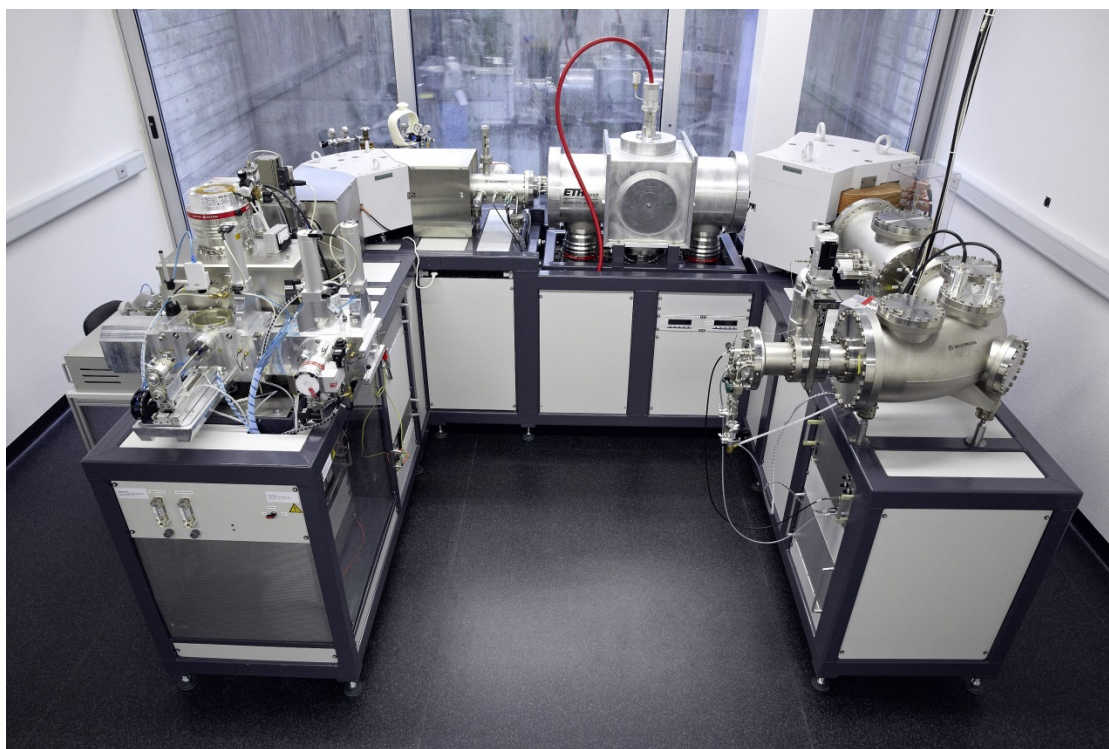
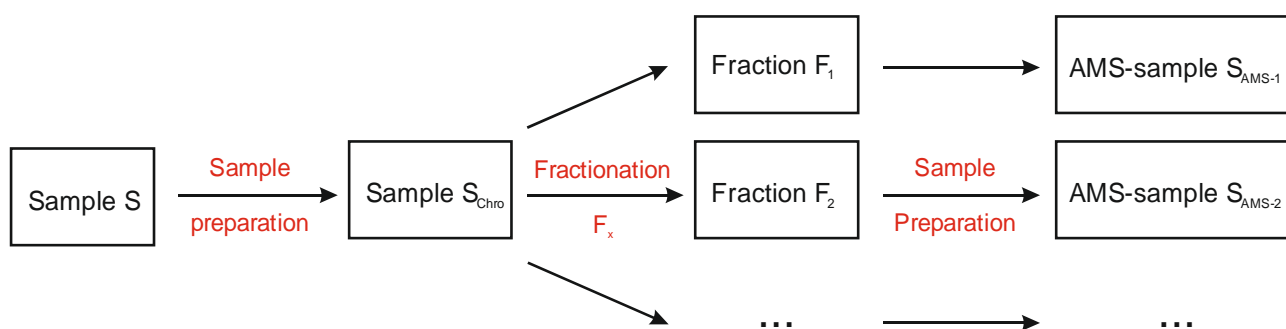


Fig. 5.3: Top: Simplified flow chart of the chromatographic separation of ^{14}C bearing organic compounds coupled to ^{14}C detection by AMS. Bottom: Picture of the MIni CARbon DAting System (MICADAS) at the University of Bern (SZIDAT et al. 2014).

5.3.1.4 Development of a reactor for the corrosion experiment with activated steel

An experimental set-up for the long-term corrosion experiment with the activated steel nut from the Gösgen nuclear power plant is currently being developed. The set-up consists of a custom-made gas-tight overpressure reactor placed within a 10 cm thick lead shielding. The overpressure reactor is designed in such a way that all manipulations necessary for regular sampling can be carried out without removing the lead shielding to minimize exposure of the experimentalist to radiation. The lead shielding has to be opened only during the transfer of the activated steel nut into the reactor. The construction of the reactor will be finished by the end of 2014 and the testing phase with non-activated steel will take place in 2015.

5.3.2 Chemical stability of organic compounds under hyper-alkaline conditions

Carbon-14 containing LMW organic molecules released during the corrosion of activated steel may not be chemically stable under the hyper-alkaline reducing conditions of a cement-based repository. Thermodynamic calculations revealed that, in case of complete thermodynamic equilibrium, the predominant dissolved carbon bearing species are CO_2 , HCO_3^- , CO_3^{2-} and CH_4 (WIELAND & HUMMEL 2014).

However, complete thermodynamic equilibrium is rarely achieved in the C-H-O system at moderate temperatures. The kind of organic compounds that might persist in the repository at partial thermodynamic equilibria is not known.

To this end, the stability of acetic acid and formic acid under hyper-alkaline anoxic conditions is being studied. A first test experiment was carried out in 2013: An oxygen-free, portlandite-saturated solution ($\text{pH} = 12.5$) containing $3 \cdot 10^{-4}$ M Na-acetate was aged for 60 days under strict anoxic conditions and in an inert N_2 atmosphere at a pressure of 4 bar. Both the gas phase and the aqueous phase were sampled at regular time intervals. The former samples were analysed at ICB/FHNW using GC-MS to check for the presence of volatile degradation products while the latter samples were analysed in-house using HPIEC-MS and total organic carbon (TOC) analysis.

The analysis of the aqueous phase did not reveal any change in the Na-acetate concentration over time whereas GC-MS analysis showed the presence of small concentrations of propane, propene and butane (Fig. 5.4). In 2014, the same experiment was repeated to determine the reproducibility of the experimental approach. In addition a blank experiment was set up in which an oxygen-free, portlandite-saturated solutions ($\text{pH} = 12.5$) without Na-acetate was sampled up to 150 days to determine possible sources of organics in the high pressure autoclave, e.g. the teflon liner and the synthetic fittings.

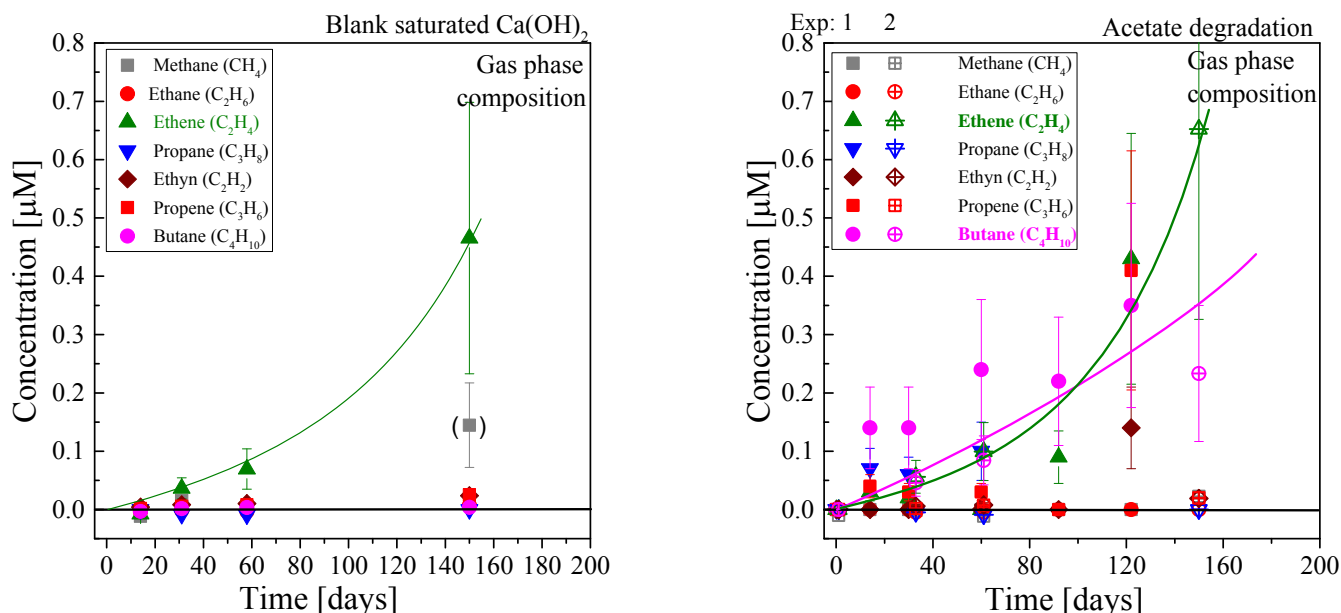


Fig. 5.4: Chemical stability of Na-acetate in a portlandite-saturated solution at $\text{pH} = 12.5$. Left: Concentration of gaseous LMW organic compounds in equilibrium with a portlandite-saturated solution without Na-acetate, right: Concentration of gaseous LMW organic compounds in equilibrium with a portlandite-saturated solution containing $3 \cdot 10^{-4}$ M Na-acetate (average concentration from two independent experiments). Lines are shown to guide the eye.

A significant concentration of ethene (up to 0.5 μM) was detected in the gas phase of the blank experiment whereas the concentrations of all other gaseous organic compounds were below the GC-MS detection limit of 0.05 μM . The experiment with acetate confirmed the presence of increasing concentrations of ethene as in the blank experiments, but in addition an increasing concentration of butane was observed at very low levels ($\sim 0.4 \pm 0.2 \mu\text{M}$) compared to the Na-acetate concentration in solution ($3 \cdot 10^{-4} \text{ M}$). At present, the reaction leading to the formation of butane in the gas phase is not known.

5.4 Immobilization of redox-sensitive radionuclides by cementitious materials

5.4.1 Actinides

Sorption data for actinides are often difficult to determine experimentally due to the high dose rates of some actinides (e.g. Pu) or the limited stability of relevant redox states (e.g. U(IV)). Therefore, chemical analogy of the radionuclides with the same redox state was checked by comparing the sorption behaviour of several lanthanides and actinides in different redox states on C-S-H phases, the main component of HCP. Uptake of Eu(III), Cm(III),

Th(IV), Np(IV,V,VI), and U(VI) by C-S-H phases with C:S ratios 1.07 and 1.2 in ACW (pH = 13.3) was determined (Fig. 5.5). In the case of the trivalent and tetravalent actinides and lanthanides, the R_d values were found to be constant, hence independent of the aqueous concentration of the actinides (linear sorption). The R_d values determined for Eu(III) and Cm(III), as well as for Th(IV) and Np(IV) are identical which supports the assumption that radionuclides with the same redox state show the same sorption behaviour.

In the case of the pentavalent and hexavalent actinides, the R_d values significantly decrease with increasing aqueous concentration (non-linear sorption) indicating that the affinity of the C-S-H phases for these actinides decreases with increasing occupation of sorption sites (Fig. 5.5). In addition, the R_d values for Np(VI) were found to be considerably lower than those for U(VI). Sorption experiments carried out at different pH on C-S-H phases with different C:S ratios confirmed this observation (Fig. 5.5b). The difference in the R_d values for Np(VI) and U(VI) uptake by C-S-H phases can be explained by the difference in the stepwise hydrolysis constants, $\log^*K_4^0$, for the two actinyl ions (GAONA et al. 2013):

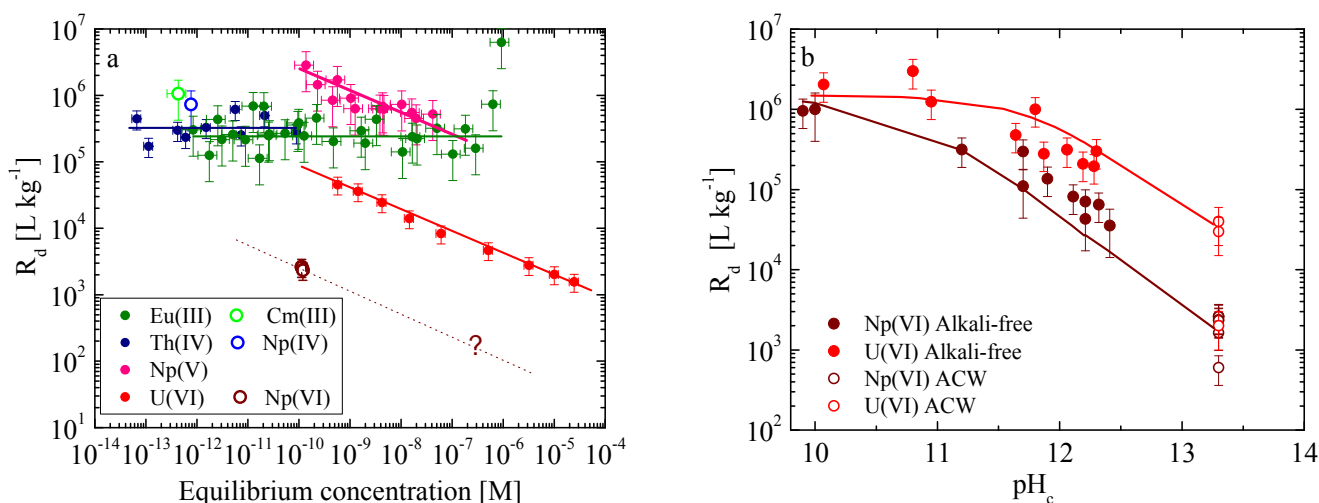


Fig. 5.5: R_d values for Eu(III), Cm(III), Th(IV), Np(IV), Np(V), U(VI) and Np(VI) sorption onto C-S-H phases in ACW at pH = 13.3. a) R_d values as a function of the equilibrium concentration from measurements of sorption isotherms (lines are shown to guide the eye.) b) Effect of pH on the sorption of hexavalent actinides: experimental (symbols), modelled (lines) (TITS et al. 2014b).

Previously it was shown that tetrahydroxo actinyl ions are not bound by solids such as C-S-H phases whereas the trihydroxy actinyl ions strongly sorb (TITS et al. 2014a). Competition between the formation of the tetrahydroxo complex in solution and the surface sorption of the Np(VI) and U(VI) species as well as the difference in the thermodynamic stability of $\text{UO}_2(\text{OH})_4^{2-}$ and $\text{NpO}_2(\text{OH})_4^{2-}$ explains the difference in the sorption behaviour (Fig. 5.5b). Thus, chemical analogy also holds in the case of the uptake of hexavalent actinides by C-S-H phases because the same processes are involved. Only the absolute sorption values are different due to differences in the hydrolysis constants.

5.4.2 Selenium

^{79}Se (half-life $3.27 \cdot 10^5$ years) is an important redox-sensitive, dose-determining radionuclide in an L/ILW repository (NAGRA 2002). The selenium speciation under oxidizing conditions is dominated by SeO_4^{2-} and SeO_3^{2-} (e.g. OLIN et al. 2005) while in alkaline, reducing conditions, i.e. $10.0 < \text{pH} < 13.5$ and $-750\text{mV} < E_h < -230\text{mV}$, $\text{Se}(0)$, HSe^- and polyselenide species exist along with SeO_3^{2-} . Robust sorption data and in particular, a mechanistic understanding of the retention of Se(-II) in a cementitious environment are lacking.

The influence of the transition of Se from oxidizing to reducing conditions on the immobilization of Se in cementitious materials is being investigated in a subproject within in the "Immorad" project. It is expected that oxidizing conditions prevail during solidification of the waste materials with cement and in the early phase of the repository. This implies that Se exists as SeO_3^{2-} which can sorb onto the different cement phases (C-S-H, AFm, Aft,...) of HCP. After the closure of the repository, however, conditions will slowly become reducing, which might eventually result in the reduction of SeO_4^{2-} and SeO_3^{2-} to Se(-II).

In 2014, kinetics of the Se(-II) uptake by cement phases, i.e. C-S-H phases with different C:S ratios, monocarbonate (AFm- CO_3) and hemicarbonate (AFm-OH- CO_3) was studied (Fig. 5.6). The uptake by all the investigated cement phases is fast, thus reaching equilibrium within 2 days. Note that the R_d values for Se(-II) uptake by C-S-H phases are lower than those for the AFm phases, although the latter phases have a lower surface area (BAUR et al. 2004).

This finding implies that Se(-II) could be stabilized in the interlayer of the AFm phases (anion exchangers).

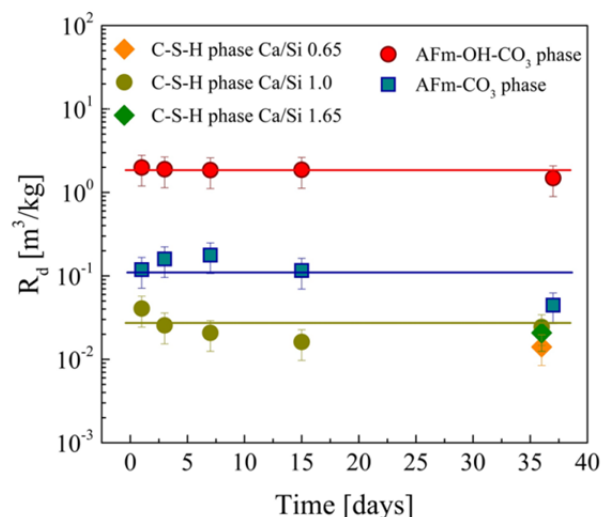


Fig. 5.6: R_d values for Se(-II) determined on different cement phases as a function of time.

The higher R_d values determined on the AFm-OH- CO_3 compared to AFm- CO_3 can be explained by the larger interlayer distance of the former phase.

R_d values determined for Se(-II) uptake by cement phases were found to be generally lower than those determined for Se(IV) uptake (Table 5.2).

Spectroscopic studies are currently being performed to determine the mechanisms controlling the Se(IV) and Se(-II) uptake.

Batch sorption experiments were carried out with the aim of determining the effect of the transition from oxidizing to reducing conditions on the redox state of Se(IV) taken up by AFm- CO_3 and AFm-OH- CO_3 . First, Se(IV) was allowed to sorb on the two cement phases for 1 month and then the Se(IV) – AFm- CO_3 and Se(IV) – AFm-OH- CO_3 suspensions were transferred to electrochemical cells in which they were exposed to reducing conditions ($E_h = -1.29$ V) for another month. The Se loaded AFm pastes were prepared for XANES measurements at the ROBL/ESRF (Grenoble, France). The measurements were carried out at cryogenic temperature (~ 15 K). The results show that Se(IV) sorbed on the AFm- CO_3 phase was reduced in the electrochemical cell while Se(IV) taken up by AFm-OH- CO_3 largely remained in the +IV redox state (Fig. 5.7). One may speculate that Se(IV) is adsorbed on the outer surface of AFm- CO_3 , in accordance with the low R_d value (Table 5.2), and therefore Se(IV) is more easily accessible to a reducing agent. In contrast, Se(IV) bound in the interlayer of AFm-OH- CO_3 , in accordance with the high R_d value (Table 5.2), prevents Se(IV) from being reduced. This hypothesis, however, needs further confirmation.

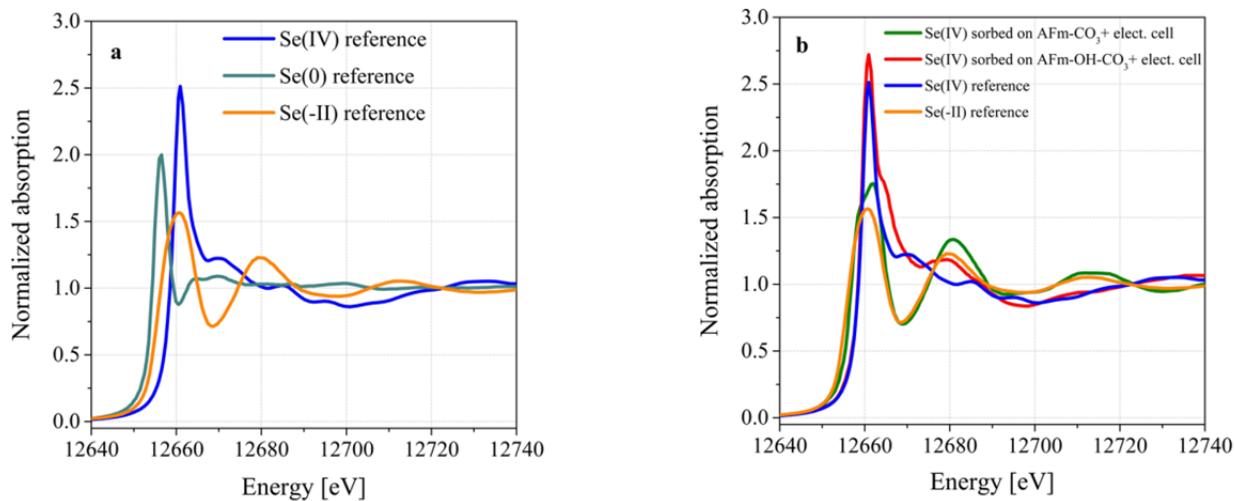


Fig. 5.7: a) XANES spectra of Se reference samples in different redox states. b) XANES spectra of Se(IV) sorbed on two AFm phases after exposure to reducing conditions for 1 month in an electrochemical cell.

Table 5.2: R_d values for Se(IV) and Se(-II) sorbed on different cement phases (uncertainties are given on the basis of the 95% confidence interval).

Cement phase	R_d (Se(IV)) [m ³ kg ⁻¹]	R_d (Se(-II)) [m ³ kg ⁻¹]
C-S-H		
C:S = 0.65	0.48±0.02	(2.5±0.4)·10 ⁻²
C:S = 1.07	-	(1.4±0.7)·10 ⁻²
C:S = 1.65	0.55±0.03	(2.0±1.0)·10 ⁻²
AFm-CO ₃	1.2±0.7	0.12±0.02
AFm-OH-CO ₃	21±2	1.80±0.07

5.5 References

- BAUR I., KELLER P., MAVROCORDATOS D., WEHRLI B., JOHNSON C.A. (2004)
Dissolution-precipitation behaviour of ettringite, monosulfate, and calcium silicate hydrate. *Cement Concr. Res.* 34, 341-348.
- DENG B. L., CAMPBELL T. J., BURRIS D. R. (1997)
Hydrocarbon formation in metallic iron/water systems. *Environ. Sci. Technol.* 31, 1185-1190.
- GAONA X., FELLHAUER D., ALTMAIER M. (2013)
Thermodynamic description of Np(VI) solubility, hydrolysis, and redox behaviour in dilute to concentrated alkaline NaCl solutions. *Pure Appl. Chem.* 85, 2027-2049.
- NAGRA (2002)
Project Opalinus Clay: Safety report. Demonstration of disposal feasibility for spent fuel, vitrified high-level waste and long-lived intermediate-level waste (Entsorgungsnachweis). Nagra Tech. Rep. NTB 02-05.
- NAGRA (2008)
Modellhaftes Inventar für radioaktive Materialien, Nagra Tech. Rep. NTB 08-06.
- OLIN Å., NOLÅNG B., OSADCHII E.G., ÖHMAN L.-O., ROSÉN E. (2005)
Chemical Thermodynamics of Selenium. *Chemical Thermodynamics Vol. 7.* Elsevier, Amsterdam, Netherlands.
- SCHUMANN D., STOWASSER T., VOLMERT B., GÜNTHER-LEOPOLD I., LINDER H.-P., WIELAND E. (2014)
Determination of the ^{14}C content in activated steel components from a neutron spallation source and a nuclear power plant. *Anal. Chem.* 86, 5448-5454.
- SZIDAT S., SALAZAR G.A., VOGEL E., BATTAGLIA M., WACKER L., SYDAL H.-A., TÜRLER A. (2014)
 ^{14}C analysis and sample preparation at the new Bern Laboratory for the analysis of radiocarbon with AMS (LARA). *Radiocarbon* 56, 561-566.
- TITS J., LAUBE A., WIELAND E., GAONA X. (2014a)
Neptunium(IV/V/VI) sorption behaviour under hyperalkaline conditions: Batch sorption studies on titanium dioxide and calcium silicate hydrates. *Radiochim. Acta* 102, 385-400.
- TITS J., LAUBE A., WIELAND E. (2014b)
Comparison of actinide (III,IV,V,VI) uptake by cementitious materials. *Appl. Geochem.* (in prep.).
- WIELAND E., HUMMEL W. (2014)
Formation and stability of carbon-14 containing organic compounds in alkaline iron-water-systems: Preliminary assessment based on a literature survey and thermodynamic modelling. *Mineral. Mag.* (submitted).
- WIELAND E., KOSAKOWSKI G., BERNER U. (2014)
Preliminary assessment of the temporal evolution of waste packages in the near field of an L/ILW repository. Nagra Arbeitsbericht NAB (in prep.).

6 COLLOID CHEMISTRY

C. Degueldre, S. Frick

6.1 Overview

The aim of the colloid sub-program is to understand the role of colloids in the migration of radionuclides in the geosphere. The studied colloid properties are their concentration, size distribution and nature that dictate their behaviour under safety relevant conditions. The main activities over the past year were within the framework of the Grimsel colloid project: "Colloid Formation and Migration" (CFM) and were focused on measuring colloid size distributions in batch and in quasi-stagnant conditions using single particle counting (SPC). The knowledge and understanding gained over the last decade allows well founded estimates for colloid assisted migration of radionuclides in the argillaceous rock to be made. These data and models are used for provisional safety assessments in the frame of the Sectoral Plan.

6.2 Activities in the CFM Project

The CFM project is conducted at the Grimsel Test Site (GTS), Switzerland, in the framework of Phase VI of the research program, which runs from 2004 to originally 2013 but was extended and shall continue through 2016 - 2018. The program is dedicated to repository-relevant (i.e. large-scale, long-term) in-situ experiments.

No radionuclide-colloid tests have been performed in the migration shear zone at the GTS since July 2013. Instead, the work was focussed on the Long-term In-situ Test (LIT), which includes installation of doped clay source for the follow up monitoring of the generated/eroded colloids in the surrounding ground water (see Fig. 6.1).

In addition, breakthrough tests are also foreseen including injection of suspension of FEBEX bentonite colloids doped with selected radionuclides. The colloid tracer tests involve injection into borehole and extraction downstream at the surface spring in the access tunnel wall approximately 6.1 m away as depicted in Fig. 6.1.

The 2nd RN migration test will be performed in the previous CRR dipole D1 (see Fig. 6.1) configuration. The hydraulic parameters are as follows:

- Outflow for injection - 5 ml/min
- Extraction from Pinkel (see Fig. 6.1) - 25 ml/min (constant since October 2011)
- Injection with low flow rate 0.33 ml/min

- Rates are approximately 30 times lower flow rates than former project tests

Only difference in set-up from 13-04 (last year) is inclusion of injection side samplers (total 30 ml volume), modification for online RN & colloid detection and collection in tanks

Cocktail to contain bentonite and synthetic clay colloids, radionuclide tracers (^{22}Na , ^{133}Ba , ^{137}Cs , ^{232}Th , ^{233}U , ^{237}Np , ^{242}Pu , ^{243}Am) and conservative dye tracer AGA.

Offsite colloid measurements are conducted at PSI using a single-particle counter (SPC). The colloid concentrations are also measured in the field using mobile laser-induced breakdown detection (LIBD) system operated by KIT personnel. The general trends in the LIBD and SPC data are in good agreement. The SPC data are size normalized. They show that the colloid size ranges relevant for the breakthrough are between 50-100 and 100-150 nm, and that sizes above 200 nm have little effect on the transport in the tests.

6.3 Other colloid activities

Currently, the main aim of co-operation with CIEMAT is to optimize the radio-analytical effort required to measure colloid breakthrough curves in the CFM experiment at the GTS. Colloid properties are also investigated in a methodological way.

Radionuclides transporting colloids can form due to bentonite erosion by flowing water. Several bentonite colloid stability studies have been carried out, analyzing aggregation behaviour as function of pH, electrolyte type and ionic strength (MISSANA et al. 2003), or kinetics of generation and sedimentation pseudo-equilibrium (GARCIA et al. 2009; ALBARRAN et al. 2014). It is known that low ionic strength ($I \sim 10^{-3}$ M), low concentration of bivalent cations and neutral-alkaline conditions favor colloid stability. Nevertheless, to the best of our knowledge, studies on colloid disaggregation due to changes in ionic strength from higher to lower values are scarce. This scenario occurs due to mixing of saline porewater with a low mineralized water of different origin (a lake, a glacier, a river or the rain). The entry of diluted water would promote a decrease of ionic strength that could favor disaggregation of bentonite particles. The size and stability recovered by these disaggregated particles would condition their further transport.

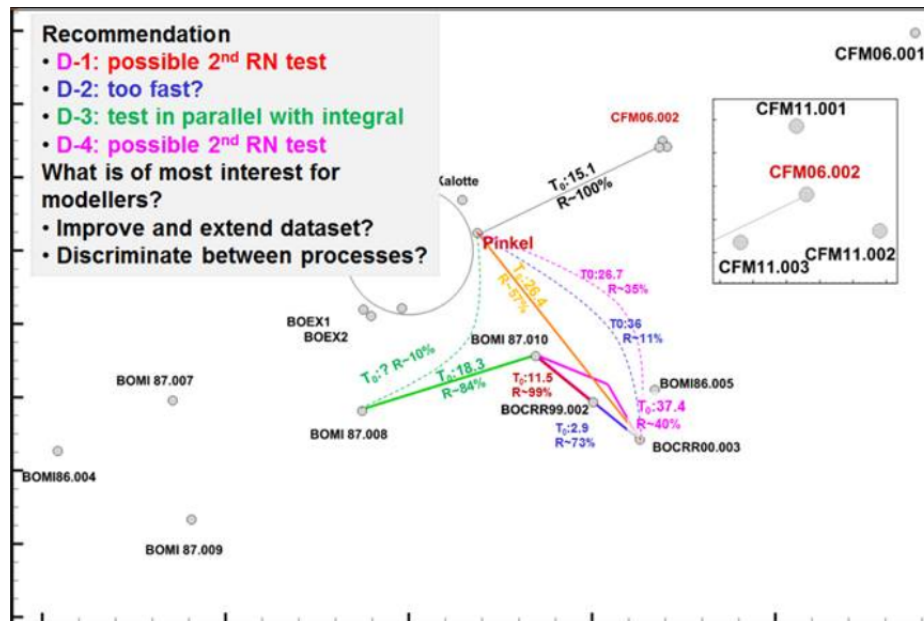


Fig. 6.1: Schematic illustration of the CFM field test zone. For LIT: the clay source is located in CFM06.002 (see insert) and colloid samplings are performed in CFM11.1-3 boreholes (low flow rate 0.3 ml/min) as well as at the Pinkel. For further breakthrough tests: injections in various bore hole and breakthrough downstream at the surface spring in the access tunnel wall or other bore holes are evaluated. CRR (Colloids & Radionuclides Retention project) D1 dipole (in red). D1 recommended (99% recovery (R)); recovery from source CFM06.002 to Pinkel: 100%.

The aim of the work performed by a PhD student from CIEMAT (MAYORDORMO et al. 2015) was to study the disaggregation behaviour of bentonite colloid suspensions after changing electrolyte background and ionic strength. Colloid size distribution was measured in the range 50 to 5000 nm by the SPC technique (Fig. 6.2).

An initial bentonite colloids suspension at $5 \cdot 10^{-4}$ M NaClO_4 was considered as reference stable suspension (*mom*). This sample was aggregated by increasing ionic strength to 0.1 M with NaClO_4 electrolyte (*agr*). Aliquots of *agr* were diluted into different salinity environments: NaClO_4 or NaCl-CaCl_2 mixed water, whose ionic strengths values were $1 \cdot 10^{-2}$ M, $1 \cdot 10^{-3}$ M and $5 \cdot 10^{-4}$ M. These represent samples at intermediate dilutions, to be compared with that of aggregated (*agr*) and initial *mom* sample.

In the intermediate diluted samples, SPC measurements showed that the population related to the lowest size channels (size < 200 nm) is higher when NaClO_4 is used to dissolve the suspension, whilst particle concentration in higher size channels (size > 200 nm) is higher when mixed water is used as electrolyte background. Fig. 6.2 presents the

normalized concentration associated to different size channels obtained by SPC measurements of the different diluted suspensions in NaClO_4 or mixed electrolyte.

Colloid formation scenarios for the potential argillaceous host rocks proposed by Nagra in the frame of the Sectoral Plan (Effingen Member, 'Brauner Dogger', and Helvetic Marl) have been estimated on the basis of our colloid formation studies at field, laboratory and model. The study will also include calculations of colloid concentrations in the relevant systems using the suspension pseudo-equilibrium model derived recently (DEGUELDRE et al. 2009). This field/lab experimental study and modelling will be published in 2015.

The Bangombe colloid data produced in 1996 in the frame of a local colloid campaign have been revisited according to our colloid generation models. A comprehensive study has been recently published (DEGUELDRE & LAAKSOHARJU 2014).

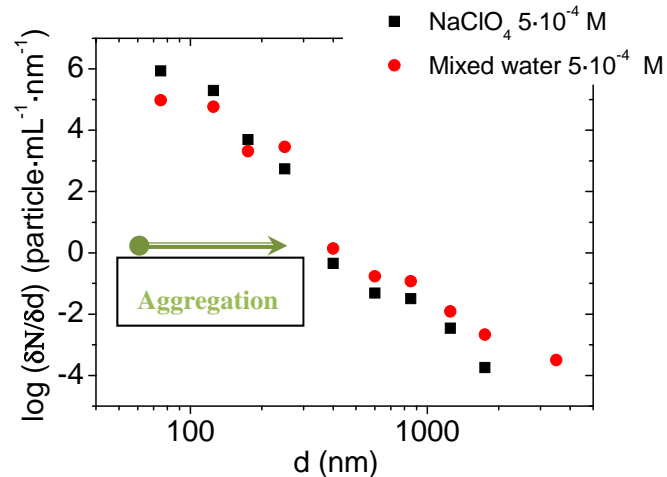


Fig. 6.2: Normalized concentration associated to different size values obtained by SPC measurements on unshaken suspensions at the lowest ionic strength 24 hours after starting experiments. Conditions: test at room temperature, sampling in the middle of the batch.

Note: the small colloids in mixed water (Na^+ , Ca^{2+}) aggregate with time (see decrease for size <200 nm) yielding larger colloidal particles (aggregates see increase for size >200 nm).

6.4 Future work

Long term in situ test of the CFM program at GTS shall continue until 2016. The SPC units currently located at PSI will be transferred to the Grimsel Test Site in May-June 2015. This will assure the continuity of activities within the CFM project and avoid the need for transport of radioactive samples from the GTS to PSI. Furthermore, the on-site measurement is always an advantage for colloid suspension analysis.

6.5 References

DEGUELDRE C., AEBERHARD PH., KUNZE P., BESSHO K. (2009)

Colloid generation/elimination dynamic processes: Toward a pseudo-equilibrium? *Colloids Surf. A*, 337 117-126.

MISSANA T., ALONSO U., TURRERO M.J. (2003)

Generation and stability of bentonite colloids at the bentonite/granite interface of a deep geological radioactive waste repository. *J. Contam. Hydrol.* 61, 17-31.

GARCIA-GARCIA S., DEGUELDRE C., WOLD S., FRICK S. (2009)

Determining pseudo-equilibrium of montmorillonite colloids in generation and sedimentation experiments as a function of ionic strength, cationic form, and elevation. *J. Colloid Interface Sci.* 335 54-61.

ALBARAN N., DEGUELDRE C., MISSANA T., ALONSO U., GARCIA-GUTIERREZ M., LOPEZ T. (2014)

Size distribution analysis of colloid generated from compacted bentonite in low ionic strength aqueous solutions. *Appl. Clay Sci.* 95 284-293.

7 DIFFUSION PROCESSES

L.R. Van Loon, M.A. Glaus, S. Frick, P. Bunic, Y. Chen (PhD student), C. Wigger (PhD student)

7.1 Overview

The foci of the activities in the Diffusion Processes group are (i) measuring diffusion parameters (effective diffusion coefficients and rock capacity values) which can be used in performance assessment studies, and (ii) understanding the diffusion mechanism(s) of radionuclides in compacted argillaceous materials.

Within the framework of the Sectoral Plan (Sachplan geologische Tiefenlager) diffusion measurements with $^{22}\text{Na}^+$ on fresh samples (of Opalinus Clay and 'Brauner Dogger') from the deep borehole in Schlattingen were performed. The results of the measurements and a compilation of effective diffusion coefficients for the different Swiss host rocks currently under investigation were summarised in a Nagra NTB (VAN LOON 2014). This diffusion data base is used for provisional safety analyses in the SGT-E2.

The EU CatClay project was finished by May 31st. The main results and outcomes of the project were summarised in a final report.

The TRAPHICCS programme on pure clay minerals has been continued. The mobility of the Sr-EDTA complex in montmorillonite was studied in order to investigate the effect of speciation on the diffusion.

Two PhD projects on reactive transport are ongoing in close co-operation with the Transport Mechanisms Group.

Another PhD project related to the migration behaviour of organic molecules with different chemical structures in compacted clay systems has been continued. Infiltration experiments with 3-hydroxypropanoic acid and 2-hydroxypropanoic acid in illite showed that the chemical structure has a clear effect on the migration behaviour of these molecules.

A new PhD project concerning the anion accessible porosity in clay rocks was started in February 2014. The project is supported by NWMO Canada. A series of Swiss and Canadian rock samples were selected for the project. The Swiss samples were characterised in terms of mineralogy, specific surface area and pore structure, and first diffusion measurements with $^{36}\text{Cl}^-$ as a function of the chemical composition of the porewater were performed.

A QM-system based on the ISO 9001 norm was developed, together with the Hot Laboratory (AHL) and the Laboratory for Nuclear Materials (LNM). The system will be stepwise implemented in 2014/2015.

7.2 Activities in support of the Sectoral Plan

Diffusion measurements with $^{22}\text{Na}^+$ were finished early 2014. All measurements with HTO, $^{36}\text{Cl}^-$ and $^{22}\text{Na}^+$ on the new samples confirm the applicability of the extended Archie's relation ("e-Archie") for estimating effective diffusion coefficients based on the accessible porosities (VAN LOON 2014). In the case of $^{22}\text{Na}^+$, surface diffusion had to be considered in order to explain the observed results. The effective diffusion coefficient estimated by Archie's law had to be corrected by a factor (CF) that was derived from the model of GIMMI & KOSAKOWSKI (2011) as described in VAN LOON (2014):

$$CF = 1 + \mu_{Na} \cdot \left(\frac{1 - \varepsilon}{\varepsilon} \cdot \rho_g \cdot \frac{f_{Na}}{C_{Na}} \cdot CEC \right) \quad (7.1)$$

where μ is the surface mobility; ε is porosity; ρ_g is the grain density; f_{Na} is the fraction of Na on the surface; CEC is the cation exchange capacity and C_{Na} is the concentration of Na in the porewater.

The K_d of $^{22}\text{Na}^+$ was estimated by taking a representative CEC value for the clay rocks of 0.1 eq/kg. The equivalent fraction of stable $^{23}\text{Na}^+$ on the surface (f_{Na}) was 50%, i.e. 0.05 eq/kg or 0.05 mol/kg (BRADBURY & BAEYENS 1998; WABER 2008; WERSIN et al. 2013). With an average concentration $C_{Na} = 0.2$ mol/L for $^{23}\text{Na}^+$ in solution, this results in a K_d value for $^{23}\text{Na}^+$ of 0.25 L/kg. The surface mobility of Na (μ_{Na}) was taken from GIMMI & KOSAKOWSKI (2011) and has a value of 0.45. Figure 7.1 shows the measured and estimated effective diffusion coefficients for $^{22}\text{Na}^+$ for a series of argillaceous rocks calculated by (VAN LOON 2014):

$$D_e = CF \cdot (D_w \cdot \varepsilon^{m_1} + A \cdot \varepsilon^{m_2}) \quad (7.2)$$

where D_w is the diffusion coefficient in water and D_e is the effective diffusion coefficient. A , m_1 and m_2 are empirical parameters.

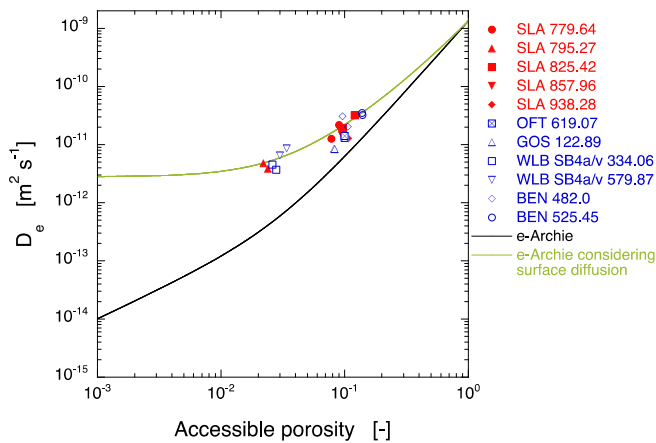


Fig. 7.1: Effective diffusion coefficients of $^{22}\text{Na}^+$ in different clay rocks, together with predicted data with and without surface diffusion (SLA: Schlattingen borehole (Opalinus Clay); OFT: Oftringen borehole (Effingen Member); WLB: Wellenberg (Helvetic Marl); BEN: Benken borehole (Opalinus Clay)).

7.3 CatClay

In the framework of WP2 of the CatClay project a comprehensive data set for diffusion in compacted illite was measured for $^{85}\text{Sr}^{2+}$, $^{60}\text{Co}^{2+}$ and $^{65}\text{Zn}^{2+}$ at pH 5 and 9, and in background NaClO_4 conditions ranging from 0.01 to 1.0 M. One of the main objectives followed in the Catclay project was to compile sets of experimental diffusion data, by which the validity of the various models for cation diffusion reported in the literature can be tested. Effective diffusion coefficients as high as 10^{-8} to $10^{-7} \text{ m}^2 \text{ s}^{-1}$ were derived from measured steady state flux at the lowest ionic strength both at pH 5 and 9 assuming that the gradient is defined by the cations concentration in the external reservoirs. The large D_e values are a clear indication that surface diffusion effects are also active for these types of cations. The reference effective diffusion coefficient for the uncharged tritiated water molecule (HTO) was of the order of $2 \cdot 10^{-10} \text{ m}^2 \text{ s}^{-1}$. Simple diffusion models in which the D_e values are derived from diffusion coefficients in bulk water and rock capacity factors (α) from batch sorption experiments are thus inadequate to describe cation diffusion in compacted illite. No correlation was found in general between the D_e values and the sorption distribution coefficients (K_d) derived from the rock capacity factors. For this reason, a diffusion model in which mass transfer rates are correlated with the total amount of sorbed cations (GLAUS et al. 2007) is neither applicable. Possible approaches for the interpretation of the measured diffusion data can be found by applying a normalisation procedure proposed by GIMMI & KOSAKOWSKI (2011), in

which the observed D_e values are viewed as the result of two parallel fluxes of an aqueous phase species and a mobile surface species. D_e values of a given element are normalised using D_e values of tritiated water (D_0^{HTO}) as a reference in order to account for the different mobilities of different elements in bulk water. The normalised effective diffusion coefficient (D_{erw}) is defined as:

$$D_{erw} = \frac{D_e D_w^{\text{HTO}}}{D_w D_e^{\text{HTO}}} \quad (7.3)$$

where D_w values denote the diffusion coefficients in bulk water. In an equivalent expression to Eq. (7.1), D_{erw} values can be expressed as a function of K_d and a relative surface mobility, μ ($\mu = D_{s0}/D_w$, with D_{s0} being an intrinsic surface diffusion coefficient on a flat surface) according to:

$$D_{erw} = 1 + K_d \frac{1 - \varepsilon}{\varepsilon} \rho_g \mu = 1 + \kappa \mu \quad (7.4)$$

with κ defined as a capacity factor describing the relative equilibrium distribution of a given species between the surface and the aqueous phase as drewed in batch experiments.

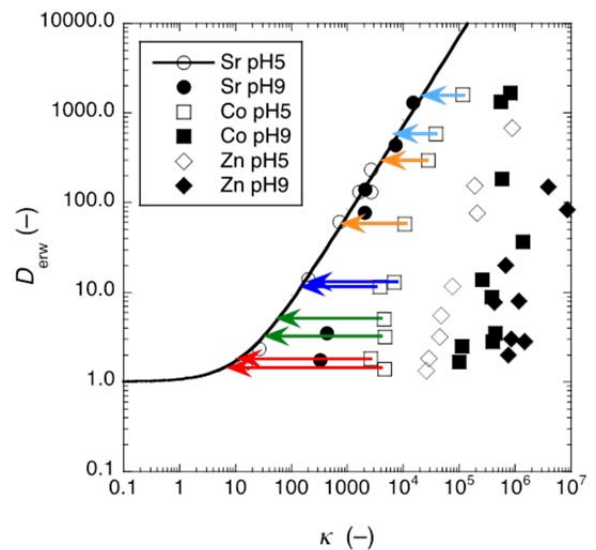


Fig. 7.2: Representation of the measured diffusion data for $^{85}\text{Sr}^{2+}$, $^{60}\text{Co}^{2+}$ and $^{65}\text{Zn}^{2+}$ in compacted illite according to the normalisation procedure proposed by GIMMI & KOSAKOWSKI (2011). Large D_{erw} values are generally found for low salinities within a single group of data. The solid curve has been obtained by fitting the $^{85}\text{Sr}^{2+}$ data measured at pH 5 to Eq. (7.4). For the interpretation of the arrows the reader is referred to the text.

As can be seen from Fig. 7.2 the agreement of the experimental data with the parallel-flux model is in general poor. In many cases large variations of D_{erw} values can be observed for relatively small variations of κ values. Only in the case of the Sr^{2+} data at pH 5 a satisfying picture was obtained. The general disagreement can be interpreted in the sense that the model of GIMMI & KOSAKOWSKI (2011) assumes the presence of two species only. This may not be an adequate assumption for the elements tested in this study. According to the 2SPNE SC/CE model (BRADBURY & BAEYENS 2009) it may well be assumed that surface species may be present in the cation exchange and/or in different types of surface complexing sites. It is further a reasonable assumption that these species may have different relative surface mobilities owing to their different chemical interaction with the surface. A feasible explanation for the different correlations observed can thus be found in the assumption that surface complexes, the dominant surface species for Co(II) and Zn(II) at higher pH values, are immobile while minor species in the cation exchange (or electrical double layer) sites are mobile and contribute to diffusion. The observed D_e values would thus be the result of (i) the stoichiometric ratio of such species compared to the aqueous phase species and (ii) their relative molecular mobility compared to aqueous phase diffusion. This ambiguity cannot be solved simply from the observed D_e values. Different strategies for a reasonable parameter assignment can be envisaged.

As a first option the fit curve of the Sr data at pH 5 is used as master curve for fully mobile surface species. Under the assumption that mobile Co(II) and Zn(II) surface species have the same mobility as Sr^{2+} , it is possible to estimate their amount from the measured D_{erw} values as indicated by the arrows in Fig. 7.2. For the element under consideration a reduced κ for mobile species κ' , can be derived by shifting the data on a constant D_{erw} line to the left until it meets the master curve. The new κ' value read out can be used to calculate a K_d value valid for mobile species only.

The proposition of a reduced κ for mobile species has a rather hypothetical character. It is, however, supported to a large degree by the qualitative trends generally observed in the experimental data. The length of the arrows, which are inversely proportional to the mole fraction of mobile surface species, increase with increasing ionic strength and increasing pH. They further increase in the order of elements Sr

→ Co → Zn corresponding to the trend of these ions to form hydrolysed species (acidity of metal cations). It further confirms the hypothesis that binding mechanism of Sr^{2+} on illite is almost pure cation exchange at low pH, whereas an increasing contribution of specific surface complexes becomes noticeable at higher pH (BRADBURY & BAEYENS 2005).

An alternative strategy is to directly apply a speciation model to calculate the relative proportions of surface and solution species, which may contribute to the diffusive flux. This has been done using an electrostatic approach, in which the clay porosity is subdivided in three fractions consisting of (i) free uncharged porewater, (ii) a Donnan layer (DL) with averaged concentrations of counter cations and reduced concentrations of anions and (iii) a fraction devoid of anions containing surface cations directly neutralising part of the negative clay surface charge. Using conventional assumptions regarding the equilibrium distribution of cations and anions between these pore compartments a relation between D_e values and the respective diffusion coefficients in bulk water can be established according to Eq. (7.5)

$$D_e = D_w \frac{\varepsilon_{tot}}{G} \left(f_{free} + f_{DL} \frac{c_{DL}}{c} \right) \quad (7.5)$$

where ε_{tot} is the total porosity, G a geometric factor, f_{free} and f_{DL} the fractional porosities of free and DL water, and c and c_{DL} the cation concentrations in the latter two porosities. Fig. 7.3 shows a comparison of model curves obtained from Eq. (7.5) with the experimental diffusion data.

One of the most important conclusions from the experiments is that mass transfer rates of transition elements in compacted clay minerals have to be viewed partly as the result of chemical speciation of the diffusing species. Effective diffusion coefficients are thus inherently depending on the chemical conditions and on the speciation model used. A second important conclusion is related to worst case assumptions applied for radionuclide transport. Competition for sorption sites between radionuclides and other metal cations present in the clay porewater may result in a redistribution of radionuclides to weaker sorption sites, by which the capacity of the clay for radionuclide uptake decreases. As a result from surface diffusion effects, the surface mobility of such species and thus the diffusive fluxes may also be changed.

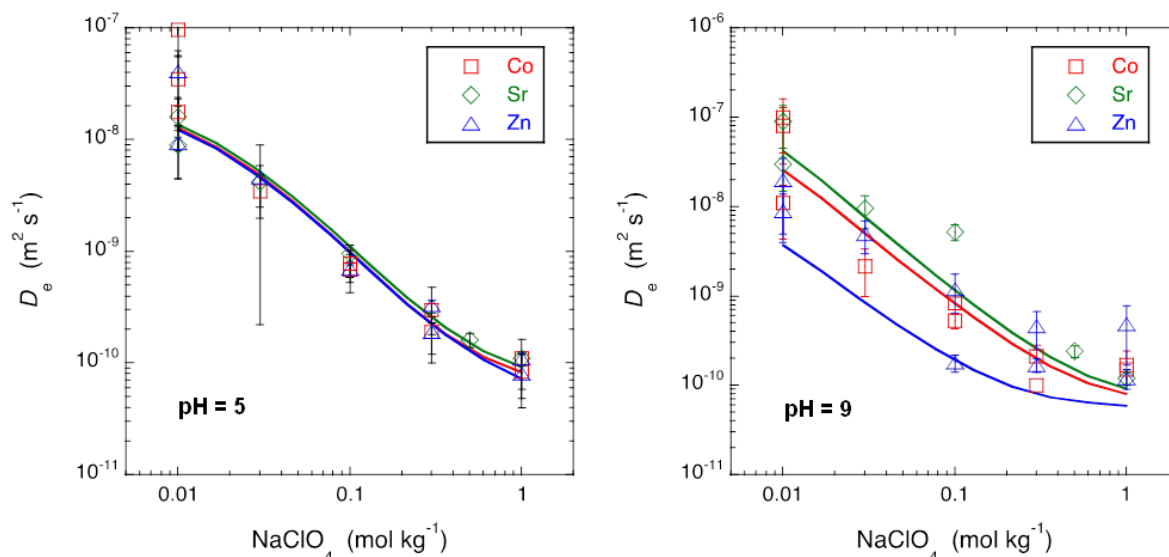


Fig. 7.3: Effective diffusion coefficients measured for $^{85}\text{Sr}^{2+}$, $^{60}\text{Co}^{2+}$ and $^{65}\text{Zn}^{2+}$ in illite at pH 5 and 9 as a function of the NaClO_4 concentration. Fit curves are calculated using the model given by Eq. (5).

Competition of other cations with radionuclides may thus have an adverse effect on the barrier function of clay not only with regards to radionuclide retardation but also to mass transfer rates.

In the framework of WP3 of the CatClay project diffusion results of $^{60}\text{Co}(\text{II})$ and $^{65}\text{Zn}(\text{II})$ on Opalinus Clay samples from the Mont Terri URL were modelled using PHREEQC. To this end, the sorption model of BRADBURY & BAEYENS (2011) was implemented in PHREEQC.

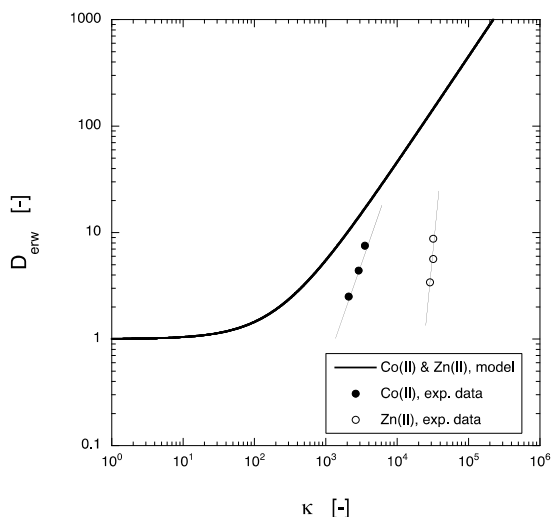


Fig. 7.4: Representation of the measured diffusion data for $^{60}\text{Co}^{2+}$ and $^{65}\text{Zn}^{2+}$ in Opalinus Clay according to the normalisation procedure proposed by GIMMI & KOSAKOWSKI (2011). Larger D_{erw} values are generally found for low salinities within a single group of data.

It could be demonstrated that the strong sorption sites suggested by Bradbury & Baeyens are not in agreement with the measured diffusion profiles. Only when competition with trace elements such as Fe(II) and lanthanides (e.g. Eu) was introduced, the effect of the strong sorption sites was annihilated and the diffusion profiles could be reproduced by the model. Competition with these trace elements is plausible because of the abundance of such elements in nature.

When applying the parallel-flux model, one can see that a similar behaviour is observed as in the case of illite (Fig. 7.4). A closer inspection indicates that a small increase of κ results in a larger increase of D_{erw} compared to the model. This indicates that also in the case of Opalinus Clay the sorbed species has to be subdivided in mobile and immobile sorbed species. The former ones probably are sorbed species that can be allocated to the diffuse layer.

7.4 Transport phenomena in compacted clay systems (TRAPPHICS)

Tracer diffusion experiments were carried out in the presence of strong ligands in order to investigate the influence of radionuclide speciation and species charge on the rates of tracer mass transfer. Radiolabelled ligands were added in part of these experiments to test whether the radionuclides might diffuse as negatively charged complexes in the pore space of negatively charged clay minerals. One group of these experiments comprised diffusion of hexavalent uranyl in carbonate containing electrolytes and the other group diffusion of Sr^{2+} in electrolytes containing ethylene-diamine-tetraacetate (EDTA), a frequently used hexadentate ligand. Both

experiments were carried out at pH values in the bulk solution resulting in dominant formation of negatively charged uranyl-carbonato and strontium-EDTA complexes. While the former experiments could not be evaluated successfully because of unexpected difficulties in radioactivity measurements, no such problems were encountered in the latter case. The diffusion of $^{85}\text{Sr}^{2+}$ and ^{14}C labelled EDTA was measured separately in Na-conditioned montmorillonite compacted to a bulk dry density of 1600 kg m^{-3} . The contacting solutions contained different concentrations of NaClO_4 (0.1, 0.5, 1.0 M), 1 mM EDTA and were buffered to pH 9. The clay was previously treated exhaustively with EDTA in order to remove mobile metal fractions. First experiments showed that such a pre-treatment was necessary, otherwise EDTA was rapidly saturated with trace metals mobilised from the clay phase. On a longer term the present experiments were also affected by slow processes related to the interaction of EDTA with montmorillonite as indicated by element analysis of the contacting solutions. Nevertheless, a couple of interesting observations were made during the course of the diffusion experiments. The negatively charged free EDTA clearly showed the typical features of anion diffusion, characterised by low effective diffusion coefficients (ca. $10^{-13} \text{ m}^2 \text{ s}^{-1}$) and rapid break-through times. It was not possible to estimate the EDTA accessible porosity, because a significant interaction between the clay and this ligand took place, as indicated by a significant loss of EDTA from the source reservoir solution. The diffusion of $^{85}\text{Sr}^{2+}$ in 1 mM EDTA resulted in effective diffusion coefficients which were lower by orders of magnitude than effective diffusion coefficients measured in systems devoid of EDTA. Similarly the rock capacity factors were much lower. The effective diffusion coefficients and rock capacity factors for $^{85}\text{Sr}^{2+}$ were, however, significantly larger than those of EDTA. Experiments carried out in the presence of a stable background concentration of $\sim 1 \text{ mM Sr}^{2+}$ resulted in the same breakthrough curves for $^{85}\text{Sr}^{2+}$ and ^{14}C -EDTA as in the experiments carried out only with $^{85}\text{Sr}^{2+}$ tracer (Fig. 7.5). The results can be interpreted qualitatively in the sense that the diffusion of EDTA and $^{85}\text{Sr}^{2+}$ occur independently and most probably in different pore types. The larger effective diffusion coefficients of Sr compared to those of EDTA indicate that an equilibrium fraction of $^{85}\text{Sr}^{2+}$ may be present in the interlayers of montmorillonite, while the EDTA molecule is excluded from this porosity. Note that EDTA is present as a bi-valent anionic species in bulk water under the conditions of the experiments.

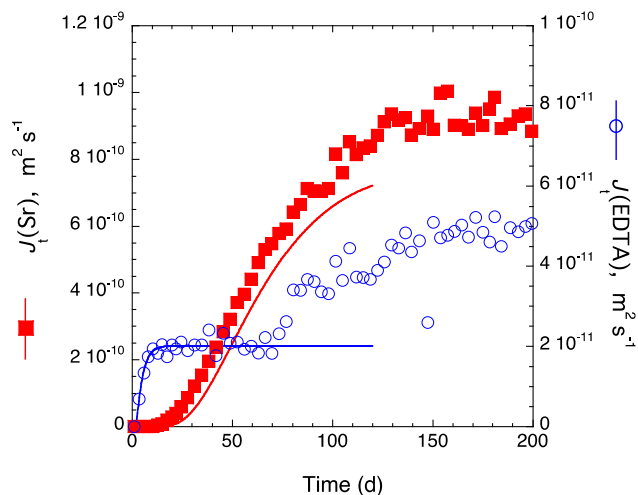


Fig. 7.5: Fluxes (J) measured at the downstream boundary in a through diffusion experiment in which the source reservoir contained each 1 mM stable Sr^{2+} and 1 mM EDTA, plus their respective radiotracer species. Lines are fit curves from the early phase (0–70 days) of experiments with separate additions of Sr and EDTA to the source reservoir. The good agreement between data and fit curves indicates that diffusion of Sr and EDTA occurs independent of each other and that Sr-EDTA complexes are unimportant in clay porewater. The slow increase of the EDTA flux after ~ 70 days is probably related in some way to the saturation of EDTA with metal cations dissolved from the clay.

If $^{85}\text{Sr}^{2+}$ was transported as an EDTA complex, even lower effective diffusion coefficients would be expected owing to the fact that such complexes are also bi-valent anionic species and that they are significantly larger than the metal-free EDTA molecules. Future experiments of such types will require shorter experimental time scales in order to avoid secondary effects induced by metal saturation of EDTA.

7.5 Porosity changes in porous media

Due to dissolution-precipitation reactions occurring at interfaces with strong chemical gradients (e.g. cement-clay), porosity changes can result in changes in the transport properties of solutes and gases. In order to achieve a better understanding of dissolution-precipitation reactions and their effect on solute transport, two projects are ongoing, one on the interface between cement and montmorillonite, another on the effect of porosity changes on transport phenomena. The projects are a co-operation between the Transport Mechanisms group, the Diffusion Processes group and the University of Bern. More information on these projects is given in Chapter 3.

7.6 Transport of small organic molecules in dense clay systems

Corrosion of activated steel can release ^{14}C -labelled organic molecules. The migration/retention behaviour of such small molecules is unknown and needs to be elucidated. The retention behaviour of a suite of organic molecules was studied using an infiltration technique. A constant advective flow through a column of compacted clay (illite in our case) was generated by pressurised helium. A pulse of tracers (^{14}C -labelled Na-acetate, Na-propanoate, Na-2-hydroxypropanoate (=Na-lactate), Na-3-hydroxypropanoate, Na-D-gluconate) was injected and their breakthrough was monitored. A non-sorbing tracer, tritiated water (HTO), was used as a conservative reference. The effluent concentrations were measured with ion chromatography and the activities of HTO and ^{14}C -labelled Na-acetate were measured by liquid scintillation counting. Breakthrough curves are shown in Figure 7.6. Within the given limits for peak resolution, the breakthrough times of propanoate and HTO were identical. Similar behaviour was observed for 3-hydroxypropanoate and acetate. Lactate, however, was significantly retarded with an R_d value of $4 \cdot 10^{-4} \text{ m}^3/\text{kg}$, and gluconate had the most significant retardation. Mass balance calculations showed that all compounds were almost completely recovered in the effluents except acetate, gluconate and 3-hydroxypropanoate.

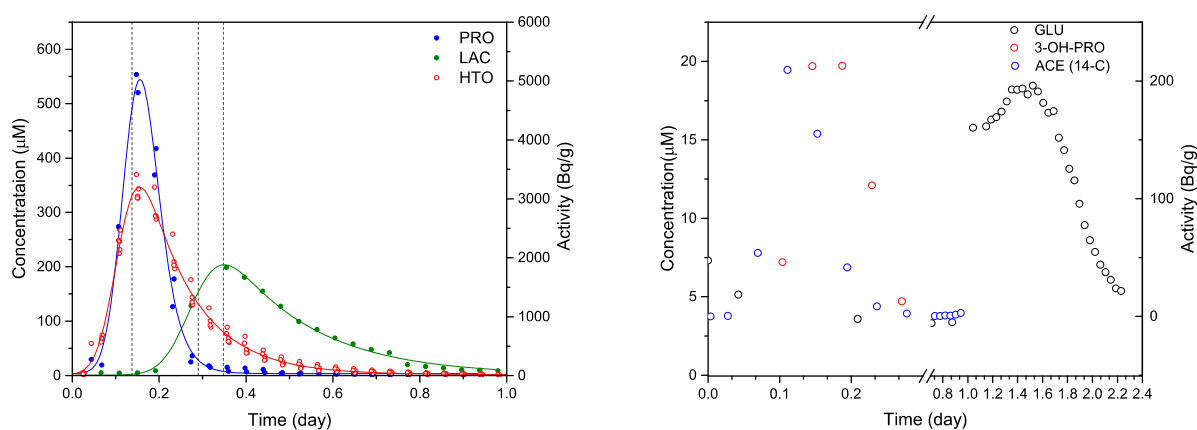


Fig. 7.6: Breakthrough curves for HTO, propanoate, lactate (left), and gluconate, 3-hydroxypropanoate, and ^{14}C labelled acetate (right). Concentrations/activity of tracers were plotted in dots as a function of elution time. Solid curves are only shown for visualization purpose.

The breakthrough of the individual tracers will be modelled with a 1D advection/diffusion model implemented in COMSOL Multiphysics.

The strong sorption of lactate and gluconate might be caused by the hydroxy group in the alpha position. This will be verified by studying the retention behaviour of butanoate and 2-hydroxybutanoate. Also a series of alcohols and aldehydes will be tested. Besides illite, infiltration experiments using kaolinite and Opalinus Clay as the solids are also planned.

7.7 Anion exclusion phenomena in low porosity clay rocks (ANPOR)

Although anion exclusion can be explained qualitatively, a quantitative explanation in the case of clay rocks cannot be given. A new PhD project to study anion exclusion into more detail and to relate diffusion to the mineral composition and pore structure of the rock was started in cooperation with NWMO Canada and the University of Bern (ANPOR). A PhD student (Cornelia Wigger) started working on the project in February 2014. For this study a selection of Swiss and Canadian clay rock samples was characterised in terms of mineralogy, specific surface area and pore size distribution. Different techniques were used such as mercury intrusion, N_2 and H_2O adsorption, CO_2 adsorption, NMR spectroscopy and cryoporometry. Cryoporometry was performed in cooperation with Dr. Beau Webber (University of Kent, UK).

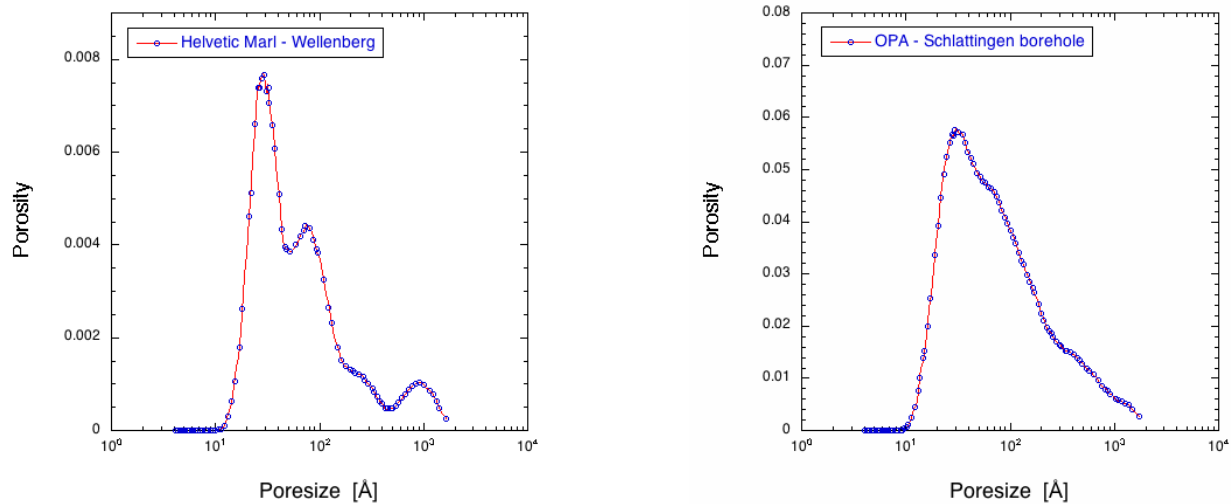


Fig. 7.7: Pore size distribution of an Opalinus Clay sample (left) and an Helvetic Marl sample (right) as measured with cryoporometry.

Figure 7.7 gives the pore size distribution for an Opalinus Clay sample (Schlattigen borehole) and a Helvetic Marl sample (Wellenberg). It can be seen that the proportion of pores with a diameter of 3 nm is larger for the Helvetic Marl sample than in the case of Opalinus Clay.

Samples of Opalinus Clay and Helvetic Marl were placed in a diffusion cell and equilibrated with solutions with different ionic compositions ($I = 0.01 \text{ M}, 0.1 \text{ M}, 1 \text{ M}$ and 2 M NaCl). The change in chemical composition of the solutions due to cation exchange reactions and dissolution reactions was monitored. As soon as chemical equilibrium was reached, the solutions were labelled with ^{36}Cl to study the effect of ionic strength on the diffusion behaviour of anions.

7.8 References

- BRADBURY M.H., BAEYENS B. (1998)
A physico-chemical characterisation and geochemical modelling approach for determining porewater chemistries in argillaceous rocks. *Geochim. Cosmochim. Acta* 62, 783-795.
- BRADBURY M.H., BAEYENS B. (2005)
Modelling the sorption of Mn(II), Co(II), Ni(II), Zn(II), Cd(II), Eu(III), Am(III), Sn(IV), Th(IV), Np(V) and U(VI) on montmorillonite: Linear free energy relationships and estimates of surface binding constants for some selected heavy metals and actinides. *Geochim. Cosmochim. Acta* 69, 875-892.
- BRADBURY M.H., BAEYENS B. (2009)
Sorption modelling on illite Part I: Titration measurements and the sorption of Ni, Co, Eu and Sn. *Geochim. Cosmochim. Acta* 73, 990-1003.
- GIMMI T., KOSAKOWSKI G. (2011)
How mobile are sorbed cations in clays and clay rocks? *Environ. Sci. Technol.* 45, 1443-1449.
- GLAUS M.A., BAEYENS, B., BRADBURY M.H., JAKOB A., VAN LOON L.R., YAROSHCHUK A. (2007)
Diffusion of ^{22}Na and ^{85}Sr in montmorillonite: Evidence of interlayer diffusion being the dominant pathway at high compaction. *Environ. Sci. Technol.* 41, 478-485.
- VAN LOON L.R. (2014)
Effective diffusion coefficients and porosity values for argillaceous host rocks: measured and estimated values for provisional safety analyses for SGT-E2. Nagra Technical Report NTB 12-03, Nagra, Wetztingen, Switzerland.
- VAN LOON L.R., HOBBS M., AL T., GIMMI T., MÄDER U. (2013)
Anion accessibility in low porosity argillaceous rocks (ANPOR). PhD proposal, Paul Scherrer Institut, Villigen, Switzerland.
- WABER H.N. (2008)
Borehole Oftringen: mineralogy, porosimetry, geochemistry, porewater chemistry. Nagra Arbeitsbericht NAB 08-18.
- WERSIN P., MAZUREK M., WABER H.N., MÄDER U.K., GIMMI TH., RUFER D., DE HALLER A. (2013)
Rock and porewater characterisation on drillcores from the Schlattigen borehole. Nagra Arbeitsbericht NAB 12-54.

8 PUBLICATIONS

8.1 Peer reviewed journals

Aldaba D.¹, Glaus M.A., Leupin O.², Van Loon L.R., Vidal M.¹, Rigol A.

Suitability of various materials for porous filters in diffusion experiments. *Radiochim. Acta.* 102, 723-730 (2014).

¹ University of Barcelona, Barcelona, Spain

² NAGRA, Wettingen, Switzerland

Bhatt J.S.¹, McDonald P.J.¹, Faux D.A.¹, Howlett N.C.¹, Churakov S.V.

NMR relaxation parameters from molecular simulations of hydrated inorganic nanopores. *Int. J. Quantum Chem.* 114, 1220–1228 (2014).

¹ University of Surrey, Surrey, UK

Churakov S.V., Gimmi T., Unruh T.¹, Van Loon L.R., Juranyi F.

Resolving diffusion in clay minerals at different timescales: Combination of experimental and modelling approaches. *Appl. Clay Sci.* 96, 36-44 (2014).

¹ Forschungsneutronenquelle Heinz Maier-Leibnitz, Garching, Germany

Churakov S.V., Labbez C.¹, Pegado L., Sulpizi M.²

Intrinsic acidity of surface sites in calcium-silicate-hydrates and its implication to their electrokinetic properties. *J. Phys. Chem. C.* 118, 11752-11762 (2014).

¹ Université de Bourgogne, Dijon, France

² Johannes Gutenberg University, Mainz, Germany

Curti E., Froideval-Zumbiehl A., Günther-Leopold I., Martin M., Bullemer A., Linder H.P., Borca C.N., Grolimund D.

Selenium redox speciation and coordination in high-burnup UO₂ fuel: Consequences for the release of ⁷⁹Se in a deep underground repository. *J. Nucl. Mat.* 453, 98-106 (2014).

Dähn R., Popov D.¹, Schaub P., Pattison P.², Grolimund D., Mäder U.³, Jenni A.³, Wieland E.

X-ray micro-diffraction studies of heterogeneous interfaces between cementitious materials and geological formations. *Phys. Chem. Earth* 70-71, 96-103 (2014).

¹ HPCAT, Carnegie Institution of Washington, Argonne, USA

² SNBL/ESRF, Grenoble, France, and EPFL, Lausanne, Switzerland

³ University of Bern, Bern, Switzerland

Deguedre C., Pin S., Poonosamy J., Kulik D.A.

Redox state of plutonium in irradiated mixed oxide fuels. *J. Phys. Chem. Solids* 75, 358–365 (2014).

Dilnesa B.Z.¹, Lothenbach B.¹, Renaudin G.², Wichser A.¹, Kulik D.A.

Synthesis and characterization of hydrogarnet Ca₃(Al_xFe_{1-x})₂(SiO₄)_y(OH)_{4(3-y)}. *Cement Concrete Res.* 59, 96-111 (2014).

¹ Empa, Dübendorf, Switzerland

² CNRS, Clermont-Ferrand, France

Dilnesa B.Z.¹, Wieland E., Lothenbach B.¹, Dähn, R., Scrivener K.L.²

Fe-containing phases in hydrated cements. *Cement Concrete Res.* 58, 45-55 (2014).

¹ Empa, Dübendorf, Switzerland

² EPFL, Lausanne, Switzerland

Gimmi T., Leupin O.X.¹, Eikenberg J., Glaus M.A., Van Loon L.R., Waber H.N.², Wersin P.², Wang H.A.O., Grolimund D., Borca C., Dewonck S.³, Wittebrodt C.⁴

Anisotropic diffusion at the field scale in a 4-year multi-tracer diffusion and retention experiment – I: Insights from the experimental data. *Geochim. Cosmochim. Acta.* 125, 373-393 (2014).

¹ NAGRA, Wettingen, Switzerland

² University of Bern, Bern, Switzerland

³ ANDRA, Bure, France

⁴ IRSN, Fontenay-aux-Roses, France

Hingerl F.F., Wagner T.¹, Kulik D.A., Thomsen K.², Driesner T.³

A new aqueous activity model for geothermal brines in the system Na-K-Ca-Mg-H-Cl-SO₄-H₂O from 25 to 300 °C. *Chem. Geol.* 381, 78-93 (2014).

¹ University of Helsinki, Helsinki, Finland

² TU Denmark, Lyngby, Denmark

³ ETH, Zürich, Switzerland

Hingerl F.F., Kosakowski G., Wagner T.¹, Kulik D.A., Driesner T.²

GEMSFIT: a generic fitting tool for geochemical activity models. *Computat. Geosci.*, 18(2), 227-242 (2014).

¹ University of Helsinki, Helsinki, Finland

² ETH Zürich, Zürich, Switzerland

Jacques D.¹, Lothenbach B.², Wieland E.

Mechanisms and modelling of waste-cement and cement-host rock interactions. *Phys. Chem. Earth* 70-71, 1-2 (2014).

¹ SCK-CEN, Mol, Belgium

² Empa, Dübendorf, Switzerland

Kosakowski G., Watanabe N.¹

OpenGeoSys-Gem: A numerical tool for calculating geochemical and porosity changes in saturated and partially saturated media. *Phys. Chem. Earth*, 70-71, 138-149 (2014).

¹ UFZ Leipzig, Leipzig, Germany

Kulasinski K.¹, Keten S.², Churakov S.V., Derome D.¹, Carmeliet J.¹

A comparative molecular dynamics study of crystalline, paracrystalline and amorphous states of cellulose. *Cellulose* 21, 1103-1116 (2014).

¹ Empa, Dübendorf, Switzerland

² Northwestern University, Evanston, USA

Kulasinski K.¹, Keten S.², Churakov S.V., Guyer R.¹, Carmeliet J.¹, Derome D.¹

Molecular mechanism of moisture-induced transition in amorphous cellulose. *ACS Macro Letter* 3, 1037-1040 (2014).

¹ Empa, Dübendorf, Switzerland

² Northwestern University, Evanston, USA

Lothenbach B.¹, Rentsch D.¹, Wieland E.

Hydration of a silica fume blended low-alkali shotcrete cement. *Phys. Chem. Earth* 70-71, 3-16 (2014).

¹ Empa, Dübendorf, Switzerland

Osán J.¹, Kéri A.¹, Breitner D.¹, Fábrián M.¹, Dähn R., Simon R.², Török S.¹

Microscale analysis of metal uptake by argillaceous rocks using positive matrix factorization of microscopic X-ray fluorescence elemental maps. *Spectrochim. Acta B: Atomic Spectroscopy* 91, 12-23 (2014).

¹ Hungarian Academy of Sciences, Budapest, Hungary

² KIT-INE, Karlsruhe, Germany

Pegado L., Labbez C.¹, Churakov S.V.

Mechanism of aluminium incorporation in C-S-H from ab initio calculations. *J. Mater. Chem. A* 2, 3477-3483 (2014).

¹ Université de Bourgogne, Dijon, France

Pfingsten W.

The influence of stable element inventory on the migration of radionuclides in the vicinity of a high level nuclear waste repository exemplified for ⁵⁹Ni. *Appl. Geochem.* 49, 103-115 (2014).

Schumann D., Stowasser T., Volmert B.¹, Günther-Leopold I., Linder H.-P., Wieland E.

Determination of the ¹⁴C content in activated steel components from a neutron spallation source and a nuclear power plant. *Anal. Chem.* 86, 5448-5454 (2014).

¹ Nagra, Wetztingen, Switzerland

Soltermann D., Marques Fernandes M., Baeyens B., Miehé-Brendlé J.¹, Dähn R.

Competitive Fe(II)-Zn(II) uptake on a synthetic montmorillonite. *Environ. Sci. Technol.* 48, 190-198 (2014).

¹ Université de Haute Alsace, Mulhouse, France

Soltermann D., Marques Fernandes M., Baeyens B., Dähn R., Joshi P.¹, Scheinost A.², Gorski C.¹

Fe(II) uptake on natural montmorillonites. I. Macroscopic and spectroscopic characterization. *Environ. Sci. Technol.* 48, 8688-8697 (2014).

¹ Pennsylvania State University, Pennsylvania, USA

² HZDR, Dresden, Germany; ROBL, Grenoble, France

Soltermann D., Baeyens B., Bradbury M.H., Marques Fernandes M.

Fe(II) uptake on natural montmorillonites. II. Surface complexation modelling. *Environ. Sci. Technol.* 48, 8698-8705 (2014).

Thien B.M.J., Kulik D.A., Curti, E.

A unified approach to model uptake kinetics of trace elements in complex aqueous - Solid solution system. *Appl. Geochem.* 41, 135-150 (2014).

Thien B.M.J.

A simple way to constrain the stoichiometry of secondary smectites upon aqueous glass alteration. *Appl. Geochem.* 42, 45-46 (2014).

Tits J., Gaona X.¹, Laube A., Wieland E.

Influence of the redox state on the neptunium sorption under alkaline conditions: Batch sorption studies on titanium dioxide and calcium silicate hydrates. *Radiochim. Acta* 102, 385-400 (2014).

¹ KIT-INE, Karlsruhe, Germany

Torapava N.¹, Ramebäck H.², Curti E., Lagerkvist P.², Ekberg Ch.¹

Recrystallization of ²²³Ra with barium sulfate. *J. Radioanal. Nucl. Chem.* 301, 545-553 (2014).

¹ Chalmers University of Technology, Gothenburg, Sweden

² Swedish Defence Research Agency, Umea, Sweden

Van Loon L.R., Müller W.

A modified version of the in-diffusion/abrasive peeling technique for measuring diffusion of strongly sorbing tracers in argillaceous rocks: a case study for diffusion of caesium in Opalinus Clay. *Appl. Radiat. Isotopes* 90, 197-202 (2014).

Vespa M.¹, Dähn R., Wieland E.

Competition behaviour of metal uptake in cementitious systems: An XRD and EXAFS investigation of Nd- and Zn-loaded 11 Å tobermorite. *Phys. Chem. Earth* 70-71, 32-38 (2014).

¹ KIT-INE, Karlsruhe, Germany

Wieland E., Lothenbach B.¹, Glaus M.A., Thoenen T., Schwyn B.²

Influence of superplasticizers on the long-term properties of cement pastes and possible impact on radionuclide uptake in a cement-based repository for radioactive waste. *Appl. Geochem.* 49, 126-142 (2014).

¹ Empa, Dübendorf, Switzerland

² Nagra, Wetztingen, Switzerland

Wu T.¹, Wang H.², Zeng Q.¹, Zao Y.L.², Van Loon L.R.

Diffusion behaviour of Se(IV) and Re(VII) in GMZ bentonite. *Appl. Clay Sci.* 101, 136-140 (2014).

¹ Huzhou Teachers College, Huzhou, PR China

² Xi'an Jiaotong University, Xi'an, PR China

8.2 PSI and Nagra reports

Baeyens B., Thoenen T., Bradbury M.H., Marques Fernandes M.

Sorption data bases for the host rocks and lower confining units and bentonite for provisional safety analyses for SGT-E2. Nagra Tech. Rep. NTB 12-04 (2014).

Baeyens B., Marques Fernandes M., Bradbury M.H. Comparison between host rock and bentonite sorption measurements and predictions using the SDB approach applied in the provisional safety analyses for SGT-E2. Nagra Tech. Rep. NTB 12-05 (2014).

Berner U.

Löslichkeitslimiten für das Bentonit-Nahfeld für die provisorischen Sicherheitsanalysen für SGT-E2. Nagra Tech. Rep. NTB 14-06 (2014).

Berner U.

Löslichkeitslimiten für das Zement-Nahfeld für die provisorischen Sicherheitsanalysen für SGT-E2. Nagra Tech. Rep. NTB 14-07 (2014).

Bradbury M.H., Berner U., Curti E., Hummel W., Kosakowski G., Thoenen T.

The long term evolution of the nearfield of the HLW repository. Nagra Tech. Rep. NTB 12-01 (2014).

Kosakowski G., Smith P.¹

Long-term evolution of the engineered gas transport system. Nagra Arbeitsberichte NAB 14-16 (2014).

¹ Safety Assessment Management, Klingnau, Switzerland

Kosakowski G., Berner U., Wieland E., Glaus M.A., Degueldre C.

Geochemical evolution of the L/ILW near field. Nagra Tech. Rep. NTB 14-11 (2014).

Thoenen T.

Speciation calculations supporting the sorption data bases for argillaceous rocks and bentonite for the provisional safety analyses for SGT-E2. Nagra Arbeitsberichte NAB 12-52 (2014).

Thoenen T., Hummel W., Curti E., Berner U.

The PSI/Nagra Chemical Thermodynamic Data base 12/07. Nagra Arbeitsberichte NAB 14-49 (2014).

Thoenen T., Hummel W., Berner U., Curti E.

The PSI/Nagra Chemical Thermodynamic Database 12/07. PSI Bericht Nr. 14-04 (2014).

Tits J., Fujita T.¹, Harfouche M., Dähn R., Tsukamoto M.¹, Wieland E.

Radionuclide uptake by calcium silicate hydrates: Case studies with Th(IV) and U(VI). PSI Bericht Nr. 14-03 (2014).

¹ Central Research Institute of the Electric Power Industry, Tokyo, Japan

Van Loon L.R.

Effective diffusion coefficients and porosity values for argillaceous rocks and bentonite: Measured and estimated values for the provisional safety analyses for SGT-E2 Nagra Tech. Rep. NTB 12-03 (2014).

Wieland E.

Sorption data base for the cementitious near field of L/ILW and ILW repositories for performance assessment analyses for SGT-E2. Nagra Tech. Rep. NTB 14-08 (2014).

8.3 Conference proceedings

Savoie S., Altmann S., Appelo T., Gaboreau S. Maes N., Schäfer T., Van Loon L.

CATCLAY: "Processes of cation migration in clayrocks". Euradwaste'13, 8th EC Conference on the Management of Radioactive Waste Community Policy and Research on Disposal, Vilnius, Lithuania. EU 26846 EN, 14-16 October 2013, 275-283 (2014).

Soler J.M., Leupin O.X., Van Loon L.R., Gimmi T.

The DR-A in-situ diffusion experiment at Mont Terri. Effects of changing salinity on diffusion and retention properties. *Mat. Res. Soc. Symp. Proc.*, 63-69 (2014).

8.4 Conferences/workshops/presentations

Berner U.

A solid solution approach for Opalinus Clay porewaters; robustness and phase rule considerations. Workshop Porewater Chemistry of Clayrocks in Repository Environments, Basel, Switzerland, 27-29 October 2014.

Chollet M., Martin Ph., Degueldre C., Poonosamy J., Belin R.C., Henning C.H.

Neptunium characterization in uranium dioxide fuel: Combining a XAS and a thermodynamic approach" 7th Workshop on Speciation, Techniques, and Facilities for Radioactive Materials at Synchrotron Light Sources (AnXAS). Schloss Böttstein, Switzerland, 20-22 May 2014.

Curti E.

X-ray spectroscopic evidence on the chemical state of ⁷⁹Se in high-burnup UO₂ spent fuel, Spent Fuel Workshop, Karlsruhe, 3-5 September 2014.

Cvetković B.Z., Rothardt J., Schlotterbeck G., Kunz D., Büttler A., Wieland E.

¹⁴C-Freisetzung in zementbasierten geologischen Tiefenlagern: Identifizierung organischer Korrosionsprodukte, Swissnuclear Day, Leibstadt, Switzerland, 7 May 2014.

Cvetković B.Z., Rothardt J., Schlotterbeck G., Kunz D., Büttler A., Szidat S., Wieland E.

Speciation of carbon-14 in a cementitious repository for radioactive waste: identification of organic compounds in anoxic corrosion experiments with iron powders, 17th Radiochemical Conference (Radchem 2014), Mariánské Lázně, Czech Republic, 11-16 May 2014.

Dähn R., Schaub P., Popov D., Pattison P., Jenni A., Mäder U., Wieland E.

Synchrotron-based micro X-ray diffraction investigations of cement-clay interfaces. International Mineralogical Association 2014, Johannesburg, South Africa, 1-5 September 2014.

Driesner Th., Scott S., Kulik D.A., Kosakowski G., Thien B.M.J., Greenhalgh S., Maurer H., Grab G., Stefansson A., Hermanska M., Arnason K.

COTHEM - Combined hydrological, geochemical and geophysical modelling of geotHERMAL systems. Geophysical Research Abstracts Vol. 16, EGU2014-15056, 2014, EGU General Assembly 2014, Vienna, Austria, 27 April – 2 May 2014.

Gabitov R., Thien B.M.J., Sadekov A.

Disequilibrium effects on elemental incorporation into CaCO₃. 24th Annual V.M. Goldschmidt Conference, Sacramento, USA, 8-13 June 2014.

Gimmi T., Churakov, S.V.

Up-scaling of diffusion coefficients in saturated and unsaturated clays. TRePro III – Workshop on Modelling of Coupled Reactive and Transport Processes, Karlsruhe, Germany, 5-7 March 2014.

Gimmi T., Leupin, O.X., Soler J.M., Van Loon L.R.

Effect of porewater chemistry on diffusion – Findings from the DR-A experiment. Workshop on Porewater Chemistry of Clayrocks in Repository Environments, Basel, Switzerland, 27–29 October 2014.

Juranyi F., Bestel M., Breitling J., Gimmi T., Churakov S., Van Loon L.R., Glaus M.A., Diamond L.W., Zamponi M.

Water distribution in montmorillonite as a function of temperature and pressure. 7th Mid-European Clay Conference, Dresden, Germany, 16-19 September 2014.

Kolditz O., Bauer S., Beyer C., Kalbacher T., Kosakowski G., McDermott C.I., Nagel T., Park C.H., Shao H., Taron J., Xie, M.

OpenGeoSys (OGS) – An open source modelling platform for simulation of thermo-hydro-mechanical-chemical processes in fractured-porous media: Reactive Transport Modelling, Subsurface Environmental Simulation Benchmarking Workshop IV (SeS Bench IV), Château de Cadarache, France, 6-8 October, 2014.

Kolditz O., Bauer S., Bilke L., Böttcher N., Delfs J.O., Fischer T., Görke U.J., Helbig C., Kalbacher T., Kosakowski G., McDermott C.I., Nagel T., Naumov D., Park C.H., Rink K., Sachse A., Schelenz S., Selle B., Shao H., Shao H.B., Singh A.K., Taron J., Walther M., Wang W., Watanabe N., Zolfaghari R.

OpenGeosys: An open-source initiative for numerical simulation of Thermo-Hydro-Mechanical/Chemical (THM/C) processes in porous media. 11th International Conference on Hydroinformatics, HIC 2014, New York City, USA, 17-21 August, 2014

Kosakowski G.

Reactive transport calculations on porosity changes at material interfaces. TRePro III – Workshop on Modelling of Coupled Reactive and Transport Processes, Karlsruhe, Germany, 5-7 March 2014.

Kulik D.A.

Improvement of C-(A)-S-H solid solution models. Workshop on Calcium Silicate Hydrates Containing Aluminium (C-A-S-H), Dübendorf, Switzerland, 5–6 May 2014.

Kulik D.A., Thien B.M.J., Curti E.

Accounting for aqueous- solid solution interaction kinetics in computer-aided calculations of partial equilibria. 16th International Symposium on Solubility Phenomena and Related Equilibrium Processes (ISSP-16), Karlsruhe Institute of Technology, Germany, 21-25 July 2014.

Miron G.D., Kulik D.A., Dmytrieva S.V., Wagner T.

GEMSFITS: A code package for input parameter optimization of chemical thermodynamic models. 16th International Symposium on Solubility Phenomena and Related Equilibrium Processes (ISSP-16), Karlsruhe Institute of Technology, Germany, 21-25 July 2014.

Pfingsten W., Jakob A.

Benchmark for nonlinear sorption processes of Cs migration through Opalinus Clay using a single species (COMSOL) and a multi-species (MCOTAC) reactive transport model. TRePro III - Workshop on Transport and Reaction Processes, Karlsruhe, Germany, 5-7 March 2014.

Pfingsten W., Jakob A.

Cs migration through Opalinus Clay modelled by a single species (COMSOL) and a multi-species (MCOTAC) reactive transport model. Subsurface Environmental Simulation Benchmark Workshop IV (SeS Bench IV), Cadarache, France, 5-9 October 2014.

Poonoosamy J., Kosakowski G., Van Loon L.R.

Tank experiments for testing numerical transport code. TRePro III – Workshop on Modelling of Coupled Reactive and Transport Processes, Karlsruhe, Germany, 5-7 March 2014.

Poonoosamy J., Kosakowski G., Van Loon L.R., Mäder U.

Experimental and numerical benchmark in 2D reactive transport system. Subsurface Environmental Simulation Benchmark Workshop IV (SeS Bench IV), Cadarache, France, 5-9 October 2014.

Poonoosamy J., Kosakowski G., Van Loon L.R., Mäder U.

Precipitation processes in tank experiments for testing numerical models for reactive transport calculations. 5th PhD Workshop: Reactive Transport Modelling and Experiment, University of Tübingen, Germany, 13-14 November 2014.

Riera A., Pfingsten W.

Uncertainty propagation of Linear-Free-Energy-Relationship sorption parameters to their application in reactive transport calculations. TRePro III – Workshop on Modelling of Coupled Reactive and Transport Processes, Karlsruhe, Germany, 5-7 March 2014.

Rojo H., Tits J., Wieland E.

Selenium uptake by C-S-H phases under anoxic and reducing conditions. Workshop on Calcium Silicate Hydrates Containing Aluminium (C-A-S-H), Dübendorf, Switzerland, 5-6 May 2014.

Rojo H., Gaona X., Rabung Th., Garcia-Gutierrez M., Missana T., Altmaier M.

Nd(III)/Cm(III) complexation with gluconate in NaCl and CaCl₂ alkaline solutions: solubility and TRLFS studies. 2nd International Symposium on Cement-based Materials for Nuclear Wastes (NUWCEM 2014), Avignon, France, 3-6 June 2014.

Rojo H., Tits J., Scheinost A.C., Wieland E.

Retention of selenium by cementitious materials under reducing radioactive waste repository conditions. 24th Annual V.M. Goldschmidt Conference, Sacramento, USA, 8-13 June 2014.

Rojo H., Tits J., Scheinost A.C., Wieland E.

Retention of selenium by cementitious materials under anoxic and reducing conditions. IGD-TP - Geodisposal 2014 Conference. Manchester, United Kingdom, 24-26 June 2014.

Rojo H., Tits J., Scheinost A.C., Wieland E.

Retention of selenium by cementitious materials under oxidizing and reducing conditions. SELEN 2014 Workshop, Karlsruhe, Germany, 13-14 October 2014.

Shafizadeh A., Gimmi T., Van Loon L., Churakov S.V., Kaestner A., Lehmann E., Mäder U.

Evolution of structural and transport properties at cement-clay interfaces. 6th Swiss Bentonite Meeting, Bern, Switzerland, 6 June 2014.

Shafizadeh A., Gimmi T., Van Loon L., Churakov S.V., Kaestner A., Lehmann E., Mäder U.

Time-resolved study of porosity evolution near cement-clay interfaces using high resolution neutron radiography. 10th World Conference on Neutron Radiography, Grindelwald, Switzerland, 5-10 October 2014.

Thien B.M.J.

Aqueous glass dissolution - Effect of Mg, pH, and secondary phases. Swiss Cement Meeting, Bern, 24 March 2014.

Thien B.M.J., Kosakowski G., Kulik D.A.

COTHERM: Modelling fluid-rock interactions in Icelandic geothermal systems. Geophysical Research Abstracts Vol. 16, EGU2014-10622, 2014, EGU General Assembly 2014, Vienna, Austria, 27 April – 2 May 2014.

Thien B.M.J., Kosakowski G., Kulik D.A.

What key factors control the rock alteration in Icelandic hydrothermal systems? 12th Swiss Geoscience Meeting, Fribourg, Switzerland, 21-22 November 2014.

Thien B.M.J., Kosakowski G., Kulik D.A.

Porosity evolution in Icelandic hydrothermal systems. AGU Fall Meeting, San Francisco, USA, 15-19 December 2014.

Tits J., Gaona X., Laube A., Wieland E.

Influence of the redox state on the actinide sorption under highly alkaline conditions: batch sorption studies on titanium dioxide and calcium silicate hydrates. 17th Radiochemical Conference (Radchem 2014), Mariánské Lázně, Czech Republic, 11-16 May 2014.

Tits J., Stumpf T., Walther C., Gaona X., Wieland, E.

Sorption of actinides onto titanium dioxide, calcium silicate hydrates and hardened cement paste. 2nd International Symposium on Cement-based Materials for Nuclear Wastes (NUWCEM 2014), Avignon, France, 3-6 June 2014.

Wieland E., Cvetković B. Z., Rothardt J., Schumann D., Stowasser T., Büttler A., Schlotterbeck G., Kunz D., Tits J., Linder H.-P., Günther-Leopold I., Szidat S.

Langzeitkorrosionsexperiment zur Freisetzung von ¹⁴C aus aktiviertem Stahl, Swissnuclear Day, Leibstadt, Switzerland, 7 May 2014.

Wieland E., Schenzel J., Schlotterbeck G.

The fate of organic compounds in a cement-based repository: Impacts on the engineered barrier and the release of C-14 from the near field. 2nd International Symposium on Cement-based Materials for Nuclear Wastes (NUWCEM 2014), Avignon, France, 3-6 June 2014.

Wieland E., Rothardt J., Cvetković B. Z., Szidat S., Schlotterbeck G.

Speciation of carbon-14 in the cementitious near field of a repository for radioactive waste. First insights from corrosion experiments with iron powder. IGD-TP - Geodisposal 2014 Conference, Manchester, United Kingdom, 24-26 June 2014.

Wigger C., Van Loon L.R., Gimmi T., Mäder U. (2014)

Anion accessibility in low porosity argillaceous rocks: ANPOR. NWMO. 12th Annual Geoscience Meeting, Ontario, Canada, 9–11 June 2014.

8.5 Invited talks

Marques Fernandes M., Soltermann D., Dähn R., Gorski C.A., Baeyens B.

Fe(II) uptake on montmorillonites: Surface complexation and oxidation. 248th ACS National Meeting & Exposition, San Francisco, USA, 10-14 August 2014.

Pegado L., Labbez C., Churakov S. V.

C-A-S-H: mechanism of Al incorporation and the road to multi-scale molecular modelling of ion sorption. Workshop on Calcium Silicate Hydrates Containing Aluminium (C-A-S-H), Dübendorf, Switzerland, 5–6 May 2014.

Pfingsten W.

Endlagerforschung in der Schweiz. Symposium des Deutsch-Schweizerischen Fachverbandes für Strahlenschutz e.V. Zwischenlager–Dauerlager–Endlager, wo bleiben wir mit unseren radioaktiven Abfällen, Mainz, Germany, 22-24 September 2014.

Van Loon L.R., Gimmi T., Wigger C.

Anion accessibility in low porosity argillaceous rocks: ANPOR. NWMO, 12th Annual Geoscience Meeting, Ontario, Canada, 9–11 June 2014.

Wieland E.

Combined wet chemistry and spectroscopic studies on radionuclide uptake by cementitious materials. 7. Workshop des Verbundprojekts "Rückhaltung endlagerrelevanter Radionuklide im natürlichen Tongestein und in salinaren Systemen". Universität des Saarlands, Saarbrücken, Germany, 28-29 October 2014.

8.6 Teaching

Gimmi T.

Lecture and examinations "Fluids in the Crust", Master Course in Environmental and Resource Geochemistry, University of Bern, Fall semester 2014.

Hummel W.

Lectures and examinations "Nuclear Energy Systems", (Spring Semester 2014) and "Landfilling, nuclear repositories and contaminated sites" (Spring and Fall Semester 2014).

Kulik D.A.

GEMS course in cement chemistry at Empa, 6-7 May 2014.

Kulik D.A.

GEMS training for reactive transport applications, MU Leoben, 7-11 July 2014.

Pfingsten W.

Modelling of Processes in Soils and Aquifers: 701-1334-00L, Department for Environmental Sciences, ETH, Zürich, Spring Semester 2014.

Pfingsten W.

Seminar für Bachelorstudierende: Biogeochemie: 701-0419-01L, Department for Environmental Sciences, ETH, Zürich, Fall Semester 2014.

8.7 PhD thesis and master projects

Bestel M.

Water-montmorillonite systems: Neutron scattering and tracer throughdiffusion studies. PhD Diss. Universität Bern, May 2014.

L'Hopital E.

Aluminium and alkali uptake in calcium silicate hydrates (C-S-H). PhD Diss., EPFL, Lausanne, October 2014.

Riera A.

Reactive transport modelling within the bentonite backfill of a deep nuclear waste repository. Comparing the migration of radionuclides through FEBEX (Spain) and MX-80 (Switzerland) bentonite taking into account sorption competition effects. Master thesis of (International Industrial Master (UPC, Spain). Thesis grade 10 (of 10), April 2014.

Meng S.

Modeling of radionuclide migration in radial symmetry using MCOTAC. Master thesis of Nuclear Engineering Master, ETHZ & EPFL, (Switzerland). Thesis grade 5.5 (of 6), September 2014.

Soltermann D.

Ferrous iron uptake mechanisms at the montmorillonite-water interface under anoxic and electrochemically reduced conditions. PhD Diss. No. 22103, ETH, Zürich, July 2014.

8.8 Other

Dähn R., Degueldre C., Grolimund D.

Organizers of ANXAS 2014 Workshop on speciation, techniques and facilities for radioactive materials at Synchrotron Light Sources in Böttstein, Switzerland, 20-22 May 2014.

Gimmi T.

Associate Editor at the Applied Geochemistry Journal.

Kulik D.A.

Member of ISSP-16 International Scientific Advisory Committee.

Kulik D.A.

Executive Guest Editor, Special Issue on geochemical speciation codes and data bases. Applied Geochemistry.

Pfingsten W.

Co-organiser of the TRePro III Workshop on Transport and reaction processes in Karlsruhe, Germany, 5-7 March 2014.

Wieland E.

Guest Editor for the journal "Physics and Chemistry of the Earth" for a special issue (Vol. 70-71, 2014) on "Mechanisms and modelling of waste-cement and cement-host rock interactions".

